

Mesenteric Fibrosis in Neuroendocrine Tumors

An entangled conundrum



Anela Blažević

Mesenteric Fibrosis in Neuroendocrine Tumors

An Entangled Conundrum

Anela Blažević

Author	Anela Blažević
Cover design and lay-out	Miranda Pouw, Mirakels Ontwerp
Print	Gildeprint
ISBN	978-94-6419-762-4

© Copyright 2023, A. Blažević

All rights reserved. No parts of this publication may be reproduced, stored in a retrieval system, or transmitted in any form or by any means, without prior written permission of the author.

Mesenteric Fibrosis in Neuroendocrine Tumors

An entangled conundrum

Mesenteriale fibrose in neuro-endocriene tumoren

Een verstrengeld vraagstuk

Thesis

to obtain the degree of Doctor from the
Erasmus University Rotterdam
by command of the
Rector Magnificus

Prof.dr. A.L. Bredenoord

and in accordance with the decision of the Doctorate Board.

The public defence shall be held on
Wednesday 10 May 2023 at 15:30 hrs
by

Anela Blažević,
Born in Zenica, Former Yugoslavia

Doctoral Committee

Promotors

prof.dr. W.W. de Herder

prof.dr. L.J. Hofland

Other members

prof.dr. E.J.M. Nieveen Van Dijkum

prof.dr. M.C.W. Spaander

prof.dr. F.A. Verburg

Copromotor

dr. R.A. Feelders

Table of contents

Chapter 1	General introduction	08
Chapter 2	Evolution of the mesenteric mass in small intestinal neuroendocrine tumors	34
Chapter 3	Mesenteric fibrosis and palliative surgery in small intestinal neuroendocrine tumors	52
Chapter 4	Predicting symptomatic mesenteric mass in small intestinal neuroendocrine tumors using radiomics	74
Chapter 5	Sexual dimorphism in small-intestinal neuroendocrine tumors: lower prevalence of mesenteric disease in premenopausal women	104
Chapter 6	Aberrant tryptophan metabolism in stromal cells is associated with mesenteric fibrosis in small intestinal neuroendocrine tumors	124
Chapter 7	Proteomic analysis of small intestinal neuroendocrine tumors and mesenteric fibrosis	146

Chapter 8	General discussion	172
Chapter 9	Summary	188
	Samenvatting	191
Appendix	Portfolio	198
	List of publications	201
	Dankwoord	202
	Curriculum Vitae	209



Chapter 1

General introduction

Small-intestinal neuroendocrine tumors

Prevalence and prognosis

Small intestinal neuroendocrine tumors (SI-NETs) are rare tumors with an rising incidence of approximately 1 per 100.000¹⁻³. The first description of a SI-NET was made by Oberndorfer in 1907, who introduced the term carcinoid for these tumors. This diminutive term was used to characterize the seemingly benign nature of these tumors. Compared to many other small intestinal neoplasms such as adenocarcinomas, lymphomas and sarcomas, SI-NETs have a considerably more indolent disease progression⁴. However, it is wrong to classify these tumors as benign. The majority of patients present with metastasized disease at diagnosis, with locoregional metastases in 38% and distant disease in 48%^{1,3-5}. SI-NETs predominantly metastasize to the liver and mesenteric lymph nodes^{5,6}.

The survival of patients has increased in recent decades, especially for metastasized disease.^{1, 2, 4, 7} The 5-year survival of patients with distant metastasis is currently 60-70%.^{2, 4} The development of targeted treatment options such as somatostatin analogues (SSAs), everolimus, and peptide receptor radionuclide therapy with ¹⁷⁷Lu-DOTATATE (PRRT) has largely contribute to improving the survival of patient with advanced SI-NETs.^{6,8}

Prognostic factors in SI-NETs

The most established prognostic factors in SI-NETs are disease stage and grade. Therefore, SI-NETs are classified according to TNM-staging and Ki-67 grading (**Table 1**).⁴ Age at diagnosis is also prognostic for survival. Patients older than 60 years at diagnosis have a worse survival, however this may be related to other age-related causes of death.^{1,4} Furthermore, male patients seem to have a worse prognosis, even when corrected for age, tumor stage and grade^{1,3}. The underlying mechanism of the sex difference in SI-NET prognosis is unclear. Therefore in **Chapter 5**, we explore this sex difference in more detail.

TABLE 1.

A. Staging of SI-NETs						B. Grading of SI-NETs		
Stage	TNM	Disease				Grade	Ki-67 index (%)	Mitotic index (mitoses / 10 HPF)
0		Tis	N0	M0	Localized	G1	≤ 2	< 2
I		T1	N0	M0		G2	3 - 20	2 - 20
II	a	T2	N0	M0		G3	> 20	> 20
	b	T3	N0	M0				
III	a	T4	N0	M0				
	b	Any T	N1	M0	Regional			
IV		Any T	Any N	M1	Distant			

SI-NETs are known to secrete a wide range of molecules and this has resulted in a widespread search for circulating prognostic biomarkers. Chromogranin A (CgA) and 5-hydroxyindoleacetic acid (5-HIAA), the main metabolite of serotonin, are the most often used biomarkers⁴. However, when corrected for other known prognostic factors such as tumor stage and grade, the additional prognostic value of a baseline measurement is limited.^{9, 10} On the other hand, these biomarkers are useful for the detection of hormonal syndromes and during follow-up to monitor disease progression and response to treatment.^{4, 10} Other recent prognostic biomarker candidates are based on circulating tumor-derived transcripts such as mRNAs and microRNAs.¹¹ An innovative approach has been the NETest[®].¹² This test is a multi-analyte biomarker that gives a single readout through an undisclosed algorithm. An increased NETest[®] score seems to be a predictor for disease progression and decreased survival.^{13, 14} However, there is a need for additional validation to establish the role of the NETest[®] in clinical practice.

The prognosis of patients with SI-NETs is also attenuated by tumor-specific hypersecretion-related symptoms. Typical clinical manifestations of hypersecretion that comprise the carcinoid syndrome are secretory diarrhea (60-80%) and flushing (60-85%)⁴. These symptoms are correlated with a significant decreased quality of life¹⁵. However, the effect on survival, independent of other prognostic factors, is unclear and seems limited, except in the case of significant heart failure caused by heart valve fibrosis, also known as carcinoid heart disease.^{4, 16-18} Fibrotic complications also occur in mesenteric

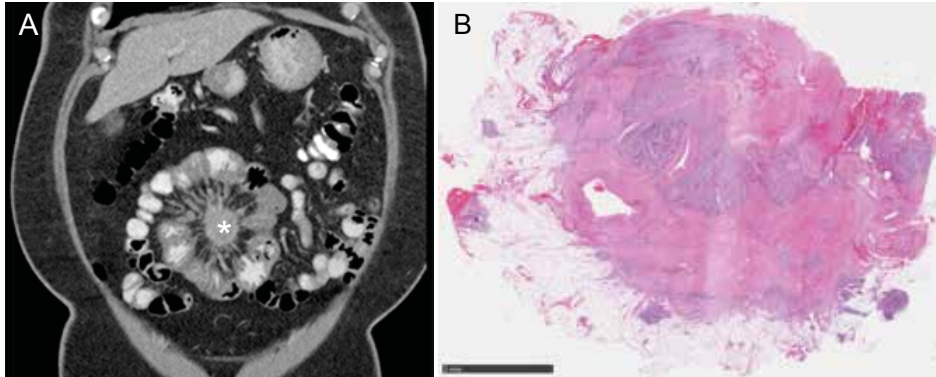
1 disease. Mesenteric metastases with vessel encasement and surrounding fibrosis can cause severe complications such as intestinal obstruction, edema and ischemia.¹⁹⁻²¹ However, there was surprisingly limited literature on the effect of mesenteric metastasis and fibrosis on survival.^{22,23} Therefore, we assessed this in a large cohort (**Chapter 3**).

Mesenteric metastasis and fibrosis

Prevalence

Mesenteric metastases are present in 65% of SI-NETs at diagnosis^{5,20,24,25}. The mesenteric metastases often present with one dominant mesenteric mass²⁶. This metastatic mass is known to induce fibrosis in the surrounding mesentery, which can cause serious complications such as bowel obstruction and ischemia.^{6, 21, 24, 26} However, there is a scarcity in literature on the progression or development of mesenteric metastases over time²⁴. Therefore, we conducted a retrospective study to assess the evolution of SI-NET-associated mesenteric mass over time in the era of targeted therapy (**Chapter 2**).

Mesenteric fibrosis occurs almost exclusively surrounding a dominant metastatic mesenteric mass and can be assessed on radiological and histopathological level^{20, 26-28}. In clinical studies, the presence of mesenteric fibrosis is typically assessed radiologically using computed tomography (CT) imaging. Mesenteric fibrosis is characterized by radiating strands of soft tissue on CT imaging, often described as a “stellate” or “spoke-wheel” pattern (**Figure 1A**).²⁶ Radiologically, mesenteric fibrosis can be detected in 55 - 75% of SI-NET patients with mesenteric metastases^{5, 20, 25, 26, 28}. Histopathological grading of mesenteric fibrosis requires removal of the complete mesenteric metastatic node (**Figure 1B**). Histopathological mesenteric fibrosis is graded based on the width of the band of fibrous tissue: grade 1 (< 1 mm); grade 2 (1-2 mm); grade 3 (> 2 mm)²⁵. However, the definition varies as some studies confine assessment of the fibrous band to intratumoral stroma, while others include the fibrous band surrounding the mesenteric tumor^{26, 27}. When assessing the intratumoral fibrous bands, fibrosis grade 2 and 3 is detected in 48% of SI-NETs with mesenteric metastases and shows a good correlation with radiological assessment of mesenteric fibrosis.²⁶

FIGURE 1. Typical examples of mesenteric fibrosis

A. Coronal CT image showing typical mesenteric fibrosis as radiating strands of soft tissue surrounding a metastatic mesenteric mass (asterisk). **B.** Photomicrograph of hematoxylin and eosin stained whole section of a metastatic mesenteric node showing extensive areas of fibrotic tissue surrounding tumor cells. Scale 5 mm.

Prognostic factors

There is a lack of predictors of development of mesenteric fibrosis. There is a co-occurrence of mesenteric fibrosis with increased 5-HIAA excretion and other SI-NETs specific complications as carcinoid syndrome and carcinoid heart disease.^{25, 28} However, this association has not been found in all studies.²⁰ Also, it is unclear if increased 5-HIAA excretion is independently associated with mesenteric fibrosis or correlated with other disease characteristics such as disease stage or tumor burden.^{20, 25, 28} In order to potentially find more or better predictors of mesenteric metastases and fibrosis, we analyzed patient and disease characteristics in a large cohort of SI-NET patients for predictors of mesenteric metastases and fibrosis (**Chapter 3**).

Pathogenesis of mesenteric fibrosis

In order to find better prognostic factors and treatment options, it is important to understand pathogenesis of SI-NET-associated mesenteric fibrosis. SI-NETs arise from enterochromaffin cells in the intestinal tract and often retain the ability to secrete bioactive amines and peptides.^{4, 69} As SI-NET-associated fibrosis can occur both locally around a tumor location and at a distance as in case of carcinoid heart disease, the secretion of the bioactive molecules has been early on implicated in the development of fibrosis⁶⁹.

Serotonin

As enterochromaffin cells are the main source of peripheral serotonin (5-hydroxytryptamine; 5-HT) and SI-NETs are known to have increased serotonin production, serotonin was considered as the causal agent of fibrosis.^{57, 70, 71} Serotonin promotes fibrosis by stimulating myofibroblastic proliferation and inducing expression of fibrogenic factors such as transforming growth factor beta (TGF β).⁵⁷ Development of fibrotic complications by drugs such as methysergide and cabergoline confirmed the profibrotic effects of serotonin signalling.⁷² These drugs can function as 5-HT_{2B} receptor agonist and are known to induce retroperitoneal fibrosis (methysergide) and heart valve fibrosis (cabergoline).^{73, 74}

The mitogenic and profibrotic potential of serotonin has also been shown in SI-NETs. In KRJ-I cells, a small intestinal enterochromaffin cell-derived NET cell line, serotonin stimulation increased proliferation, which could be reversed by ketanserin, a 5-HT_{2A/C} receptor antagonist.⁷⁵ Also, a 5-HT_{2B} receptor antagonist resulted in decreased viability of KRJ-I cells and reduced secretion of serotonin and the profibrotic growth factors; TGF β , connective tissue growth factor (CTGF) and basic fibroblast growth factor (FGF2).⁵⁸

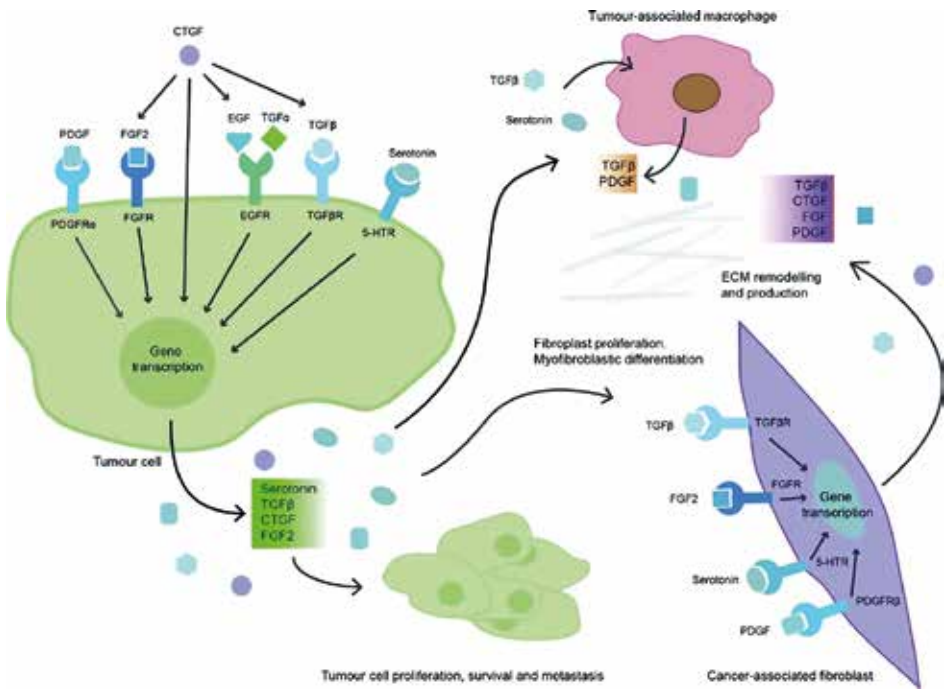
Even though serotonin seems to be the main driver of SI-NET-associated fibrotic complications, the mechanistic pathways are not fully elucidated. First, it is unclear why certain locations, i.e. heart valves and mesentery, are more susceptible to the profibrotic effect of serotonin. Second, serotonin production by tumor cells as measured by 5-HIAA levels is a poor predictor for the individual risk of mesenteric fibrosis development.^{5, 76}

Thus, the fibrotic potential of serotonin seems to differ both between different tissues and individual patients. This could be due to alternations in the tryptohan metabolism. This pathway is involved in the formation and degradation of serotonin.⁷⁷ A decrease in rate of degradation of serotonin could result in prolonged effect of serotonin in the tumor microenvironment. In **Chapter 6**, we explored if differences in the tryptophan metabolism in tumor cells or surrounding stroma could be linked to differences in profibrotic potential of serotonin.

Growth factors

Next to serotonin, various growth factors have been described to have a profibrotic effect in SI-NETs. Growth factors regulate cell proliferation and differentiation by a combination of autocrine and paracrine signalling. TGF β , CTGF, FGF2 and platelet-derived growth factor (PDGF) have all been implicated in SI-NET-associated fibrogenesis (**Figure 2**).

The TGF β family of cytokines is a pivotal regulator of proliferative and profibrotic processes. The cellular effects of TGF β signalling are mediated via SMAD pathway. TGF β signalling has a dual role with on the one hand antitumor and antiproliferative effects in physiological and early neoplastic conditions, and on the other hand, protumorigenic effects such as proliferation and invasion in later stages of malignant disease. Also, it stimulates stromal cells to induce myofibroblastic differentiation and altered extracellular matrix (ECM) production. Once differentiated to myofibroblast, these cells secrete TGF β creating a self-sustained, profibrotic feedback loop.^{78, 79} Due to its profibrotic and tumorigenic effects, TGF β is one of the most extensively studied growth factors in SI-NETs. SI-NETs express both TGF β transcripts and receptors.⁸⁰⁻⁸² *In vitro*, the dual role of TGF β signalling on proliferation during tumorigenesis has been demonstrated as proliferation is stimulated by TGF β in KRJ-I cells and inhibited in normal enterochromaffin cells.⁸³ The profibrotic effects are also demonstrated *in vitro*. Medium conditioned by BON1 cells, a pancreatic NET cell line, induced TGF β -mediated proliferation of fibroblasts. Furthermore, TGF β stimulation increased production of TGF β by these fibroblasts, confirming a positive autocrine feedback loop.⁸⁴ TGF β signalling is further implicated as an important regulator of SI-NET tumorigenesis as in a series of 48 SI-NETs, 22 had mutations or deletions in *SMAD* genes.⁸⁵

FIGURE 2. Development of mesenteric fibrosis in SI-NETs

Interactions of profibrotic growth factors within the tumor microenvironment, which consists among others of tumor cells, fibroblasts, immune cells and extracellular matrix (ECM). 5-HT_R, serotonin receptor; CTGF, connective tissue growth factor; EGF, epidermal growth factor; EGFR, epidermal growth factor receptor; FGF2, basic fibroblast growth factor; FGFR, fibroblast growth factor receptor; PDGF, platelet-derived growth factor; PDGFR, platelet-derived growth factor receptor; TGF α , transforming growth factor alpha; TGF β , transforming growth factor beta; TGF β R, transforming growth factor beta receptor.

CTGF is involved in the coordination of various biological processes including tissue repair and fibrosis. Although CTGF can influence cell processes independently, it acts mainly by modifying signalling of other molecules. CTGF enhances profibrotic actions of TGF β and FGF2 by increasing collagen synthesis, fibroblast proliferation and differentiation into myofibroblasts.⁸⁶ SI-NETs have a high expression of CTGF compared to other neuroendocrine tumors, especially fibrotic SI-NETs. Immunoreactivity for CTGF was strongest in SI-NET cells adjacent to fibrovascular stroma, suggesting a profibrotic effect at the tumor invasion border.^{87, 88}

FGF2 is an important regulator of wound healing and is known to have a strong mitogenic effect on fibroblasts. It can be induced by TGF β and is linked to several fibrotic disorders.⁴⁴ Its role in cancer is less obvious. FGF2 is suggested to have anti-apoptotic, proliferative effects on tumor cells and to stimulate angiogenesis. Conversely, other studies have shown that in some conditions, FGF2 has a tumor suppressive role, making it a complex signalling factor to investigate.⁸⁹ Studies performed on SI-NETs demonstrated positive IHC staining for FGF2 and FGF receptors in most SI-NETs and adjacent stroma.⁹⁰⁻⁹² However, there was no correlation of FGF2 expression in SI-NETs and mesenteric fibrosis.⁹¹

PDGF is released in response to tissue injury, and it is shown to be involved in multiple fibrotic diseases such as scleroderma, intestinal fibrosis in Crohn's disease and renal fibrosis.⁹³ Next to a proliferative effect on fibroblasts, PDGF can also induce proliferation of epithelial cancer cells.⁴⁴ The profibrotic effects of PDGF are mediated by binding to the PDGF α - and β -receptors. Expression of the receptors can be induced by diverse factors, such as TGF β , and upregulation of both receptors is found in many fibrotic diseases, although it depends on the involved tissue which of the PDGF receptors is predominantly upregulated.⁹³

In SI-NETs both the PDGF α - and β -receptors are present, albeit at different location within the tumor microenvironment. Expression of PDGF and PDGF α -receptor was found in the majority of SI-NET tumor cells with limited focal staining in the stroma surrounding positive tumor cells. Conversely, expression PDGF β -receptor was selectively found in stromal cells, especially adjacent to tumor cells. The PDGF β -receptor positive cells showed frequently a fibroblastic morphology with muscle actin antigen positivity, suggesting an activated phenotype characteristic of cancer-associated fibroblasts⁹⁰. Moreover, PDGF β -receptor immunoreactivity was more prevalent in metastases and associated with the presence of macrophages^{94, 95}. Increased expression of PDGF β -receptor on the invasive border and in metastases, links PDGF signalling to metastatic potential. An important role for PDGF signalling in SI-NET tumorigenesis is further suggested by the finding that 20% of SI-NETs show copy number gains of *PDGFR*, suggesting augmented activation of this pathway in a subset of SI-NETs.⁸⁵

Tumor microenvironment (TME)

The TME consists of immune cells, fibroblasts, capillaries, basement membrane and ECM. This network of cells has intricate interactions and is crucial for tumor growth, invasion and metastasis. The TME also shows many commonalities with chronic wound healing that results in fibrosis.^{44,96} Therefore, understanding the SI-NET TME is crucial in order to decipher the pathogenesis of SI-NET-associated fibrosis. The tumor stroma of SI-NETs differs from other cancers with a characteristic desmoplastic reaction as it has limited leukocytic infiltration.^{26, 91, 95} The sparsely found leukocytes are mostly macrophages, as identified by Leu M5 antibody staining.^{94, 95} These macrophages also stained strongly for TGF β and PDGF, suggesting a polarized, tumor-associated macrophage phenotype, which is associated with cancer-promoting effects.^{95,97}

Fibroblasts are the dominant cellular component of the tumor stroma, next to tumor cells. The majority of these fibroblasts have a modified phenotype, similar to fibroblasts during wound healing. These cancer-associated fibroblasts (CAFs) are identified by expression of α -smooth muscle actin (α SMA) and are able to proliferate, produce growth factors and ECM.⁹⁸ Compared to other neuroendocrine tumors, SI-NETs have a high expression of α SMA in the fibroblast component of the TME both in primary tumors and metastases.^{87, 88, 92} Further evidence on the presence of these activated fibroblasts in SI-NETs was detected in primary cultures in which cells from the tumor stroma developed the typical stellate shape of CAFs and increased growth factor transcription after stimulation TGF β .⁸⁷

The ECM is another important constituent of the TME. Next to giving structural support, it is providing biochemical and biomechanical cues necessary for tissue homeostasis. Remodelling of the ECM has been shown to be important both in fibrotic and neoplastic diseases.⁹⁹ Mechanical stress has been shown to induce release of signalling molecules such as serotonin in normal enterochromaffin and NET tumor cells.^{100,101} Thus, changes in ECM composition might influence tumor functionality in SI-NETs by biochemical and biomechanical. Unfortunately, little is known about the specific composition and changes in the ECM of SI-NETs. Therefore, we analysed in **Chapter 7** the stroma and tumor proteome of SI-NETs and assessed the differences between patients with and without mesenteric fibrosis.

Management of mesenteric fibrosis

Surgery

In contrast to the significant improvements in treatment options for disease progression and hormonal secretion symptoms, the mainstay of treatment for complications due to mesenteric metastases and fibrosis remains limited to intestinal resection or bypass.^{6, 21} In distant disease, the current European Neuroendocrine Tumor Society (ENETS) guideline advises to consider prophylactic palliative surgery in SI-NET patients with mesenteric metastases. However, improved overall outcome has not been reproducible in all studies.⁴ To address the question if there is a role for prophylactic palliative surgery in SI-NETs, we compared the effect of prophylactic palliative surgery to symptomatic palliative surgery or no surgery on overall survival (**Chapter 3**).

Moreover, not all patients with mesenteric metastases and fibrosis develop abdominal complications, approximately 30-50% of patients with mesenteric disease are asymptomatic.^{25, 29} Nonetheless, it has been suggested that a certain subsets of these asymptomatic patients might benefit from early, preventive surgical intervention.^{30, 31} However, there is currently no method to identify these patients. The radiological severity of mesenteric fibrosis is not associated with survival or hospitalisation for fibrotic complications.¹⁸ In search of a prediction model for development of symptomatic fibrotic disease, we analyzed asymptomatic and symptomatic SI-NET patients with mesenteric metastases with multiple techniques including CT-based radiomics models (**Chapter 4**).

Somatostatin analogues (SSAs)

SSAs are first-line therapy with proven efficacy on tumor growth control and reduction of carcinoid syndrome symptoms.⁶ Treatment with SSAs also reduced secretion of tumor related metabolites such as 5-HIAA.³² However, complete biochemical response occurs only in a minority of patients treated with SSAs.³² Since increased urinary 5-HIAA excretion is associated with mesenteric fibrosis, effective reduction could attenuate the risk of fibrosis development. Moreover, SSAs are known to attenuate fibrosis in other diseases such as peritoneal sclerosis, pulmonary and liver fibrosis.³³⁻³⁵ However, the effect of SSAs on mesenteric fibrosis, prevention or treatment, has not been examined.

Interferon-alpha (IFN-alpha)

Next to SSAs, IFN-alpha is an established therapy for SI-NETs. IFN-alpha has immunoregulatory, antifibrotic and antiproliferative actions.³⁶ In SI-NETs, IFN-alpha has proven symptomatic and antiproliferative efficacy.⁶ As IFN-alpha has also antifibrotic effects and is used as treatment for fibrotic skin diseases, it could have a role in the treatment of mesenteric fibrosis.³⁶ However, the side-effects of flu-like symptoms and chronic fatigue, preclude a widespread use in SI-NETs and there is no data on the effect of mesenteric fibrosis.

Molecular targeted therapies

Everolimus is a mechanistic target of rapamycin (mTOR) inhibitor. The mTOR signalling network plays a pivotal role in regulating cell growth and metabolism and deregulation is described in neuroendocrine tumors.^{37, 38} A small retrospective study showed the everolimus therapy caused a reduction in common carcinoid syndrome symptoms such as diarrhea and flushing.^{39, 40} However, clinical use is often limited due to treatment resistance, both primary and acquired, and the toxicity profile.^{6, 38} The effect of everolimus on SI-NET-associated mesenteric fibrosis is unknown and as everolimus has been described both as a potential profibrotic and antifibrotic agent it is difficult to predict⁴¹⁻⁴³.

Tyrosine kinases consist of a large family of enzymes that are important mediators of cellular signal transduction and are involved in tumori- and fibrogenesis.⁴⁴ Targeting these signalling pathways by tyrosine kinase inhibitors (TKIs) might therefore be efficient in reducing SI-NET progression and the development of fibrotic complications. Unfortunately, the efficacy of TKIs in SI-NETs on tumor growth suppression is not demonstrated and is accompanied by significant toxicity.⁴⁵⁻⁴⁸ While the focus in neuroendocrine tumors has been on inhibition of angiogenesis by targeting enzymes such as vascular endothelial growth factor (VEGF), research on fibrotic disease such as scleroderma focuses on TKIs targeting c-abl kinases and PDGF receptors. By blocking these kinases, important profibrotic signalling molecules such as TGF β are reduced.⁴⁹ Imatinib, a TKI that targets c-abl kinases and PDGF receptors, showed decreased organ fibrosis in patients with scleroderma and pulmonary fibrosis.⁴⁹ Since the signalling

pathways involved in the development of fibrosis in SI-NETs are similar to other fibrotic diseases, the use of TKIs in SI-NETs could be extended beyond tumor growth control and also be evaluated as antifibrotic therapy.

Peptide Receptor Radionuclide Therapy (PRRT)

PRRT with radiolabelled somatostatin analogs is an effective treatment for SI-NETs that improves progression-free survival and reduces carcinoid syndrome symptoms.^{8, 50} However, radiolabelled peptides induce tissue inflammation at delivery that could result in increased fibrogenesis. Recently, two studies showed that a small percentage of patients, approximately 5%, developed obstructive complications during PRRT treatment. Interestingly, all these patients had both peritoneal and mesenteric metastasized disease.^{51, 52} Thus there seems to be an increased risk for fibrotic complications during PRRT treatment. On the other hand, a reduction in mesenteric tumor volume could result in decreased symptoms. In the NETTER-1 trial on PRRT in SI-NETs, 18% of the patients had an objective response according to Response Evaluation Criteria in Solid Tumors (RECIST).⁸ However, there was no data available on the response of mesenteric disease. Therefore, we assessed the rate of objective response of PRRT on mesenteric disease (**Chapter 2**).

Serotonin Synthesis Inhibitors and 5-HT Receptor Antagonists

As described above, serotonin is considered the main driver of SI-NET-associated fibrosis. Therefore, it has been implied that inhibition of peripheral serotonin synthesis and signalling could be effective in preventing SI-NET-associated fibrotic complications. The first attempts to block peripheral serotonin synthesis aimed at inhibiting 5-hydroxytryptophan decarboxylation. These drugs had a moderate effect on decreasing serotonin production and side effects limited their clinical use.^{53, 54} The next step was to inhibit tryptophan hydroxylase (THP). Using para-chlorophenylalanine (PCPA), serotonin production and carcinoid syndrome symptoms could be reduced. However, the therapeutic use was precluded by the psychiatric side effects.⁵⁵ The search for THP inhibitors that primarily inhibit peripheral serotonin synthesis finally resulted in the development of telotristat ethyl. Treatment of SI-NETs patients with telotristat ethyl resulted in significant reduction

1 of urinary 5-HIAA levels and diarrhea frequency.⁵⁶ However, to date there is no evidence of an effect of SI-NET-associated fibrotic complications.

Next to inhibition of serotonin synthesis, targeting 5-HT receptors can modify serotonin signalling. As the profibrotic effects of serotonin seem to be mainly mediated via the 5-HT_{1A/B} and 5-HT_{2A/B} receptors, drugs targeting these receptors should be considered for antifibrotic treatment.⁵⁷⁻⁵⁸ Non-selective 5-HT₂ receptor antagonists such as cyproheptadine and ketanserin were found to be able to reduce carcinoid syndrome symptoms such as flushing and diarrhea. However, due to the modest effects compared to SSAs and serious adverse effect of ketanserin, the clinical utility of these drugs is limited.^{59,60} Yet, advancements have been made with new potential antifibrotic agents. Terguride, a 5-HT_{2A/B} receptor antagonist, is proven to reduce the profibrotic effects of serotonin in animals.⁶¹ Furthermore, in a phase II study in scleroderma patients it was well tolerated and resulted in amelioration of the skin fibrosis.⁶² Even though more research is needed to establish the effect of terguride on SI-NET-associated fibrosis, it sparks hope for a potent, well-tolerated anti-fibrotic therapy.

Tamoxifen

Tamoxifen is another antifibrotic agent used in fibrotic diseases such as desmoid tumors and retroperitoneal fibrosis.⁶³ Tamoxifen is a synthetic nonsteroidal selective oestrogen receptor modulator, developed for the treatment of breast cancer. The antifibrotic effect seems to be mediated by an inhibitory effect of tamoxifen on TGF β secretion by fibroblasts.⁶⁴ Tamoxifen has also been used in SI-NETs for tumor growth control and amelioration of carcinoid syndrome symptoms with varying success.⁶⁵⁻⁶⁸ However, better patient selection and focus on the antifibrotic effects might establish tamoxifen as a treatment option for fibrotic complications of SI-NETs.

Aim and outline of this thesis

Since the development of a variety of palliative treatments, the survival of patients with metastasized SI-NETs has improved. As a result, morbidity caused by mesenteric metastases and fibrosis in combination with the lack of therapeutic options have become major issues for SI-NET management. In order to improve care for SI-NET patients, it is important to understand the effect of current treatments on mesenteric metastases and fibrosis. Also, it is important to find new effective treatment options. For this it is key to gain better insight in the processes involved in mesenteric metastases and fibrosis. The aim of this thesis is to address both issues.

In **Chapter 2**, we evaluated the development and growth of mesenteric metastases and fibrosis over time in this new era of targeted therapy. This includes the effect of PRRT on mesenteric disease.

Chapter 3 reviews the results on prophylactic palliative surgery in patients with advanced SI-NETs compared to symptomatic palliative surgery or no surgery.

In **Chapter 4**, we evaluated clinical characteristics and CT imaging in order to find predictors for development of symptomatic mesenteric metastases. We used both systematic evaluation by clinicians and a radiomics approach.

Chapter 5 describes the differences between male and female SI-NETs patients and investigates possible mechanisms inducing sexual dimorphism by analysing sex steroid receptors.

Chapter 6 examines the tryptophan metabolism pathway in primary SI-NETs and mesenteric metastases with and without fibrosis.

In **Chapter 7**, the proteome of primary SI-NETs and paired mesenteric metastases is studied and the differences between patients with and without mesenteric fibrosis are evaluated.

Funding

This work was supported by an unrestricted fund of IPSEN.

References

1. Yao JC, Hassan M, Phan A, et al. One Hundred Years After “Carcinoid”: Epidemiology of and Prognostic Factors for Neuroendocrine Tumors in 35,825 Cases in the United States. *Journal of Clinical Oncology*. 2008;26(18):3063-3072. doi:10.1200/jco.2007.15.4377
2. Dasari A, Shen C, Halperin D, et al. Trends in the Incidence, Prevalence, and Survival Outcomes in Patients With Neuroendocrine Tumors in the United States. *JAMA Oncol*. Oct 1 2017;3(10):1335-1342.
3. Hallet J, Law CHL, Cukier M, Saskin R, Liu N, Singh S. Exploring the rising incidence of neuroendocrine tumors: A population-based analysis of epidemiology, metastatic presentation, and outcomes. *Cancer*. 2015;121(4):589-597. doi:10.1002/cncr.29099
4. Niederle B, Pape UF, Costa F, et al. ENETS Consensus Guidelines Update for Neuroendocrine Neoplasms of the Jejunum and Ileum. *Neuroendocrinology*. 2016;103(2):125-38.
5. Blazevic A, Zandee WT, Franssen GJH, et al. Mesenteric fibrosis and palliative surgery in small intestinal neuroendocrine tumours. *Endocr Relat Cancer*. Mar 2018;25(3):245-254.
6. Pavel M, O’Toole D, Costa F, et al. ENETS Consensus Guidelines Update for the Management of Distant Metastatic Disease of Intestinal, Pancreatic, Bronchial Neuroendocrine Neoplasms (NEN) and NEN of Unknown Primary Site. *Neuroendocrinology*. 2016;103(2):172-85.
7. Lawrence B, Gustafsson BI, Chan A, Svejda B, Kidd M, Modlin IM. The Epidemiology of Gastroenteropancreatic Neuroendocrine Tumors. *Endocrinol Metab Clin North Am*. 2011/03/01/2011;40(1):1-18. doi:https://doi.org/10.1016/j.ecl.2010.12.005
8. Strosberg J, El-Haddad G, Wolin E, et al. Phase 3 Trial of (177)Lu-Dotatate for Midgut Neuroendocrine Tumors. *N Engl J Med*. Jan 12 2017;376(2):125-135.
9. Zandee WT, Kamp K, van Adrichem RCS, Feelders RA, de Herder WW. Limited value for urinary 5-HIAA excretion as prognostic marker in gastrointestinal neuroendocrine tumours. *Eur J Endocrinol*. 2016/11// 2016;175(5):361-366. doi:10.1530/eje-16-0392
10. Rossi RE, Ciafardini C, Sciola V, Conte D, Massironi S. Chromogranin A in the Follow-up of Gastroenteropancreatic Neuroendocrine Neoplasms: Is It Really Game Over? A Systematic Review and Meta-analysis. *Pancreas*. Nov/Dec 2018;47(10):1249-1255.
11. Hofland J, Zandee WT, de Herder WW. Role of biomarker tests for diagnosis of neuroendocrine tumours. *Nature Reviews Endocrinology*. 2018/11/01 2018;14(11):656-669. doi:10.1038/s41574-018-0082-5

12. Modlin IM, Drozdov I, Kidd M. The identification of gut neuroendocrine tumor disease by multiple synchronous transcript analysis in blood. *PLoS One*. 2013;8(5):e63364.
13. Modlin IM, Kidd M, Malczewska A, et al. The NETest: The Clinical Utility of Multigene Blood Analysis in the Diagnosis and Management of Neuroendocrine Tumors. *Endocrinol Metab Clin North Am*. Sep 2018;47(3):485-504.
14. van Treijen MJC, van der Zee D, Heeres BC, et al. Blood Molecular Genomic Analysis Predicts the Disease Course of Gastroenteropancreatic Neuroendocrine Tumor Patients: A Validation Study of the Predictive Value of the NETest®. *Neuroendocrinology*. 2020;doi:10.1159/000509091
15. Pearman TP, Beaumont JL, Cella D, Neary MP, Yao J. Health-related quality of life in patients with neuroendocrine tumors: an investigation of treatment type, disease status, and symptom burden. *Supportive Care in Cancer*. 2016/09/01 2016;24(9):3695-3703. doi:10.1007/s00520-016-3189-z
16. Halperin DM, Shen C, Dasari A, et al. Frequency of carcinoid syndrome at neuroendocrine tumour diagnosis: a population-based study. *Lancet Oncology*. 2017;18:525-534. doi:10.1016/S1470-2045(17)30110-9
17. Zandee WT, de Herder WW, Jann H. Incidence and prognosis of carcinoid syndrome: hormones or tumour burden? *The Lancet Oncology*. 2017/06/01/ 2017;18(6):e299. doi:https://doi.org/10.1016/S1470-2045(17)30335-2
18. Laskaratos FM, Diamantopoulos L, Walker M, et al. Prognostic Factors for Survival among Patients with Small Bowel Neuroendocrine Tumours Associated with Mesenteric Desmoplasia. *Neuroendocrinology*. 2018;106(4):366-380. doi:10.1159/000486097
19. Makridis C, Oberg K, Juhlin C, et al. Surgical treatment of mid-gut carcinoid tumors. *World J Surg*. May-Jun 1990;14(3):377-83; discussion 384-5.
20. Druce MR, Bharwani N, Akker SA, Drake WM, Rockall A, Grossman AB. Intra-abdominal fibrosis in a recent cohort of patients with neuroendocrine ('carcinoid') tumours of the small bowel. *QJM*. 2010;103(3):177-185. doi:10.1093/qjmed/hcp191
21. Howe JR, Cardona K, Fraker DL, et al. The Surgical Management of Small Bowel Neuroendocrine Tumors: Consensus Guidelines of the North American Neuroendocrine Tumor Society. *Pancreas*. 2017;46(6):715-731. doi:10.1097/mpa.0000000000000846
22. Modlin IM, Gustafsson BI, Pavel M, Svejda B, Lawrence B, Kidd M. A Nomogram to Assess Small-Intestinal Neuroendocrine Tumor ('Carcinoid') Survival. *Neuroendocrinology*. 2010;92(3):143-157. doi:10.1159/000319784

23. Makridis C, Ekblom A, Bring J, et al. Survival and daily physical activity in patients treated for advanced midgut carcinoid tumors. *Surgery. Dec* 1997;122(6):1075-82.
24. Makridis C, Rastad J, Oberg K, Akerström G. Progression of metastases and symptom improvement from laparotomy in midgut carcinoid tumors. *World J Surg. Sep* 1996;20(7):900-6; discussion 907.
25. Laskaratos FM, Walker M, Wilkins D, et al. Evaluation of Clinical Prognostic Factors and Further Delineation of the Effect of Mesenteric Fibrosis on Survival in Advanced Midgut Neuroendocrine Tumours. *Neuroendocrinology. 2018*;107(3):292-304.
26. Pantongrag-Brown L, Buetow PC, Carr NJ, Lichtenstein JE, Buck JL. Calcification and fibrosis in mesenteric carcinoid tumor: CT findings and pathologic correlation. *AJR Am J Roentgenol. Feb* 1995;164(2):387-91.
27. Laskaratos F-M, Mandair D, Hall A, et al. Clinicopathological correlations of mesenteric fibrosis and evaluation of a novel biomarker for fibrosis detection in small bowel neuroendocrine neoplasms. *Endocrine. 2020*;67(3):718-726. doi:10.1007/s12020-019-02107-4
28. Rodríguez Laval V, Pavel M, Steffen IG, et al. Mesenteric Fibrosis in Midgut Neuroendocrine Tumors: Functionality and Radiological Features. *Neuroendocrinology. 2018*;106(2):139-147.
29. Daskalakis K, Karakatsanis A, Hessman O, et al. Association of a Prophylactic Surgical Approach to Stage IV Small Intestinal Neuroendocrine Tumors With Survival. *JAMA Oncol. Feb 1* 2018;4(2):183-189.
30. Wu L, Fu J, Wan L, et al. Survival outcomes and surgical intervention of small intestinal neuroendocrine tumors: a population based retrospective study. *Oncotarget. Jan 17* 2017;8(3):4935-4947.
31. Daskalakis K, Tsolakis AV. Upfront surgery of small intestinal neuroendocrine tumors. Time to reconsider? *World J Gastroenterol. Aug 7* 2018;24(29):3201-3203.
32. Modlin IM, Pavel M, Kidd M, Gustafsson BI. Review article: somatostatin analogues in the treatment of gastroenteropancreatic neuroendocrine (carcinoid) tumours. *Alimentary Pharmacology & Therapeutics. 2010*;31(2):169-188. doi:https://doi.org/10.1111/j.1365-2036.2009.04174.x
33. Lang A, Sakhmini E, Fidler HH, Maor Y, Bar-Meir S, Chowers Y. Somatostatin inhibits pro-inflammatory cytokine secretion from rat hepatic stellate cells. *Liver International. 2005*;25:808-816. doi:10.1111/j.1478-3231.2005.01057.x

34. Ertilav M, Hur E, Bozkurt D, et al. Octreotide lessens peritoneal injury in experimental encapsulated peritoneal sclerosis model. *Nephrology*. 2011;16:552-557. doi:10.1111/j.1440-1797.2011.01460.x
35. Borie R, Fabre A, Prost F, et al. Activation of somatostatin receptors attenuates pulmonary fibrosis. *Thorax*. 2008;63:251-258. doi:10.1136/thx.2007.078006
36. Granstein RD, Flotte TJ, Amento EP. Interferons and Collagen Production. *Journal of Investigative Dermatology*. 1990/12/01/ 1990;95(6, Supplement):S75-S80. doi:https://doi.org/10.1111/1523-1747.ep12874789
37. Saxton RA, Sabatini DM. mTOR Signaling in Growth, Metabolism, and Disease. *Cell*. 2017/03/09/ 2017;168(6):960-976. doi:https://doi.org/10.1016/j.cell.2017.02.004
38. Beyens M, Vandamme T, Peeters M, Van Camp G, Op de Beeck K. Resistance to targeted treatment of gastroenteropancreatic neuroendocrine tumors. *Endocr Relat Cancer*. 01 Mar. 2019 2019;26(3):R109-R130. doi:10.1530/erc-18-0420
39. Bainbridge HE, Larbi E, Middleton G. Symptomatic Control of Neuroendocrine Tumours with Everolimus. *Horm Cancer*. Dec 2015;6(5-6):254-9.
40. Pavel ME, Hainsworth JD, Baudin E, et al. Everolimus plus octreotide long-acting repeatable for the treatment of advanced neuroendocrine tumours associated with carcinoid syndrome (RADIANT-2): a randomised, placebo-controlled, phase 3 study. *Lancet*. Dec 10 2011;378(9808):2005-2012.
41. Eren ME, Ay Eren A, Sayan M, et al. The Impact of Everolimus and Radiation Therapy on Pulmonary Fibrosis. *Medicina (Kaunas)*. Jul 13 2020;56(7)
42. Masola V, Carraro A, Zaza G, et al. Epithelial to mesenchymal transition in the liver field: the double face of Everolimus in vitro. *BMC Gastroenterol*. Sep 14 2015;15:118.
43. Patsenker E, Schneider V, Ledermann M, et al. Potent antifibrotic activity of mTOR inhibitors sirolimus and everolimus but not of cyclosporine A and tacrolimus in experimental liver fibrosis. *J Hepatol*. Aug 2011;55(2):388-98.
44. Rybinski B, Franco-Barraza J, Cukierman E. The wound healing, chronic fibrosis, and cancer progression triad. doi: 10.1152/physiolgenomics.00158.2013. *Physiological Genomics*. 2014/04/01 2014;46(7):223-244.
45. Chan JA, Mayer RJ, Jackson N, Malinowski P, Regan E, Kulke MH. Phase I study of sorafenib in combination with everolimus (RAD001) in patients with advanced neuroendocrine tumors. *Cancer Chemother Pharmacol*. May 2013;71(5):1241-6.

- 1
46. Kulke MH, Lenz HJ, Meropol NJ, et al. Activity of sunitinib in patients with advanced neuroendocrine tumors. *Journal of Clinical Oncology*. Jul 10 2008;26(20):3403-10.
 47. Phan AT, Yao JC, Fogelman DR, et al. A prospective, multi-institutional phase II study of GW786034 (pazopanib) and depot octreotide (sandostatin LAR) in advanced low-grade neuroendocrine carcinoma (LGNEC). *Journal of Clinical Oncology*. 2010;28:4001-4001. doi:10.1200/jco.2010.28.15_suppl.4001
 48. Hobday TJ, Rubin J, Holen K, et al. Mbib44h, a phase II trial of sorafenib in patients (pts) with metastatic neuroendocrine tumors (NET): A Phase II Consortium (P2C) study. *Journal of Clinical Oncology*. 2007;25:4504.
 49. Distler JH, Distler O. Tyrosine kinase inhibitors for the treatment of fibrotic diseases such as systemic sclerosis: towards molecular targeted therapies. *Annals of the Rheumatic Diseases*. 2010;69((Supplement 1)):i48-i51. doi:10.1136/ard.2009.120196)
 50. Zandee WT, Brabander T, Blažević A, et al. Peptide Receptor Radionuclide Therapy With ¹⁷⁷Lu-DOTATATE for Symptomatic Control of Refractory Carcinoid Syndrome. *J Clin Endocrinol Metab*. 2021;doi:10.1210/clinem/dgab289
 51. Strosberg JR, Al-Toubah T, Pellè E, et al. Risk of Bowel Obstruction in Patients with Mesenteric or Peritoneal Disease Receiving Peptide Receptor Radionuclide Therapy. *J Nucl Med*. Jan 2021;62(1):69-72.
 52. Wee CE, Dundar A, Eiring RA, et al. Bowel Obstruction as a Complication of Peptide Receptor Radionuclide Therapy (PRRT). *Journal of Nuclear Medicine*. 2021;jnumed.121.262048. doi:10.2967/jnumed.121.262048
 53. Sandler M, Close HG. Biochemical effect of phenylacetic acid in a patient with 5-hydroxytryptophan-secreting carcinoid tumor. *Lancet*. 1959;2:316-318.
 54. Sjoerdsma A, Oates JA, Zaltzman P, Udenfriend S. Serotonin synthesis in carcinoid patients. *N Engl J Med*. 1960;263:585-588. doi:10.1056/nejm196009222631204
 55. Engelman K, Lovenberg W, Sjoerdsma A. Inhibition of serotonin synthesis by para-chlorophenylalanine in patients with the carcinoid syndrome. *N Engl J Med*. 1967;277:1103-1108. doi:10.1056/nejm196711232772101
 56. Kulke MH, Horsch D, Caplin ME, et al. Telotristat ethyl, a tryptophan hydroxylase inhibitor for the treatment of carcinoid syndrome. *Journal of Clinical Oncology*. 2017;35:14-23. doi:10.1200/jco.2016.69.2780

57. Mann DA, Oakley F. Serotonin paracrine signaling in tissue fibrosis. *Biochimica et Biophysica Acta (BBA) - Molecular Basis of Disease*. 2013/07/01/ 2013;1832(7):905-910. doi:<https://doi.org/10.1016/j.bbadis.2012.09.009>
58. Svejda B, Kidd M, Giovinazzo F, et al. The 5-HT(2B) receptor plays a key regulatory role in both neuroendocrine tumor cell proliferation and the modulation of the fibroblast component of the neoplastic microenvironment. *Cancer*. Jun 15 2010;116(12):2902-12.
59. Robertson JIS. Carcinoid syndrome and serotonin: Therapeutic effects of ketanserin. *Cardiovascular Drugs and Therapy*. 1990;4:53-58. doi:10.1007/bf00053427
60. Moertel CG, Kvols LK, Rubin J. A study of cyproheptadine in the treatment of metastatic carcinoid tumor and the malignant carcinoid syndrome. *Cancer*. 1991;67:33-36. doi:10.1002/1097-0142(19910101)67:1<33::Aid-cncr2820670107>3.0.Co;2-e
61. Hauso Ø, Gustafsson BI, Loennechen JP, Stunes AK, Nordrum I, Waldum HL. Long-term serotonin effects in the rat are prevented by terguride. *Regulatory Peptides*. 2007;143:39-46. doi:10.1016/j.regpep.2007.02.009
62. Distler O, Maurer B, Vettori S, et al. OP0034 the serotonin receptor 2 inhibitor terguride has beneficial effects on skin fibrosis: results from a phase 2 proof of concept study. *Annals of the Rheumatic Diseases*. 2016;75:66-66.
63. van Bommel EF, Hendriksz TR, Huiskes AW, Zeegers AG. Brief communication: tamoxifen therapy for nonmalignant retroperitoneal fibrosis. *Ann Intern Med*. Jan 17 2006;144(2):101-6.
64. Mikulec AA, Hanasono MM, Lum J, Kadleck JM, Kita M, Koch R. Effect of tamoxifen on transforming growth factor β 1 production by keloid and fetal fibroblasts. *Archives of Facial Plastic Surgery*. 2001;3:111-114. doi:10.1001/archfaci.3.2.111
65. Stathopoulos GP, Karvountzis GG, Yiotis J. Tamoxifen in carcinoid syndrome. *N Engl J Med*. Jul 2 1981;305(1):52.
66. Myers CF, Ershler WB, Tannenbaum MA, Barth R. Tamoxifen and Carcinoid Tumor. doi: 10.7326/0003-4819-96-3-383_1. *Annals of Internal Medicine*. 1982/03/01 1982;96(3):383-383. doi:10.7326/0003-4819-96-3-383_1
67. Moertel CG, Engstrom PF, Schutt AJ. Tamoxifen Therapy for Metastatic Carcinoid Tumor: A Negative Study. doi: 10.7326/0003-4819-100-4-531. *Annals of Internal Medicine*. 1984/04/01 1984;100(4):531-532.
68. Arganini M, Spinelli C, Cecchini GM, Miccoli P. Long term treatment with tamoxifen for metastatic carcinoid tumor. *Acta Chir Belg*. 1989 Jul-Aug 1989;89(4):209-211.

- 1
69. de Herder WW, Rehfeld JF, Kidd M, Modlin IM. A short history of neuroendocrine tumours and their peptide hormones. *Best Practice & Research Clinical Endocrinology & Metabolism*. 2016/01/01/ 2016;30(1):3-17. doi:<https://doi.org/10.1016/j.beem.2015.10.004>
 70. Mohammad-Zadeh LF, Moses L, Gwaltney-Brant SM. Serotonin: a review. *J Vet Pharmacol Ther*. Jun 2008;31(3):187-99.
 71. de Herder WW. Tumours of the midgut (jejunum, ileum and ascending colon, including carcinoid syndrome). *Best Practice and Research: Clinical Gastroenterology*. 2005;19:705-715. doi:10.1016/j.bpg.2005.05.007
 72. Eriksson B, Klöppel G, Krenning E, et al. Consensus guidelines for the management of patients with digestive neuroendocrine tumors--well-differentiated jejunal-ileal tumor/carcinoma. *Neuroendocrinology*. 2008;87(1):8-19.
 73. Reimund E. Methysergide and retroperitoneal fibrosis. *Lancet*. Feb 21 1987;1(8530):443.
 74. Antonini A, Poewe W. Fibrotic heart-valve reactions to dopamine-agonist treatment in Parkinson's disease. *Lancet Neurol*. Sep 2007;6(9):826-9.
 75. Drozdov I, Kidd M, Gustafsson BI, et al. Autoregulatory effects of serotonin on proliferation and signaling pathways in lung and small intestine neuroendocrine tumor cell lines. *Cancer*. 2009;115(21):4934-4945. doi:<https://doi.org/10.1002/cncr.24533>
 76. Koumariou A, Alexandraki KI, Wallin G, Kaltsas G, Daskalakis K. Pathogenesis and Clinical Management of Mesenteric Fibrosis in Small Intestinal Neuroendocrine Neoplasms: A Systematic Review. *J Clin Med*. Jun 8 2020;9(6)
 77. Roth W, Zadeh K, Vekariya R, Ge Y, Mohamadzadeh M. Tryptophan Metabolism and Gut-Brain Homeostasis. *International Journal of Molecular Sciences*. 2021;22(6):2973.
 78. Massague J. TGFbeta signalling in context. *Nature Reviews Molecular Cell Biology*. 2012;13:616-630. doi:10.1038/nrm3434
 79. Witsch E, Sela M, Yarden Y. Roles for growth factors in cancer progression. *Physiology*. 2010;25:85-101. doi:10.1152/physiol.00045.2009
 80. Chaudhry A, Oberg K, Gobl A, Heldin CH, Funa K. Expression of transforming growth factors β 1, β 2, β 3 in neuroendocrine tumors of the digestive system. *Anticancer Research*. 1994;14:2085-2091.
 81. Wimmel A, Wiedenmann B, Rosewicz S. Autocrine growth inhibition by transforming growth factor beta-1 (TGFbeta-1) in human neuroendocrine tumour cells. *Gut*. Sep 2003;52(9):1308-16.

82. Wulbrand U, Remmert G, Zöfel P, Wied M, Arnold R, Fehmann HC. mRNA expression patterns of insulin-like growth factor system components in human neuroendocrine tumours. *European Journal of Clinical Investigation*. 2000;30:729-739. doi:10.1046/j.1365-2362.2000.00700.x
83. Kidd M, Modlin IM, Pfragner R, et al. Small bowel carcinoid (enterochromaffin cell) neoplasia exhibits transforming growth factor-beta1-mediated regulatory abnormalities including up-regulation of C-Myc and MTA1. *Cancer*. 2007;109:2420-2431. doi:10.1002/cncr.22725
84. Beauchamp RD, Coffey RJ, Jr, Lyons RM, Perkett EA, Townsend CM, Jr, Moses HL. Human carcinoid cell production of paracrine growth factors that can stimulate fibroblast and endothelial cell growth. *Cancer Res*. Oct 1 1991;51(19):5253-60.
85. Banck MS, Kanwar R, Kulkarni AA, et al. The genomic landscape of small intestine neuroendocrine tumors. *The Journal of Clinical Investigation*. 2013;123(6):2502-2508. doi:10.1172/jci67963
86. Leask A, Abraham DJ. All in the CCN family: essential matricellular signaling modulators emerge from the bunker. *Journal of Cell Science*. 2006;119:4803-4810. doi:10.1242/jcs.03270
87. Kidd M, Modlin IM, Shapiro MD, et al. CTGF, intestinal stellate cells and carcinoid fibrogenesis. *World journal of gastroenterology*. 2007;13(39):5208-5216. doi:10.3748/wjg.v13.i39.5208
88. Cunningham JL, Tsolakis AV, Jacobson A, Janson ET. Connective tissue growth factor expression in endocrine tumors is associated with high stromal expression of α -smooth muscle actin. *Eur J Endocrinol*. 2010;163:691-697. doi:10.1530/eje-10-0420
89. Turner N, Grose R. Fibroblast growth factor signalling: from development to cancer. *Nature Reviews Cancer*. 2010;10:116-129. doi:10.1038/nrc2780
90. Chaudhry A, Funa K, Oberg K. Expression of growth factor peptides and their receptors in neuroendocrine tumors of the digestive system. *Acta Oncologica*. 1993;32:107-114. doi:10.3109/02841869309083898
91. Zhang PJ, Furth EE, Cai X, Goldblum JR, Pasha TL, Min KW. The role of β -catenin, TGF β 3, NGF2, FGF2, IGFR2, and BMP4 in the pathogenesis of mesenteric sclerosis and angiopathy in midgut carcinoids. *Human Pathology*. 2004/06/01/ 2004;35(6):670-674. doi:https://doi.org/10.1016/j.humpath.2003.12.010
92. Facco C, La Rosa S, Dionigi A, Uccella S, Riva C, Capella C. High expression of growth factors and growth factor receptors in ovarian metastases from ileal carcinoids. *Arch Pathol Lab Med*. 1998;122:828-832.

- 1
93. Bonner JC. Regulation of PDGF and its receptors in fibrotic diseases. *Cytokine and Growth Factor Reviews*. 2004;15:255-273. doi:10.1016/j.cytogfr.2004.03.006
 94. Funa K, Papanicolaou V, Juhlin C, et al. Expression of platelet-derived growth factor β -receptors on stromal tissue cells in human carcinoid tumors. *Cancer Research*. 1990;50:748-753.
 95. Chaudhry A, Papanicolaou V, Oberg K, Heldin CH, Funa K. Expression of platelet-derived growth factor and its receptors in neuroendocrine tumors of the digestive system. *Cancer Research*. 1992;52:1006-1012.
 96. Quail DE, Joyce JA. Microenvironmental regulation of tumor progression and metastasis. *Nature Medicine*. 2013;19:1423-1437. doi:10.1038/nm.3394
 97. Mantovani A, Allavena P, Sica A, Balkwill F. Cancer-related inflammation. *Nature*. 2008;454:436-444. doi:10.1038/nature07205
 98. Kalluri R. The biology and function of fibroblasts in cancer. *Nature Reviews Cancer*. 2016;16:582-598. doi:10.1038/nrc.2016.73
 99. Cox TR, Ertler JT. Remodeling and homeostasis of the extracellular matrix: implications for fibrotic diseases and cancer. *Disease Models and Mechanisms*. 2011;4:165-178. doi:10.1242/dmm.004077
 100. Chin A, Svejda B, Gustafsson BI, et al. The role of mechanical forces and adenosine in the regulation of intestinal enterochromaffin cell serotonin secretion. *American Journal of Physiology-Gastrointestinal and Liver Physiology*. 2012;302(3):G397-G405. doi:10.1152/ajpgi.00087.2011
 101. Linan-Rico A, Ochoa-Cortes F, Beyder A, et al. Mechanosensory signaling in enterochromaffin cells and 5-HT release: potential implications for gut inflammation. *Frontiers in Neuroscience*. 2016;10:564.



Chapter 2

Evolution of the mesenteric mass in small intestinal neuroendocrine tumors

2

Anela Blažević, Tessa Brabander, Wouter T. Zandee, Johannes Hofland, Gaston J. H. Franssen, Marie-Louise F. van Velthuysen, Richard A. Feelders and Wouter W. de Herder

Cancers 2021 Jan 25;13(3):443.

Simple Summary

Around two-thirds of patients with small intestinal neuroendocrine tumors present with a metastatic mesenteric mass. This mass is known to cause intestinal complications, however little is known on its development over time in the era of targeted therapy. Therefore, we conducted a retrospective study to assess the growth and response to therapy. We found that the growth of the mesenteric mass was detectable in 13.5% over a median time of 3.4 years and peptide receptor radionuclide therapy resulted in size reduction in only 3.8%. This site-specific static growth behavior is important to note when assessing disease progression and therapeutic options.

Abstract

Background: A metastatic mesenteric mass is a hallmark of small intestinal neuroendocrine tumors (SI-NETs). However, little is known on its development over time. Therefore, we conducted a study to assess the evolution of a SI-NET-associated mesenteric mass over time.

Methods: Retrospectively, 530 patients with proven SI-NET were included. The presence and growth of a mesenteric mass was assessed using RECIST 1.1 criteria on every consecutive CT scan until the end of follow-up or resection.

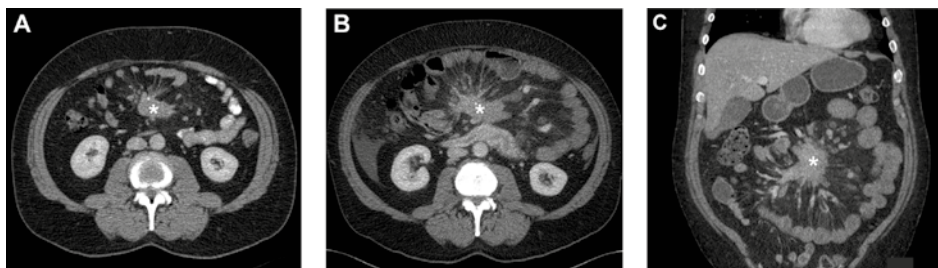
Results: At baseline, a mesenteric mass was present in 64% of the patients, of whom 13.5% showed growth of the mesenteric mass with a median time to growth of 40 months. Male gender was the only independent predictor of growth (OR 2.67). Of the patients without a mesenteric mass at the first evaluation, 2.6% developed a pathological mesenteric mass. Treatment with peptide receptor radionuclide therapy (PRRT; $n = 132$) resulted in an objective size reduction of the mesenteric mass in 3.8%.

Conclusion: The metastatic mesenteric mass in SI-NETs has a static behavior over time. Therefore, site-specific growth behavior should be taken into account when selecting target lesions and assessing disease progression and therapeutic response. PRRT appears not to be effective for size reduction of the mesenteric mass.

Introduction

Small intestinal neuroendocrine tumors (SI-NETs) are often diagnosed at an advanced stage with the mesentery being one of the dominant metastatic sites [1-3]. The metastatic mass is known to induce fibrosis in the surrounding mesentery (**Figure 1**) which can cause serious complications such as bowel obstruction and ischemia [1-5]. Even though the survival of patients with advanced SI-NETs has improved due to targeted treatment options such as somatostatin analogues (SSAs), everolimus and peptide receptor radionuclide therapy with ^{177}Lu -DOTATATE (PRRT), treatment options for intestinal complications due to mesenteric metastasis and fibrosis remain limited to primarily intestinal resection or bypass [1,5-7]. As a preventive treatment, the current European Neuroendocrine Tumor Society (ENETS) guideline advises to consider prophylactic palliative surgery in SI-NET patients with mesenteric metastasis [8]. However, not all patients develop abdominal complications, approximately 30% of patients with mesenteric disease are asymptomatic. Moreover, there is increasing evidence that prophylactic palliative resection of the primary tumor and mesenteric mass does not result in an overall improved outcome [2,9,10]. Currently, there is no method to identify patients with high risk of progressive mesenteric disease that may benefit from prophylactic palliative surgery. Increased knowledge on the clinical course of the SI-NET-associated mesenteric mass is essential in order to develop these criteria. Furthermore, understanding of the clinical course and factors associated with progressive disease could point to underlying pathways and aid the development of novel therapeutic options.

Therefore, the aim of this study was to obtain more insight in the clinical course of metastatic mesenteric masses in SI-NETs. To this end, we have used routinely obtained CT scans, and assessed the growth of the mesenteric mass over time and tried to identify patients at high risk for disease progression based on clinical criteria.

FIGURE 1. Metastatic mesenteric mass and surrounding fibrosis over time

(A) Transverse image of CT scan at baseline showing mesenteric mass (asterisk) with radiating strands of fibrotic tissue. Transverse (B) and coronal image (C) of CT scan after five year showing growth the mesenteric mass (asterisk) of > 20% on the short axis.

Methods

Patients

Patients from the NET-database, which encompassed all NET patients treated between 1993 and 2016 in the Erasmus Medical Center in Rotterdam, were included if they had proven SI-NET and at least 2 contrast-enhanced CT scans were available. As the study was retrospectively performed with anonymized data, according to the Central Committee on Research involving Human Subjects (CCMO) no approval from an ethics committee in the Netherlands was required. The disease characteristics and tumor markers were determined at the time of diagnosis or, if not available, the first measurement at our center was used. An extensive description of the methods used for tumor marker measurement was published previously ^[16]. To assess development over time, we divided the cohort based on date of diagnosis. The cut-offs were based on the publication data of the sequential ENETS guidelines resulting in 4 groups: < 2008 ($n = 188$), 2008 – 2012 ($n = 161$), 2012-2016 ($n = 150$), > 2016 ($n = 31$)^[8,17,18].

Imaging

Radiological features were assessed by means of contrast-enhanced CT. A mesenteric node of ≥ 10 mm on the short axis was considered a metastatic mass. Growth of the largest

mesenteric mass was assessed on all available CT scans in accordance with RECIST 1.1 criteria until the end of follow-up, significant growth of mesenteric mass or resection of mesenteric mass. Significant growth was determined if at least a 20% increase of the diameter of the short axis of the mesenteric mass was measured. In addition, the absolute increase needed to be at least 5 mm ^[19]. The effect of PRRT was evaluated until 12 months after the last cycle, also in accordance with RECIST 1.1 criteria. Both patients with complete response (CR; disappearance of all target and non-target lesions) and partial response (PR; at least a 30% decrease in the sum of diameters of targets lesion) were included in the objective response category ^[19]. Therefore, when assessing only the mesenteric mass, patients were considered to have an objective response if there was a disappearance of the mesenteric mass or decrease of at least 30% of the diameter on the short axis.

Statistics

SPSS software (version 21 for Windows, SPSS Inc.) was used to perform the analyses. Data were presented as median, range and IQR (25th–75th percentiles) or percentage with count. Continuous data were compared using the unpaired t-test, Mann-Whitney U test or ANOVA as appropriate. For post-hoc multiple comparison, the Dunnett's T3 test was used as equal variances were not assumed. The Fisher exact test was performed for comparison of categorical data. Odds ratios (OR) with a 95% confidence interval (CI) were determined using univariate and multivariate logistic regression. A *P*-value of < 0.05 was considered statistically significant.

Results

Patient Characteristics

From a cohort of 635 patients with SI-NETs, 530 patients had at least two accessible CT scans and were included for analysis. Of the excluded 105 patients with less than two accessible CT scans, 70 were once assessed and further follow-up was performed in another center, often outside the Netherlands, and 35 had no analyzable CT scans due to other reasons. Baseline characteristics are shown in **Table 1**. A mesenteric mass was

present in 64.2% of patients at baseline. The patients with mesenteric metastases were older, had a more advanced disease as expressed by the ENETS disease stage, presence of liver metastases and tumor marker levels. Additionally, there was a male predominance ($P \leq 0.001$).

Mesenteric Metastases Over Time

The evolution of the mesenteric metastases is shown in **Table 2**. In the overall group, 9.2% of patients showed the development or growth of the mesenteric mass. The median follow-up time was 34 months (range 1 – 186; interquartile range [IQR] 14 – 61). There was no significant difference in the follow-up time between patients with and without a mesenteric mass, and patients with and without growth. Patients with a mesenteric mass at baseline ($n = 340$), showed growth in 13.5% ($n = 46$) with a median time to growth of 40 months (range 4 – 134; IQR 15 – 61). In contrast, patients without a mesenteric mass at baseline ($n = 190$) rarely developed an objective mesenteric disease ($n = 5$, 2.6%) with an approximately equal time to development (range 7 – 113).

To obviate the bias induced by inclusion of patients at referral to a tertiary center after the initial surgical treatment, we performed a subgroup analysis of patients with a follow-up from before the first abdominal surgery and found no significant difference in the growth rate or time to growth (see Supplementary Materials).

Predictors of Growth

To find predictors of mesenteric mass growth, we analyzed patients with a mesenteric mass at baseline. Patients that underwent resection of the mesenteric mass ($n = 11$) had a significant shorter follow-up time compared to the overall follow-up time (median follow-up time 7 vs. 34 months, respectively, $P = 0.01$). As this follow-up was also notably shorter than the median time to growth of mesenteric masses (7 vs. 40 months, respectively), we excluded these patients from this analysis. To find predictors of growth, we performed the univariate analysis of the baseline patients and disease characteristics and the size of the mesenteric mass. We found male gender and tumor grade to be predictors of growth (**Table 3**). Other baseline characteristics such as age or tumor markers were not significantly associated with growth. When we combined the significant predictors in a multivariate model, only male gender remained an independent predictor of mesenteric mass growth.

TABLE 1. Characteristics

	All patients (n = 530)	Patients with mesenteric mass ≥ 10 mm (n = 340)	Patients without mesenteric mass ≥ 10 mm (n = 190)	P-Value
Patient Characteristics				
Age	60.3 (52.1-68.3)	61.6 (54.1-69.7)	57.1 (49.8-65.5)	<0.001
Male	53.2% (n = 282)	58.8% (n = 200)	43.2% (n = 82)	0.001
Disease Characteristics				
Tumor grade				0.105
Grade 1	50.0% (n = 265)	48.8% (n = 166)	52.1% (n = 99)	
Grade 2	26.4% (n = 140)	29.7% (n = 101)	20.5% (n = 39)	
Grade 3	2.1 % (n = 11)	1.8% (n = 6)	2.6% (n = 5)	
Missing	21.5% (n = 114)	19.7% (n = 67)	24.7% (n = 47)	
ENETS disease stage				< 0.001
Stage I / II	2.8% (n = 15)	0.6% (n = 2)	6.9% (n = 13)	
Stage III	20.9% (n = 111)	17.6% (n = 60)	26.8% (n = 51)	
Stage IV	75.8% (n = 402)	81.2% (n = 276)	66.3% (n = 126)	
Liver metastasis	71.1% (n = 377)	77.1% (n = 262)	60.5% (n = 115)	< 0.001
CgA (µg/L)	205.0 (90.5-748.5)	244.5 (109.5-826.0)	136.5 (63.0-546.3)	< 0.001
5-HIAA (µmol/24 h)	107.9 (42.4-439.2)	154.2 (63.4-519.0)	51.6 (24.8-241.4)	< 0.001
Treatments				
SSAs	82.8% (n = 439)	91.2% (n = 310)	67.9% (n = 129)	< 0.001
PRRT	44% (n = 233)	46.8% (n = 159)	38.9% (n = 74)	0.08
Surgery	70.6% (n = 374)	63.2% (n = 215)	83.7% (n = 159)	< 0.001
Curative	23.9% (n = 122)	14.2% (n = 48)	43.0% (n = 74)	
Palliative for symptom control	27.5% (n = 140)	26.6% (n = 90)	29.1% (n = 50)	
Prophylactic palliative	18.8% (n = 96)	18.9% (n = 64)	18.5% (n = 32)	
Indication not reported	3.1% (n = 16)	2.5% (n = 13)	1.7% (n = 1.7%)	

Numerical data are median with interquartile range in brackets. Categorical data are percentages with count in brackets. CgA: Serum chromogranin A, normal range < 94 µg/L, 5-HIAA: urinary 5-hydroxyindoleacetic acid excretion, normal range < 50 µmol /24 h

TABLE 2. Evolution of mesenteric mass over time.

	All patients (n = 530)	Patients with mesenteric mass ≥ 10 mm (n = 340)	Patients without mesenteric mass ≥ 10 mm (n = 190)	P-Value
No growth	88.3% (n = 468)	83.2% (n = 283)	97.4% (n = 185)	<0.001
Growth*	9.2% (n = 51)	13.5% (n = 46)	2.6% (n = 5)	
Resection	2.1% (n = 11)	3.2% (n = 11)	N/A	

*Growth assessed by RECIST 1.1 criteria and compared to the baseline CT scan. In case of mesenteric mass at baseline, growth is defined as increase of ≥ 20% and ≥ 5 mm on the short axis of the dominant mesenteric mass. In case of no mesenteric mass at baseline, growth is defined as development of a mesenteric node of ≥ 10 mm on the short axis.

TABLE 3. Predictors of growth in patients with mesenteric mass (n = 329)

	Univariate			Multivariate		
	OR	95% CI	P-Value	OR	95% CI	P-Value
Age	0.98	0.95 - 1.01	0.107	NS		
Male	2.15	1.06 - 4.32	0.033	2.67	1.19 - 5.99	0.017
Tumor grade						
Grade 1	Reference			Reference		
Grade 2	0.43	0.19 - 0.99	0.048	0.43	0.19 - 1.01	0.051
Grade 3	0.97	0.11 - 8.64	0.978	1.24	0.13-11.53	0.853
ENETS disease stage						
Stage I and II	Reference					
Stage III and IV	0.16	0.01 - 2.54	0.192	NS		
CgA (µg/L)	1.00	1.00 - 1.00	0.791	NS		
5-HIAA (µmol/24 h)	1.00	1.00 - 1.01	0.877	NS		
Liver metastasis	0.85	0.41 - 1.78	0.673	NS		
Mesenteric mass size (mm)	0.99	0.96 - 1.02	0.438	NS		

OR, odds ratio; 95% CI, 95% confidence interval; NS, non-significant in univariate analysis; CgA: Serum chromogranin A, normal range <94 µg/L; 5-HIAA, urinary 5-hydroxyindoleacetic acid excretion, normal range <50 µmol/24 h.

Received Treatments and Mesenteric Mass Growth

In our cohort, patients received SSAs in 82.8% and PRRT in 26.4% of cases as shown in **Table 1**. Patients with a mesenteric mass received more often SSAs, even when corrected for the ENETS disease stage (OR 3.87, 95% CI: 2.25-6.63, $P < 0.001$). There was no significant difference in the percentage of patients that received PRRT. Next, we assessed the difference in treatment received by patients with and without growth of the mesenteric mass. There was no difference regarding the rate of SSAs use (both 91%, $P = 1.000$), or PRRT administration (40% vs. 39%, $P = 0.871$, respectively).

We have also assessed surgical treatments. As shown in **Table 1**, patients with a mesenteric mass less often received surgery. However, palliative surgery for symptomatic control is performed in approximately the same percentage of patients (26.6% in patients with a mass vs. 29.1% in patients without a mass, $P = 0.77$). As the study had a long timeframe, we also assessed if the disease management changed over the years. We divided the cohort in four groups based on data of diagnosis (< 2008 , 2008 – 2012, 2012-2016 and > 2016) and found no significant shift in the percentages of patients that received surgery or in the indications for surgery. Finally, there was also an equal percentage of patients with and without growth that underwent palliative surgery for symptomatic control (33% vs. 26%, respectively, $P = 0.458$).

Of the 132 patients with a mesenteric mass that received PRRT, an objective response (30% reduction or more of the sum of diameters of all target lesions) was noted in 12.9%. In contrast, a 30% reduction or more of the mesenteric mass was only observed in 3.8% of the patients. The five patients with an objective mesenteric mass reduction (range 32-50% of the diameter on the short axis) showed no growth of the mass before PRRT and the timing between diagnosis and PRRT ranged from 2 to 96 months.

Discussion

In the current study, we analyzed the evolution of mesenteric metastases in a large cohort of patients with SI-NETs with a median follow-up time of 34 months. In our cohort, a metastatic mesenteric mass was present in 64% of the SI-NET patients. During follow-up, growth of the mesenteric mass was noted in a minority (13.5%) and when present,

the time to growth was remarkably long with a median of 40 months. Moreover, the development of a mesenteric mass in patients without mesenteric disease at baseline was very rare and only observed in five patients (2.6%).

In order to gain more insight in the mechanisms underlying mesenteric disease progression in SI-NETs, we assessed patient and disease characteristics as potential predictors of growth. In the multivariate analysis, only male gender remained a significant predictor of growth. This finding suggests an effect of sex on SI-NETs and mesenteric metastasis, possibly mediated by steroid hormone receptors [11-13]. However, further research is necessary to understand the relevance of this finding.

When analyzing the treatment response, the static growth pattern of mesenteric metastases could also be observed. When we assessed patients with a mesenteric mass that received PRRT, we found an objective response in 12.9%. This is comparable with results from the NETTER-1 trial (CR+PR: 18%) [6]. However, when we exclusively assessed the effect on the mesenteric mass, we found that only 3.8% of patients had an objective response. Therefore, PRRT does not seem to be an effective treatment to reduce the SI-NET-associated mesenteric mass size. However, PRRT might still have an effect on the surrounding fibrosis and clinical symptoms [14,15].

These outcomes illustrate the limitations of solely relying on RECIST 1.1 criteria to assess the disease progression and therapeutic effect in SI-NETs. Due to the highly static behavior of the mesenteric mass, patients with a dominant mesenteric disease might be falsely classified as stable disease and therefore not receive the proper treatment for progressive disease. Moreover, these patient might be falsely classified as nonresponsive to treatments such as PRRT. Therefore, we believe that when assessing the disease development in SI-NETs, site-specific growth behavior should be taken into account and the SI-NET-associated mesenteric mass should preferably not be included as target lesion for determining the disease progression and treatment response.

Our study has some limitations to note, including that it is performed in a single, tertiary referral center. As a result, patients often received first medical or surgical treatment before referral. However, a subgroup analysis of patients with follow-up from before the first surgical intervention did not show a difference in the growth rate. Furthermore, most patients received targeted medical treatments, such as SSAs, that could have inhibitory effects and alter the growth behavior of the mesenteric mass. However, as this reflects

the current management strategy, we believe our results accurately reflect the growth behavior of mesenteric masses in the era of targeted treatments.

Conclusion

In this study has important clinical implications as it demonstrates the static behavior of the SI-NET-associated mesenteric mass which should be taken into account when selecting target lesions and assessing disease progression, therapeutic response and treatment options. PRRT appears not to be effective for size reduction of the mesenteric mass.

Institutional Review Board Statement: Ethical review and approval were waived for the study in accordance with the regulations of the Central Committee on Research involving Human Subjects (CCMO) in the Netherlands, as it was performed retrospectively with anonymized data.

Informed Consent Statement: Patient consent was waived in accordance with the regulations of the Central Committee on Research involving Human Subjects (CCMO) in the Netherlands, as it was performed retrospectively with anonymized data.

References

1. Pavel, M.; O'Toole, D.; Costa, F.; Capdevila, J.; Gross, D.; Kianmanesh, R.; Krenning, E.; Knigge, U.; Salazar, R.; Pape, U.F., et al. Enets consensus guidelines update for the management of distant metastatic disease of intestinal, pancreatic, bronchial neuroendocrine neoplasms (nen) and nen of unknown primary site. *Neuroendocrinology* 2016, 103, 172-185.
2. Blazevic, A.; Zandee, W.T.; Franssen, G.J.H.; Hofland, J.; van Velthuysen, M.F.; Hofland, L.J.; Feelders, R.A.; de Herder, W.W. Mesenteric fibrosis and palliative surgery in small intestinal neuroendocrine tumours. *Endocr Relat Cancer* 2018, 25, 245-254.
3. Makridis, C.; Rastad, J.; Oberg, K.; Akerström, G. Progression of metastases and symptom improvement from laparotomy in midgut carcinoid tumors. *World J Surg* 1996, 20, 900-906; discussion 907.
4. Pantongrag-Brown, L.; Buetow, P.C.; Carr, N.J.; Lichtenstein, J.E.; Buck, J.L. Calcification and fibrosis in mesenteric carcinoid tumor: Ct findings and pathologic correlation. *AJR Am J Roentgenol* 1995, 164, 387-391.
5. Howe, J.R.; Cardona, K.; Fraker, D.L.; Kebebew, E.; Untch, B.R.; Wang, Y.-Z.; Law, C.H.; Liu, E.H.; Kim, M.K.; Menda, Y., et al. The surgical management of small bowel neuroendocrine tumors: Consensus guidelines of the north american neuroendocrine tumor society. *Pancreas* 2017, 46, 715-731.
6. Strosberg, J.; El-Haddad, G.; Wolin, E.; Hendifar, A.; Yao, J.; Chasen, B.; Mitra, E.; Kunz, P.L.; Kulke, M.H.; Jacene, H., et al. Phase 3 trial of 177lu-dotatate for midgut neuroendocrine tumors. *N Engl J Med*. 2017, 376, 125-135.
7. Blažević, A.; Hofland, J.; Hofland, L.J.; Feelders, R.A.; de Herder, W.W. Small intestinal neuroendocrine tumours and fibrosis: An entangled conundrum. *Endocr Relat Cancer* 2018, 25, R115-R130.
8. Niederle, B.; Pape, U.F.; Costa, F.; Gross, D.; Kelestimir, F.; Knigge, U.; Öberg, K.; Pavel, M.; Perren, A.; Toumpanakis, C., et al. Enets consensus guidelines update for neuroendocrine neoplasms of the jejunum and ileum. *Neuroendocrinology* 2016, 103, 125-138.
9. Daskalakis, K.; Karakatsanis, A.; Hessman, O.; et al. Association of a prophylactic surgical approach to stage iv small intestinal neuroendocrine tumors with survival. *JAMA Oncol* 2018, 4, 183-189.

10. Wu, L.; Fu, J.; Wan, L.; Pan, J.; Lai, S.; Zhong, J.; Chung, D.C.; Wang, L. Survival outcomes and surgical intervention of small intestinal neuroendocrine tumors: A population based retrospective study. *Oncotarget* 2017, 8, 4935-4947.
11. Arnason, T.; Sapp, H.L.; Barnes, P.J.; Drewniak, M.; Abdollell, M.; Rayson, D. Immunohistochemical expression and prognostic value of er, pr and her2/neu in pancreatic and small intestinal neuroendocrine tumors. *Neuroendocrinology* 2011, 93, 249-258.
12. Estrella, J.S.; Broaddus, R.R.; Mathews, A.; Milton, D.R.; Yao, J.C.; Wang, H.; Rashid, A. Progesterone receptor and pten expression predict survival in patients with low- and intermediate-grade pancreatic neuroendocrine tumors. *Archives of Pathology & Laboratory Medicine* 2014, 138, 1027-1036.
13. Zimmermann, N.; Lazar-Karsten, P.; Keck, T.; Billmann, F.; Schmid, S.; Brabant, G.; Thorns, C. Expression pattern of cdx2, estrogen and progesterone receptors in primary gastroenteropancreatic neuroendocrine tumors and metastases. *Anticancer Res* 2016, 36, 921-924.
14. Laskaratos, F.; Cox, B.; Woo, W.L.; Khalifa, M.; Ewang, M.; Navalkisoor, S.; Quigley, A.M.; Mandair, D.; Caplin, M.; Toumpanakis, C. In Assessment of changes in mesenteric fibrosis (mf) after peptide receptor radionuclide therapy (prrt) in midgut neuroendocrine tumours (nets). *Neuroendocrinology* 2019, 108, 217
15. Strosberg, J.R.; Al-Toubah, T.; Pellè, E.; Smith, J.; Haider, M.; Hutchinson, T.; Fleming, J.B.; El-Haddad, G. Risk of bowel obstruction in patients with mesenteric/peritoneal disease receiving peptide receptor radionuclide therapy (prrt). *J Nucl Med* 2020.
16. Zandee, W.T.; Kamp, K.; van Adrichem, R.C.; Feelders, R.A.; de Herder, W.W. Limited value for urinary 5-hiaa excretion as prognostic marker in gastrointestinal neuroendocrine tumours. *Eur J Endocrinol* 2016, 175, 361-366.
17. Pape, U.F.; Perren, A.; Niederle, B.; Gross, D.; Gress, T.; Costa, F.; Arnold, R.; Denecke, T.; Plöckinger, U.; Salazar, R., et al. Enets consensus guidelines for the management of patients with neuroendocrine neoplasms from the jejunum-ileum and the appendix including goblet cell carcinomas. *Neuroendocrinology* 2012, 95, 135-156.
18. Eriksson, B.; Klöppel, G.; Krenning, E.; Ahlman, H.; Plöckinger, U.; Wiedenmann, B.; Arnold, R.; Auernhammer, C.; Körner, M.; Rindi, G., et al. Consensus guidelines for the management of patients with digestive neuroendocrine tumors--well-differentiated jejunal-ileal tumor/carcinoma. *Neuroendocrinology* 2008, 87, 8-19.

19. Eisenhauer, E.A.; Therasse, P.; Bogaerts, J.; Schwartz, L.H.; Sargent, D.; Ford, R.; Dancey, J.; Arbuck, S.; Gwyther, S.; Mooney, M., et al. New response evaluation criteria in solid tumours: Revised recist guideline (version 1.1). *Eur J Cancer* 2009, 45, 228-247.

Supplementary material

Subgroup analysis of patients with follow-up before first abdominal surgery including patients who did not receive abdominal surgery during follow-up ($n = 282$) versus complete cohort ($n = 530$). The subgroup analysis has a median follow-up time of 32.3 months (IQR 12.0–62.1) with a median time to growth of 38.5 months (IQR 12.3 – 73.2).

SUPPLEMENTARY TABLE 1. Comparison of evolution of mesenteric mass over time in all patients.

	Complete cohort ($n = 530$)	Subgroup ($n = 282$)	P-value
No growth	88.3% ($n = 468$)	86.9% ($n = 245$)	0.453
Growth*	9.2% ($n = 51$)	9.6% ($n = 27$)	
Resection	2.1% ($n = 11$)	3.5% ($n = 10$)	

*Growth assessed by RECIST 1.1 criteria and compared to the baseline CT scan. In case of mesenteric mass at baseline, growth is defined as an increase of $\geq 20\%$ and ≥ 5 mm on the short axis of the dominant mesenteric mass. In case of no mesenteric mass at baseline, growth is defined as development of a mesenteric node of ≥ 10 mm on the short axis.

SUPPLEMENTARY TABLE 2. Comparison of evolution of mesenteric mass over time in patients with mesenteric mass ≥ 10 mm at baseline.

	Complete cohort ($n = 340$)	Subgroup ($n = 234$)	P-value
No growth	83.2% ($n = 283$)	85.5% ($n = 200$)	0.426
Growth*	13.5% ($n = 46$)	10.3% ($n = 24$)	
Resection	3.2% ($n = 11$)	4.2% ($n = 10$)	

*Growth assessed by RECIST 1.1 criteria and compared to the baseline CT scan. In case of mesenteric mass at baseline, growth is defined as an increase of $\geq 20\%$ and ≥ 5 mm on the short axis of the dominant mesenteric mass. In case of no mesenteric mass at baseline, growth is defined as development of a mesenteric node of ≥ 10 mm on the short axis.

SUPPLEMENTARY TABLE 3. Comparison of evolution of mesenteric mass over time in patients without mesenteric mass ≥ 10 mm at baseline.

	Complete cohort (n = 190)	Subgroup (n = 48)	P-value
No growth	97.4% (n = 185)	93.9% (n = 45)	0.214
Growth*	2.6% (n = 5)	6.1% (n = 3)	
Resection	N/A	N/A	

*Growth assessed by RECIST 1.1 criteria and compared to the baseline CT scan. In case of mesenteric mass at baseline, growth is defined as an increase of $\geq 20\%$ and ≥ 5 mm on the short axis of the dominant mesenteric mass. In case of no mesenteric mass at baseline, growth is defined as development of a mesenteric node of ≥ 10 mm on the short axis.



Chapter 3

Mesenteric fibrosis and palliative surgery in small intestinal neuroendocrine tumors

Anela Blažević, Wouter T Zandee, Gaston J H Franssen, Johannes Hofland, Marie-Louise F van Velthuisen, Leo J Hofland, Richard A Feelders and Wouter W de Herder

Endocrine-Related Cancer 2018; 25: 245–254

Abstract

Mesenteric fibrosis (MF) surrounding a mesenteric mass is a hallmark feature of small intestinal neuroendocrine tumors (SI-NETs). Since this can induce intestinal obstruction, oedema and ischaemia, prophylactic resection of the primary tumor and mesenteric mass is often recommended. This study assessed the predictors for mesenteric metastasis and fibrosis and the effect of MF and palliative surgery on survival. A retrospective analysis of 559 patients with pathologically proven SI-NET and available CT imaging data was performed. Clinical characteristics, presence of mesenteric mass and fibrosis on CT imaging and the effect of palliative abdominal surgery on overall survival were assessed. We found that MF was present in 41.4%. Older age, 5-HIAA excretion ≥ 67 $\mu\text{mol}/24$ h, serum CgA $\geq 121,5$ $\mu\text{g}/\text{L}$ and a mesenteric mass ≥ 27.5 mm were independent predictors of MF. In patients ≤ 52 years, mesenteric mass was less often found in women than in men (39% vs 64%, $P = 0.002$). Corrected for age, tumor grade, CgA and liver metastasis, MF was not a prognostic factor for overall survival. In patients undergoing palliative surgery, metastasectomy of mesenteric mass or prophylactic surgery did not result in survival benefit.

In conclusion, we confirmed known predictors of MF and mesenteric mass and suggest a role for sex hormones as women ≤ 52 years have less often a mesenteric mass. Furthermore, the presence of MF has no effect on survival in a multivariate analysis and we found no benefit of metastasectomy of mesenteric mass or prophylactic surgery on overall survival.

Introduction

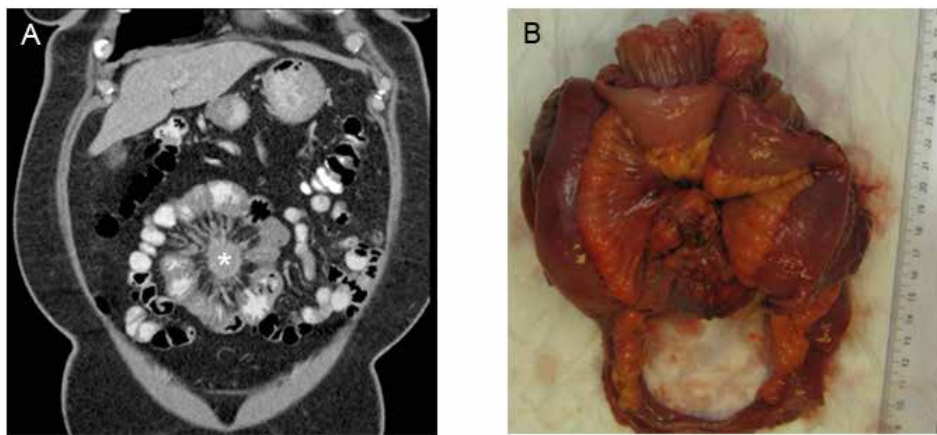
Small intestinal neuroendocrine tumors (SI-NETs) are rare neoplasms with an incidence of approximately 0.2 - 1.2 per 100,000 individuals. However, due to the mostly indolent nature and increasing incidence, their prevalence is rising^{1,2}.

Neuroendocrine tumors are able to produce and secrete bioactive amines and peptides that induce distinct clinical syndromes. SI-NETs are well known to cause the carcinoid syndrome, characterized by flushing and diarrhoea, via the release of mediators like serotonin^{3,4}. Furthermore, SI-NETs are associated with fibrosis, most notably mesenteric and right-sided endocardial fibrosis. Although this association is well documented, the pathobiology remains largely elusive⁵.

Patients with mesenteric fibrosis (MF) often present with abdominal pain and cachexia by intestinal obstruction, oedema, or ischaemia⁶. A mesenteric mass with radiating strands of soft tissue on CT imaging is a pathognomonic feature of MF associated with SI-NET (**Fig. 1A**)⁷. To date, treatment of patients with SI-NETs and complaints due to MF is limited to surgery (**Fig. 1B**)^{5,6}. Furthermore, resection of lymph nodes and the primary intestinal tumor seems to increase survival, even in patients with extensive metastatic disease^{8,9}.

We have conducted the largest retrospective study to investigate the relationships between MF and clinical factors in order to elucidate potential pathogenic mechanisms. Furthermore, we have assessed the survival of patients with MF and the effect of palliative surgery on survival.

FIGURE 1. Appearance of mesenteric fibrosis associated with SI-NETs



(A) CT imaging showing mesenteric mass (asterisk) with typical desmoplastic reaction as radiating strands of soft tissue. (B) Small bowel resection of the same patient showing mesenteric retraction due to centrally located mass.

Methods

Patients

Medical histories of patients treated for SI-NET between 1993 and 2016 in the ENETS Centre of Excellence for Neuroendocrine Tumors, Erasmus MC and Erasmus MC Cancer Institute, Rotterdam, The Netherlands were analysed. SI-NETs were diagnosed on the basis of a combination of markers, imaging and histology according to current guidelines¹⁰. Patients with NET of unknown primary despite extensive work-up including nuclear imaging by targeting somatostatin receptors were excluded. Furthermore, patients with proven SI-NET were included if there was at least one CT scan available and they were resident in the Netherlands during follow-up or continued follow-up in Erasmus MC. The disease characteristics, tumor grade, ENETS stage and presence of liver metastases were recorded at the time of diagnosis¹⁰.

Tumor markers

Serum chromogranin A (CgA, REF: < 94 µg/L) was determined at the time of diagnosis, or if this was not available at first visit to our centre. Urinary 5-hydroxyindoleacetic acid (5-HIAA) levels were determined in 24-hour urine samples (REF: < 50µmol /24 h). 5-HIAA levels <10 µmol / 24 h were excluded because of probable erroneous sampling. The methods of tumor marker measurement were described previously ¹¹.

Imaging

Radiologic features were assessed by means of contrast-enhanced CT. An enlarged mesenteric lymph node of ≥ 10 mm on the short axis was considered pathologic. As there is no possibility to radiologically distinguish between an enlarged mesenteric lymph node and mesenteric tumor mass, both were classified as mesenteric mass. MF was defined as radiating soft tissue strands in the mesentery. Furthermore, CT scans were evaluated for mesenteric infiltration, characterized by a 'misty' soft tissue attenuation and thickening of the small bowel wall.

Statistics

Analyses were performed using SPSS software (version 21 for Windows, SPSS). Data were presented as percentage with count or median and interquartile range (IQR; 25th–75th percentiles). Comparisons were performed for continuous data with unpaired t-test or Mann-Whitney U test as appropriate. For categorical data the Fisher exact test was carried out. To increase clinical relevancy continuous variables were dichotomized. Cut-off values were obtained by the receiver operating characteristic (ROC) curve and maximizing the Youden Index. Odds ratios (ORs) of predictive factors were determined using univariate and multivariate logistic regression. Survival curves were generated using Kaplan-Meier method, and the log-rank test was used to compare survival difference between groups. Hazard ratios (HRs) and 95% confidence intervals (CI) were calculated by Cox regression. In multivariate Cox regression models variables were considered independent if the F-statistic had a probability of less than 0.05. A *P* value of <0.05 was considered statistically significant, and no corrections were made for multiple testing.

Results

Mesenteric fibrosis

A total of 559 patients with SI-NET were included in this retrospective analysis. Their clinical characteristics are shown in **Table 1**. Signs of MF on CT imaging were present in 41.4% of patients. As shown in **Table 1**, the majority of these patients have a mesenteric mass. However, 4.3% had no mesenteric mass of ≥ 10 mm on the short axis. In these cases, the fibrotic strands radiated from a central node which itself was smaller than 10 mm.

To determine potential predictors of MF, we selected clinical factors that significantly differed between patients with and without MF (**Table 1**). 5-HIAA ≥ 67 $\mu\text{mol}/24$ h (AUC 0.64 (95% CI: 0.59–0.68)), CgA ≥ 121.5 $\mu\text{g}/\text{L}$ (AUC 0.61 (95% CI: 0.56–0.66)), mesenteric mass ≥ 27.5 mm (AUC 0.64 (95% CI: 0.58–0.70)), age of diagnosis ≥ 55.8 years (AUC 0.61 (95% CI: 0.51–0.66)), gender, ENETS stage IV, liver and mesenteric metastasis were all significant predictors of MF in univariate analyses (**Table 2**). Mechanical ileus, mesenteric infiltration and small bowel wall thickening were excluded from analysis, as they are generally the result of MF. In a multivariate analysis, independent predictors of MF were 5-HIAA ≥ 67 $\mu\text{mol}/24$ h, a mesenteric mass and a mass ≥ 27.5 mm. Age of diagnosis ≥ 55.8 years, ENETS stage IV, liver metastases, CgA ≥ 121.5 $\mu\text{g}/\text{L}$ and gender were not independent predictors of MF (**Table 2**).

As the presence of a mesenteric mass was a strong predictor of MF, we also evaluated predictive markers for the presence of a mesenteric mass. Since the optimal cut-offs for continuous factors predicting a mesenteric mass (5-HIAA 62 $\mu\text{mol}/24$ h, CgA 121,5 $\mu\text{g}/\text{L}$ and age of diagnosis 56.7) approximated the values found for MF, the same cut-off values were used. In univariate analyses, significant predictors of a mesenteric mass were age of diagnosis ≥ 55.8 years, gender, liver metastases, ENETS stage IV, CgA $\geq 121,5$ $\mu\text{g}/\text{L}$ and 5-HIAA ≥ 67 $\mu\text{mol}/24$ h. Fitting these variables in a multivariate model, only age of diagnosis ≥ 55.8 years, 5-HIAA ≥ 67 $\mu\text{mol}/24$ h and male gender remained independent predictors of a mesenteric mass (**Table 2**).

TABLE 1. Baseline clinical and radiologic characteristics overall

	All patients (n = 559)	Mesenteric fibrosis (n =232)	No mesenteric fibrosis (n = 327)	P-value
Age of diagnosis	60,4 (52,1-68,1)	62.7 (54.7-69.3)	58.7 (50.6-66.5)	< 0.001
Gender				0.036
Male	53.0% (n = 296)	58.2% (n = 135)	49.2% (n = 161)	
Female	47.0% (n = 263)	41.8% (n = 97)	50.8% (n = 166)	
Tumor grade				0.306
Grade 1	48.5% (n = 271)	44.4% (n = 103)	51.4% (n = 168)	
Grade 2	25.9% (n = 145)	28.4% (n = 66)	24.2% (n = 79)	
Grade 3	2.7% (n = 15)	2.2% (n = 5)	3.1% (n = 10)	
Unknown	22.9% (n = 128)	25.0% (n = 58)	20.8% (n = 68)	
ENETS stage IV	76.0% (n = 425)	85.8% (n = 199)	69.1% (n = 226)	< 0.001
Presence of liver metastases	71.0% (n = 397)	81.9% (n = 190)	63.3% (n = 207)	< 0.001
CgA (µg/L)	213.0 (91.3-770.3)	314.5 (125.3-1002.3)	159.0 (72.5-706.5)	<0.001
5-HIAA (µmol/24 h)	124.25 (46.52-457.90)	184.06 (75.53-595.26)	75.73 (37.02-314.93)	<0.001
Mechanical ileus in history	18.1% (n = 101)	23.3% (n = 54)	14.4% (n = 47)	0.008
Presence of mesenteric mass	65.3% (n = 365)	95.7% (n = 222)	43.7% (n = 143)	< 0.001
Size largest mesenteric mass (mm)	29 (22-38)	32 (24-40)	25 (19-33)	< 0.001
Mesenteric infiltration	16.8% (n = 94)	26.3 (n = 61)	10.1% (n = 33)	< 0.001
Small bowel thickening	7.0% (n = 39)	13.4% (n = 31)	2.4% (n = 8)	< 0.001

Numerical data are median with IQR in brackets.

Categorical data are percentages with count in brackets.

CgA: serum chromogranin A, normal range < 94 µg/L, 5-HIAA: urinary 5-hydroxyindoleacetic acid excretion, normal range < 50µmol /24 h

P-value: mesenteric fibrosis versus no mesenteric fibrosis

TABLE 2. Predictive factors of mesenteric fibrosis and mass in patients with SI-NETs (*n* = 559)

	Univariate			Multivariate		
	OR	95% CI	P-value	OR	95% CI	P-value
Age of diagnosis ≥ 55.8 years						
Mesenteric fibrosis	2.05	1.43-2.95	<0.001	1.43	0.89-0.2.31	0.142
Mesenteric mass	2.16	1.51-3.10	<0.001	1.93	1.28-2.90	0.002
Male						
Mesenteric fibrosis	1.44	1.02-2.01	0.037	1.15	0.75-1.79	0.522
Mesenteric mass	1.82	1.28-2.58	0.001	1.68	1.14-2.48	0.009
ENETS stage IV						
Mesenteric fibrosis	2.87	1.84-4.48	<0.001	1.19	0.42-3.39	0.749
Mesenteric mass	2.63	1.76-3.92	<0.001	0.77	0.34-1.76	0.531
Liver metastases						
Mesenteric fibrosis	2.60	1.74-3.89	<0.001	1.10	0.41-2.94	0.855
Mesenteric mass	2.64	1.81-3.86	<0.001	1.64	0.75-3.57	0.216
CgA ≥ 121,5 µg/L						
Mesenteric fibrosis	2.56	1.76-3.73	<0.001	1.12	0.65-1.93	0.684
Mesenteric mass	2.33	1.62-3.43	<0.001	0.97	0.61-1.54	0.910
5-HIAA ≥ 67 µmol/24 h						
Mesenteric fibrosis	3.28	2.21-4.87	<0.001	1.96	1.15-3.36	0.014
Mesenteric mass	3.10	2.11-4.54	<0.001	2.72	1.73-4.28	<0.001
Mesenteric mass						
Mesenteric fibrosis	28.57	14.61-55.84	<0.001	11.49	5.58-23.63	<0.001
Mesenteric mass ≥ 27.5 mm						
Mesenteric fibrosis	8.94	6.01-13.30	<0.001	3.01	1.90-4.76	<0.001

OR: odds ratio. 95% CI: 95% confidence interval.

CgA: serum chromogranin A, normal range < 94 µg/L, 5-HIAA: urinary 5-hydroxyindoleacetic acid excretion, normal range < 50µmol /24h

Gender

Male patients had a significant higher occurrence of MF than women (**Table 1**). In accordance, median urinary 5-HIAA excretion is higher (male 142.41 $\mu\text{mol}/24\text{h}$ vs female 96.94, $P = 0.001$) and the presence of a mesenteric mass is more frequent (72% vs 58% $P = 0.001$). Noteworthy, male patients also less frequently underwent abdominal surgery (male 69% vs. female 79%, $P = 0.005$). Other characteristics, including age of diagnosis and ENETS stage, did not differ significantly between male and female patients (*data not shown*).

As shown in **Table 2**, gender was an independent predictor of the presence of a mesenteric mass. As the presence and the effect of sex hormones are age-dependent, we divided the cohort in 4 equal age categories: ≤ 52.1 , 52.2-60.4, 60.5-68.1, ≥ 68.1 years. In the first group with age of diagnosis ≤ 52.1 years, there were 70 female and 70 male patients, while 39% of the female patients vs 64% of the male patients had a mesenteric mass ($P = 0.002$). This significant difference in presence of a mesenteric mass was not found in other age groups and other characteristics did not significantly differ in this age group between genders (*data not shown*).

Effect of mesenteric fibrosis on survival

During a median follow-up time of 62.3 months (IQR 32.9-103.4), 208 patients died. Kaplan-Meier analysis demonstrated that patients with MF had a significantly shorter overall survival ($P < 0.001$) with a median survival of 102 months in the group with MF vs 174 months in the group without MF (**Fig. 2**). This was in accordance with a five-year survival rate of respectively 71% vs 80%.

To assess possible prognostic factors, we performed univariate analyses on known prognostic factors, age, CgA, tumor grade and ENETS stage¹⁰, and possible prognostic factors, urinary 5-HIAA excretion, presence of liver metastases¹², mesenteric mass, MF and gender. To enhance clinical utility, ROC curve analysis was used to determine optimal cut-offs for 5-HIAA (AUC 0.70 (95% CI 0.66-0.75)) and CgA (AUC 0.72 (95% CI 0.68-0.76)) for survival. This resulted in a cut-off for 5-HIAA of 215 $\mu\text{mol}/24\text{h}$ and for CgA of 310 $\mu\text{g}/\text{L}$. These cut-off values approximated the median value in patients with ENETS stage IV disease, which were 188 $\mu\text{mol}/24\text{h}$ and 298 $\mu\text{g}/\text{L}$, respectively.

When assessed in univariate analyses, only gender and ENETS stage were not significant predictors of worse survival (**Table 3**).

The predictors of worse survival, age of diagnosis, tumor grade, CgA > 310 µg/L, 5-HIAA > 215 µmol/24 h, MF, liver and mesenteric metastasis, were further assessed in a multivariate model (**Table 3**). The known factors (age, tumor grade and CgA) were confirmed as independent prognostic markers, as well as liver metastasis and urinary 5-HIAA excretion > 215 µmol/24 h. However, MF and having a mesenteric mass were not independent prognostic factors for overall survival when added to this multivariate model (**Table 3**).

FIGURE 2. Overall survival according to presence of mesenteric fibrosis on CT imaging ($n=559$)

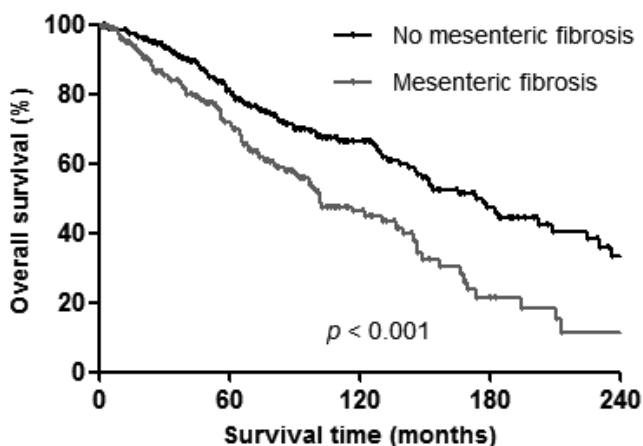


TABLE 3. Prognostic factors for overall survival

	Univariate			Multivariate		
	HR	95% CI	P-value	HR	95% CI	P-value
Age of diagnosis	1.07	1.05-1.08	<0.001	1.07	1.05-1.09	<0.001
Gender	1.08	0.82-1.42	0.580	NS		
Tumor grade						
Grade 1	Reference			Reference		
Grade 2	2.52	1.76-3.61	<0.001	2.17	1.50-3.14	<0.001
Grade 3	6.05	3.15-11.63	<0.001	4.85	2.29-10.25	<0.001
ENETS stage at diagnosis				NS		
Stage I	Reference					
Stage II	0.28	0.02-4.53	0.372			
Stage III	0.52	0.07-3.99	0.530			
Stage IV	2.08	0.29-14.90	0.465			
CgA \geq 310 μ g/L	2.87	2.17-3.79	<0.001	1.90	1.28-2.80	0.001
5-HIAA \geq 215 μ mol/24 h	2.22	1.68-2.95	<0.001	1.50	1.02-2.21	0.042
Liver metastases	3.42	2.20-5.33	<0.001	2.64	1.44-4.85	0.002
Mesenteric mass	1.62	1.19-2.20	0.002	0.73	0.45-1.17	0.185
Mesenteric fibrosis	1.78	1.35-2.35	<0.001	1.47	0.98-2.19	0.060

NS, non-significant in univariate analysis; CgA, serum chromogranin, A normal range < 94 μ g/L; 5-HIAA: urinary 5-hydroxyindoleacetic acid excretion, normal range < 50 μ mol/24 h; HR, hazard ratio; 95% CI, 95% confidence interval.

Therapy

As patients with MF had more advanced disease (**Table 1**), almost all patients were treated with somatostatin analogues (SSAs) (MF 92.2% vs no MF 74.6%, $P < 0.001$). Since the study was performed in a tertiary referral centre, the majority of patients already received SSA therapy at the first visit to our centre. Therefore, the effect of starting SSAs on 5-HIAA excretion and MF could not be evaluated. Since patients with MF had predominantly ENETS stage IV disease (**Table 1**), we

selected patients with ENETS stage IV ($n = 425$) to assess the effect of MF on surgical management of SI-NETs. The majority of patients in our cohort underwent abdominal surgery and the characteristics of the abdominal operations are shown in **Table 4**. Patients with MF had less often abdominal surgical procedures and underwent more frequent first abdominal surgery >6 months after diagnosis. However, when they did undergo surgery there was no difference in the number of procedures as compared to patients without MF (range 1-5, $P = 0.683$).

TABLE 4. Characteristics of abdominal surgery in patients with ENETS stage IV

	All patients ($n = 425$)	Mesenteric fibrosis ($n = 199$)	No mesenteric fibrosis ($n = 226$)	<i>P</i> -value
Abdominal surgery	67.8% ($n = 288$)	57.8% ($n = 115$)	76.5% ($n = 173$)	
Emergency surgery	12.5% ($n = 53$)	15.1% ($n = 30$)	10.2% ($n = 23$)	<0.001
Elective surgery	55.3% ($n = 235$)	42.7% ($n = 85$)	55.4% ($n = 150$)	<0.001
Small bowel resection	19.1% ($n = 81$)	17.6% ($n = 35$)	20.4% ($n = 46$)	
Ileocaecal resection	13.9% ($n = 59$)	8.0% ($n = 16$)	19.0% ($n = 43$)	
Right sided hemicolectomy	16.7% ($n = 71$)	10.6% ($n = 21$)	22.1% ($n = 50$)	
Other	5.6% ($n = 24$)	6.5% ($n = 13$)	4.8% ($n = 11$)	
No abdominal surgery	32.2% ($n = 137$)	42.2% ($n = 84$)	23.5% ($n = 53$)	<0.001
Resection of mesenteric mass*	16.7% ($n = 50$)	21.6% ($n = 41$)	8.2% ($n = 9$)	0.001
Surgery < 6 months after diagnosis	56.7% ($n = 241$)	42.7% ($n = 85$)	69.0% ($n = 156$)	0.002
Indication for initial surgery				<0.001
Curative	16.3% ($n = 47$)	11.3% ($n = 13$)	19.7% ($n = 34$)	
Palliative; symptomatic	42.4% ($n = 122$)	53% ($n = 61$)	35.3% ($n = 61$)	
Palliative; prophylactic	28.5% ($n = 82$)	29.6% ($n = 34$)	27.7% ($n = 48$)	
Not reported	12.8% ($n = 37$)	6.1% ($n = 7$)	17.3% ($n = 30$)	

*Percentage of patients with mesenteric mass on first available CT scan and resection afterwards.
P-value: mesenteric fibrosis vs no mesenteric fibrosis

To determine factors that influence the likelihood of undergoing surgical treatment, we performed univariate and multivariate analyses of clinically relevant factors in patients with ENETS stage IV disease (**Table 5**). We were mostly interested in the effect of MF and as patients with MF had in >95% of the cases a mesenteric mass, we excluded this variable from the multivariate model. The multivariate analysis showed that patients with MF were less likely to have abdominal surgery independent of age, sex, tumor grade and the presence of liver metastases.

TABLE 5. Predictive factors for undergoing abdominal surgery

	Univariate			Multivariate		
	OR	95% CI	P- value	OR	95% CI	P- value
Age	0.97	0.95-0.99	0.004	0.96	0.93-0.98	0.002
Male	0.63	0.42-0.96	0.029	0.57	0.34-0.96	0.035
Tumor grade						
Grade 1	Reference			Reference		
Grade 2	0.42	0.26-0.69	0.001	0.43	0.26-0.72	0.001
Grade 3	0.42	0.13-1.40	0.157	0.41	0.12-1.44	0.164
Liver metastases	0.22	0.06-0.73	0.013	0.14	0.10-1.25	0.107
Mesenteric mass	0.15	0.08-0.28	<0.001	N/A*		
Mesenteric fibrosis	0.42	0.28-0.64	<0.001	0.56	0.34-0.93	0.025

*Excluded from multivariate analysis to avoid collinearity.

OR, odds ratio; 95% CI, 95% confidence interval

Effect of surgery on survival

To assess the effect of surgery on survival in patients with SI-NETs, we categorized patients according to indication for surgery, i.e. curative, palliative prophylactic and palliative for symptomatic control. The majority of patients who underwent surgery with curative intent ($n = 131$) had ENETS stage III disease (51.1%, $n = 67$); however, 35.1% ($n = 46$) had already metastasized disease, ENETS stage IV at diagnosis. In a small percentage (6.1%, $n = 8$), the surgery was irradical and another 9.2% ($n = 12$) had recurrent disease within 1

3

year. The median disease-free survival was 117 months (95% CI: 83.6 – 150.4), with five-year disease-free survival of 64.2% and ten year of 48.1%. Importantly, we found that after ten years disease-free survival ($n = 20$), 60% of these patients ($n = 12$) developed recurrent disease with disease-free time ranging up to 300 months after initial curative surgery. The median overall survival of patients operated with curative intent was 183.5 months (95% CI: 129.1 – 237.9) with a five-year survival of 87.1%. Conversely to surgery with curative intent, if palliative resection of the primary tumor or metastasectomy in the context of metastasized disease prolongs survival is often debated as a benefit on overall survival has not been shown unequivocally¹⁰. Therefore, we fitted the previous multivariate model of survival (including age, tumor grade, CgA > 310 µg/l, 5-HIAA > 215 µmol/24 h and the presence of liver metastases) on survival of patients with ENETS stage IV disease ($n = 425$). In these patients, the presence of liver metastases (HR 1.09 (95% CI: 0.44-2.71), $P = 0.858$) and 5-HIAA > 215 µmol/24 h (HR 1.45 (95% CI: 0.99 – 2.15), $P = 0.060$) were no longer significant predictors of survival. Further survival analyses have been fitted on a multivariate model consisting of age of diagnosis, tumor grade and CgA > 310 µg/L. To investigate the effect of prophylactic palliative surgery in metastasized disease, we additionally excluded patients who underwent surgery with curative intention or for symptomatic control. The selected 217 patients had a median follow-up time of 57.0 months (IQR 29.0-89.7), during which 90 patients died. The median survival of 99 months (95% CI: 83.9 – 113.9) for non-operated patients was significantly shorter than the 147 months (95% CI: 122.77 – 170.63, $P = 0.019$) for operated patients. This corresponded with five-year survival rates of 67% vs 78%, respectively. However, when added to a multivariate model with the above-mentioned independent predictors (age, tumor grade and CgA > 310 µg/L), prophylactic abdominal surgery was no independent prognostic factor (HR 1.34 (95% CI: 0.72-2.49), $P = 0.358$). Patients who received prophylactic surgery were younger and more often female than non-operated patients (median age of diagnosis 58.9 years vs 63.2 years, $P = 0.002$, and 54.9% female vs 38.5% male $P = 0.02$). Furthermore, MF and a mesenteric mass were less frequently present in operated patients (MF in 41% vs 61% in non-operated, $P = 0.004$, and mesenteric mass in 63% vs 91% in non-operated, $P < 0.001$). Even so, also in this population, MF and mesenteric mass were not independent predictors of overall survival (HR 1.09, $P = 0.76$, HR 1.52, $P = 0.392$, respectively) when corrected for age, tumor grade and CgA.

As delayed surgery can result in developing symptoms which necessitates surgery with worse outcome, we investigated if undergoing palliative surgery for symptomatic control vs prophylactic palliative surgery is a prognostic factor. In our cohort, 276 patients received palliative surgery, of which 83 died during a median follow-up of 62.7 months (IQR 33.4-106.1). Palliative surgery was prophylactic in 34.4% ($n = 6$), in 52.2% ($n = 144$) palliative surgery was performed because of symptoms (abdominal pain in 10.5%, obstruction or ischaemia in 38.8%, and cachexia in 2.2%) and in 13.4% ($n = 37$) the intent was not clearly reported. Patients undergoing prophylactic palliative surgery had a median survival of 152.2 months (95% CI: 80.8 – 223.6). This is significantly longer than the median survival of 137.1 months (95% CI: 80.3 – 193.9, $P = 0.012$) of non-operated patients. However, when added in a multivariate model to independent predictive factors of survival (age, tumor grade and CgA > 310 $\mu\text{g/L}$), prophylactic palliative surgery is no longer an independent predictor of survival (HR 0.62 (95% CI: 0.35-1.10), $P = 0.10$)

Finally, to assess the effect of metastasectomy of the mesenteric mass on survival, we selected the patients with a mesenteric mass who underwent surgery after the first available CT scan or those who did not undergo abdominal surgery. Of these 244 patients, 110 (45.1%) underwent abdominal surgery of which 19.1% ($n = 21$) was performed with curative intent, 37.3% ($n = 41$) palliative prophylactic and in 43.6% ($n = 48$) palliative for symptomatic control. The frequency of successful resection of mesenteric mass differed significantly between surgical indication from 90.5% ($n = 19$) in patients with curative intent to 65.0% ($n = 26$) in prophylactic and 52.1% ($n = 25$) in symptomatic palliative surgery ($P = 0.009$). The median follow-up time of these 244 patients was 50.4 months (IQR 19.1-83.4), during which 91 patients died. The median survival of 81.6 months (95% CI: 43.4 – 119.8) in patients receiving metastasectomy was not significantly different as compared to 100.2 months (95% CI: 89.84 – 110.6, $P = 0.485$) of patients not undergoing metastasectomy. In addition, the number of abdominal surgical procedures did not differ between both groups (range 1-5, $P = 0.219$). Furthermore, when focusing on patients receiving palliative prophylactic surgery with a mesenteric mass on CT image preoperatively ($n = 41$), we find no effect of successful resection of mesenteric mass ($n = 14$) on survival compared to patients with residual mesenteric disease ($n = 26$) (HR 2.46 95% CI: 0.63 – 9.67, $P = 0.197$).

Discussion

Small intestinal neuroendocrine tumors are slow-growing tumors, which are characterized by their ability to secrete bioactive amines and peptides and induce associated syndromes such as carcinoid syndrome, carcinoid heart disease and MF. We have conducted the largest retrospective study so far in 559 patients with a median follow-up time of 62.3 months to assess the effect of MF and palliative surgery on survival. Because of this large patient cohort, we were able to assess predictors of MF and to search for novel insights into the pathogenic mechanisms of mesenteric fibrosis and metastasis.

In our cohort 41.4% of all patients showed the hallmark of radiating soft tissue strands which earlier research has shown to be correlated with profound fibrosis in the mesenteric fat ⁷. Most of the patients with MF had a mesenteric mass and in the small percentage (4.3%) without a mesenteric mass, the fibrotic strands radiated from a central node which itself was smaller than 10 mm on the short axis.

In accordance with other studies, increased urinary 5-HIAA excretion and larger mesenteric mass were independent predictors of MF ¹³. Additionally, in our cohort, increased urinary 5-HIAA excretion was an independent predictor for the presence of a mesenteric mass as well, affirming the above-mentioned link between secretion of biogenic molecules and mesenteric fibrosis and metastasis.

Interestingly, we found that gender was also an independent predictor of a mesenteric mass. As tumor grade, ENETS stage, serum CgA level and the presence of liver metastases did not differ between male and female patients, this seems not to be an effect of tumor aggressiveness or burden. In addition, only in the youngest quartile, patients diagnosed before 52 years of age, the prevalence of a mesenteric mass differed significantly between sexes. In this age group, women had in 39% a mesenteric mass vs 64% of the men. As this age cut-off correlates with the age before menopause in women, it is suggestive of a potential relationship between sex hormones and metastatic patterns. Further research is needed to investigate the role of gender and sex hormones in SI-NETs and the pathogenesis of mesenteric metastasis and fibrosis ^{14,15}.

Mesenteric mass and the associated MF results in considerable disease burden in patients with SI-NETs as it can cause small bowel obstruction, ischaemia and perforation. Accordingly, in our study, MF was associated with a decreased five-year survival.

However, MF did not remain a significantly negative prognostic factor when corrected for known prognostic factors¹⁰. This suggests that factors such as age, tumor aggressiveness expressed as tumor grade and tumor burden measured as serum CgA mostly determine the prognosis^{10,16,17} and the decreased survival in patients with MF reflects the presence of more advanced disease.

The cornerstone of treatment for patients with abdominal complaints due to mesenteric metastases and fibrosis remains surgery with intestinal resection and guidelines recommend surgery in patients with locally or advanced metastasized SI-NET in the case of symptoms or possible curation^{6,10,18}. In our cohort the majority of patients have local or distant metastasized disease, also the patients undergoing surgery with curative intent. In these patients, we find consistent with literature a favourable five-year survival rate of 87.1%¹⁰. However, 51.9% of patients operated with curative intent have recurrent disease after 10 years, highlighting the difficulty of achieving curation in patients with advanced SI-NETs.

Compared to clear guidelines in case of possible curation or abdominal symptoms, the place of prophylactic palliative resection of primary tumor and mesenteric mass in distantly metastasized disease remains a matter of debate as the benefits of surgery on survival remain controversial¹⁰. Based on retrospective analyses, which found survival benefit of palliative resection of primary tumors, early prophylactic surgery is often recommended to avoid complications. However, this benefit could have resulted from biased patient selection, as proper correction for known prognostic markers was often not performed. Moreover, a recent prospective cohort study found no survival benefit of prophylactic surgery¹⁹. To investigate the effect on survival of palliative surgery in patients with metastasized SI-NET, we selected patients with ENETS stage IV disease at diagnosis. Five-year survival rates for patients receiving palliative surgery were higher compared to non-operated patients. However, when corrected for age of diagnosis, tumor grade and serum CgA, prophylactic palliative surgery did not result in better survival rates. Also, we found no survival benefit or reduction in number of surgical procedures in patients who received metastasectomy of the largest mesenteric mass. Furthermore, when we assessed survival in a multivariate analysis with known independent prognostic factors, prophylactic palliative surgery in an asymptomatic stage resulted in no survival benefit compared to palliative surgery for symptom control.

3

However, it is also important to note that although overall patients with advanced SI-NET may not benefit from prophylactic surgery, some patient populations might ². In order to be able to identify patients who might benefit from prophylactic surgery, more insight is needed on the development of MF ^{10,20}. The robust correlation between 5-HIAA excretion and mesenteric metastasis and fibrosis suggests a pathogenic relation ^{5,13}. It can therefore be hypothesized that medical therapy such as SSAs and serotonin synthesis inhibitors should aim to fully normalize serotonin production in order to minimize development MF, although this should be evaluated in prospective studies. Additionally, SI-NETs are generally slow-growing tumors, and it is possible that certain patients without MF or with asymptomatic MF will never develop obstructive or ischaemic complaints. Furthermore, intestinal resection with metastasectomy can result in significant postoperative morbidity due to short-bowel syndrome, adhesions and bile-salt diarrhoea. Therefore, as there seems to be no potential survival benefit of prophylactic surgery in the overall populations of patients with advanced SI-NET, we would generally advise a watchful wait-and-see approach and in case of symptoms, tumor growth or MF to consider palliative surgery in a tailor-made approach.

This study has several limitations. It is a retrospective study and performed in a tertiary referral centre. Patients often already received their first (medical) treatment before referral, making the evaluation of initial serum CgA and urinary 5-HIAA excretion biased. Also, it is possible that a selection of patients is not referred, such as curatively operated patients, or patients with rapidly progressive disease and poor clinical condition. Despite efforts to adjust for known prognostic factors, a biased patient selection can still occur. Due to conflicting findings on the effect of palliative surgery for SI-NETs, this study emphasizes again the need for randomized controlled trials.

Conclusion

We have confirmed known predictors of MF in patients with SI-NETs and presented that these are congruent with the predictors of a mesenteric mass. We also found that in patients aged ≤ 52 years, female gender is associated with lower incidence of a mesenteric mass. In our cohort, MF is not an independent prognostic factor for overall survival. In addition, we found no general benefit of palliative resection of mesenteric mass, or prophylactic surgery on survival.

References

1. Fraenkel M, Kim M, Faggiano A, de Herder WW, Valk GD, Knowledge N. Incidence of gastroenteropancreatic neuroendocrine tumours: a systematic review of the literature. *Endocr Relat Cancer*. Jun 2014;21(3):R153-63.
2. Wu L, Fu J, Wan L, et al. Survival outcomes and surgical intervention of small intestinal neuroendocrine tumors: a population based retrospective study. *Oncotarget*. Jan 17 2017;8(3):4935-4947.
3. de Herder WW. Tumours of the midgut (jejunum, ileum and ascending colon, including carcinoid syndrome). Article. *Best Practice & Research in Clinical Gastroenterology*. Oct 2005;19(5):705-715.
4. Halperin DM, Shen C, Dasari A, et al. Frequency of carcinoid syndrome at neuroendocrine tumour diagnosis: a population-based study. *Lancet Oncol*. Apr 2017;18(4):525-534.
5. Modlin IM, Shapiro MD, Kidd M. Carcinoid tumors and fibrosis: An association with no explanation. *Am J Gastroenterol*. 2004;99(12):2466-2478. doi:10.1111/j.1572-0241.2004.40507.x
6. Makridis C, Oberg K, Juhlin C, et al. Surgical treatment of mid-gut carcinoid tumors. *World J Surg*. May-Jun 1990;14(3):377-383; discussion 384-375.
7. Pantongrag-Brown L, Buetow PC, Carr NJ, Lichtenstein JE, Buck JL. Calcification and fibrosis in mesenteric carcinoid tumor: CT findings and pathologic correlation. *AM J ROENTGENOL*. 1995;164(2):387-391.
8. Landry CS, Lin HY, Phan A, et al. Resection of at-risk mesenteric lymph nodes is associated with improved survival in patients with small bowel neuroendocrine tumors. *World J Surg*. Jul 2013;37(7):1695-700.
9. Guo J, Zhang Q, Bi X, et al. Systematic review of resecting primary tumor in MNETs patients with unresectable liver metastases. *Oncotarget*. Mar 07 2017;8(10):17396-17405.
10. Niederle B, Pape UF, Costa F, et al. ENETS Consensus Guidelines Update for Neuroendocrine Neoplasms of the Jejunum and Ileum. *Neuroendocrinology*. 2016;103(2):125-38.
11. Zandee WT, Kamp K, van Adrichem RC, Feelders RA, de Herder WW. Limited value for urinary 5-HIAA excretion as prognostic marker in gastrointestinal neuroendocrine tumours. *Eur J Endocrinol*. Nov 2016;175(5):361-6.

12. Janson ET, Holmberg L, Stridsberg M, et al. Carcinoid tumors: analysis of prognostic factors and survival in 301 patients from a referral center. *Ann Oncol.* Jul 1997;8(7):685-90.
13. Rodriguez Laval V, Pavel M, Steffen IG, et al. Mesenteric Fibrosis in Midgut Neuroendocrine Tumors: Functionality and Radiological Features. *Neuroendocrinology.* Apr 07 2017;
14. Viale G, Doglioni C, Gambacorta M, Zamboni G, Coggi G, Bordi C. Progesterone receptor immunoreactivity in pancreatic endocrine tumors. An immunocytochemical study of 156 neuroendocrine tumors of the pancreas, gastrointestinal and respiratory tracts, and skin. *Cancer.* Nov 1 1992;70(9):2268-77.
15. Estrella JS, Ma LT, Milton DR, et al. Expression of Estrogen-Induced Genes and Estrogen Receptor Beta in Pancreatic Neuroendocrine Tumors: Implications for Targeted Therapy. *Pancreas.* 2014;43(7):996-1002. doi:10.1097/mpa.0000000000000203
16. Kolby L, Bernhardt P, Sward C, et al. Chromogranin A as a determinant of midgut carcinoid tumour volume. *Regul Pept.* Aug 15 2004;120(1-3):269-73.
17. Capdevila J, Meeker A, Garcia-Carbonero R, et al. Molecular biology of neuroendocrine tumors: from pathways to biomarkers and targets. *Cancer Metastasis Rev.* Mar 2014;33(1):345-51.
18. Öhrvall U, Eriksson B, Juhlin C, et al. Method for dissection of mesenteric metastases in mid-gut carcinoid tumors. *World J Surg.* 2000;24(11):1402-1408. doi:10.1007/s002680010232
19. Daskalakis K, Karakatsanis A, Hessman O, et al. Association of a Prophylactic Surgical Approach to Stage IV Small Intestinal Neuroendocrine Tumors With Survival. *JAMA Oncol.* Feb 1 2018;4(2):183-189.
20. Norlen O, Stalberg P, Oberg K, et al. Long-term results of surgery for small intestinal neuroendocrine tumors at a tertiary referral center. *World J Surg.* Jun 2012;36(6):1419-31.



Chapter 4

Predicting symptomatic mesenteric mass in small intestinal neuroendocrine tumors using radiomics

4

Anela Blažević, Martijn P. A. Starmans, Tessa Brabander, Roy S. Dwarkasing, Renza A. H. van Gils, Johannes Hofland, Gaston J. H. Franssen, Richard A. Feelders, Wiro J. Niessen, Stefan Klein and Wouter W. de Herder

Endocrine Related Cancer 2021 Jun 21;28(8):529-539

Abstract

Metastatic mesenteric masses of small intestinal neuroendocrine tumors (SI-NETs) are known to often cause intestinal complications. The aim of this study was to identify patients at risk to develop these complications based on routinely acquired CT scans using a standardized set of clinical criteria and radiomics. Retrospectively, CT scans of SI-NET patients with a mesenteric mass were included and systematically evaluated by five clinicians. For the radiomics approach, 1128 features were extracted from segmentations of the mesenteric mass and mesentery, after which radiomics models were created using a combination of machine learning approaches. The performances were compared to a multidisciplinary tumor board (MTB). The dataset included 68 patients (32 asymptomatic, 36 symptomatic). The clinicians had AUCs between 0.62 and 0.85 and showed poor agreement. The best radiomics model had a mean AUC of 0.77. The MTB had a sensitivity of 0.64 and specificity of 0.68. We conclude that systematic clinical evaluation of SI-NETs to predict intestinal complications had a similar performance compared to an expert MTB, but poor inter-observer agreement. Radiomics showed a similar performance and is objective, and thus is a promising tool to correctly identify these patients. However, further validation is needed before the transition to clinical practice.

Introduction

Small intestinal neuroendocrine tumors (SI-NETs) are rare neoplasms with a mostly slow, progressive course ¹. Patients frequently present with metastasized disease, the liver and mesentery being the dominant metastatic sites ². SI-NETs are known to induce fibrosis, most notably surrounding a metastatic mesenteric mass, via production of mediators like serotonin. This mesenteric fibrosis causes distortion and traction on the surrounding intestine and can encase mesenteric vessels. In the majority of patients, this leads to severe complications such as intestinal obstruction and ischemia.

In order to prevent future complications, the current European Neuroendocrine Tumor Society (ENETS) guideline advises consideration of prophylactic surgery in these patients ³. However, not all of these patients may benefit from surgery: approximately 30% of patients with mesenteric metastasized disease has no abdominal symptoms ^{4,5}. In addition, recent studies found no survival or clinical benefit of prophylactic palliative surgery in asymptomatic patients ^{4,6}. Nonetheless, it has been suggested that a certain subset of patients might benefit from early surgical intervention ¹. Often the presence of a mesenteric mass and the severity of mesenteric fibrosis are used to determine the necessity of prophylactic palliative surgery. However, there is discordance between the histological and radiological severity of mesenteric fibrosis and the symptomatology ^{7,8}. To our knowledge, there is currently no method to reliably identify patients prone to develop intestinal complications due to a SI-NET mesenteric mass.

The currently developed stratification methods for SI-NETs focus solely on overall survival and prognosis and do not include risk factors for intestinal complications due to mesenteric metastasis and fibrosis ⁹⁻¹¹. Therefore, we propose two novel methods for the identification of complications based on contrast-enhanced abdominal computed tomography (CT) scans. First, a visual systematic clinical evaluation of the scan. Second, a data-driven approach to identify predictive features of symptomatic mesenteric masses. To this end, we use radiomics, in which quantitative medical imaging features are related to clinical outcome. Radiomics has been used in combination with CT in various clinical applications, such as liver cancer ¹², lung cancer ¹³, clear cell renal carcinoma ¹⁴, and many more ¹⁵. In neuroendocrine tumors, radiomics has been used to predict the grade of pancreatic neuroendocrine tumors ¹⁶. Given the success in these previous studies and the

fact that CT scans are routinely acquired for assessing disease progression, we hypothesize that radiomics may be used to quantify the appearance of the SI-NET mesenteric mass and surrounding mesentery. Besides developing a prediction model using radiomics, further analysis of the radiomics features of symptomatic patients may elucidate new insights in the processes involved in the development of symptomatic mesenteric masses.

The aim of this study was to find a method to reliably identify patients at high risk of developing complications from a mesenteric mass and surrounding fibrosis. To this end, routinely acquired CT scans were assessed by five clinicians using systematic clinical evaluation, and a radiomics approach was used in which we assessed the predictive value of 1) the SI-NET mesenteric mass; 2) the surrounding mesentery; and 3) the mesenteric mass location. To compare the performance with clinical practice, a multidisciplinary tumor board (MTB) evaluated the patients as well.

Materials and methods

Study population

This study was performed in accordance with the Dutch Code of Conduct for Medical Research of 2004. As the study was retrospectively performed with anonymized data, no approval from the ethical committee or informed consent was required. Patients were retrospectively included from the Rotterdam NET-database, which encompassed all NET patients treated between January 1993 and December 2018 in the Erasmus MC, University Medical Center Rotterdam, the Netherlands. Included cases had a pathologically proven SI-NET and radiological evidence of a metastatic mesenteric mass. A metastatic mesenteric mass was diagnosed if the lesion met the criteria of a malignant mesenteric lymph node on CT scan in accordance with the RECIST 1.1 guidelines, as these are validated criteria to determine disease progression with clear criteria for a malignant lymph node^{3,17}.

Patients were included in the symptomatic group in case of palliative abdominal surgery because of intestinal complications, for example, obstruction, ischemia, or perforation. For this group, a venous phase contrast-enhanced abdominal CT scan performed up to 365 days before the surgery was used. Patients were included in the

asymptomatic group when none of the mentioned intestinal complications were present, and thus no abdominal surgery was performed, for at least 3 years after the included venous phase contrast-enhanced abdominal CT scan was performed.

Due to the low quality of older scans and to make the outcome more applicable to the current CT technology, only scans between 2008 and 2018 were included. No other restrictions on the acquisition parameters or contrast administration protocol were imposed. It was recorded whether positive enteric contrast was used or not. Baseline characteristics included age, sex, tumor grade according to WHO criteria, ENETS disease stage, plasma chromogranin A (CgA) level, and 24-h urinary 5-hydroxyindoleacetic acid (5-HIAA) excretion ³.

Segmentation

For each patient, three regions of interest (ROIs) were segmented: (1) the mesenteric mass (MM); (2) the surrounding mesentery (SM); and (3) the origin of the superior mesenteric artery (SMA). Segmentation was performed manually per voxel by a clinician (AB) and reviewed by a nuclear physician (TB). For segmentation of the MM, a mesenteric node of 15 mm or more on the short axis was selected in accordance with RECIST 1.1 criteria for target lymph nodes ¹⁷. In case of multiple pathological mesenteric nodes, the largest mesenteric node was selected, since the desmoplastic reaction occurs principally around the dominant mesenteric node ¹⁸. The SM was segmented by annotating the mesentery between the MM and the surrounding bowel wall with a maximum distance of 30 mm between the MM and SM contour. This cutoff was chosen instead of annotating the entire mesentery between the MM and bowel wall to reduce differences in the segmentations due to variations in mesenteric retraction across patients. Determination of the exact middle of the SMA origin, that is, one point on one slice, is difficult due to the variable and often high slice thickness (e.g. 5 mm) of the scans, and is potentially observer dependent. Instead, to improve reproducibility, for all scans, the first 10 mm of the SMA branching from the abdominal aorta were manually delineated per voxel. The center of this ROI was used to calculate the location features as described in the “Radiomics” section.

Systematic clinical evaluation by clinicians

The criteria for the systematic clinical evaluation are shown in **Supplementary Table 1**, see section on supplementary materials given at the end of this chapter. Fibrosis was classified as: grade 1 (< 10 thin radiating strands), grade 2 (> 10 thin and < 10 thick radiating strands), grade 3 (> 10 thick radiating strands) ¹⁸. Mesenteric mass staging was classified as: stage I when the mesenteric mass is located close to the intestine; stage II involves arterial branches close to the origin in the mesenteric artery; stage III extends along the SMA; and stage IV masses grow around the mesenteric artery with involvement of the first jejunal arteries ¹⁹. As mesenteric metastases are known to compromise mesenteric vasculature, vessel encasement (tumor tissue surrounding the vessel), signs of intestinal edema (thickened mucosal and submucosal layers) or bowel wall ischemia (thickened bowel wall with diminished contrast-enhancement) were also scored. The criteria were scored by five clinicians: two radiologists (Rad1 and Rad2, 15 and 5 years of experience, respectively), a nuclear medicine physician (Nucl, 4 years of experience), a surgeon (Surg, 10 years of experience), and an endocrinologist (End, 30 years of experience).

Radiomics

From both the MM and the SM segmentations, 564 features quantifying intensity, shape, and texture were extracted: these will be referred to as the MM features and the SM features, respectively. The MM and SM features total 1128 imaging features per patient. More details on the extracted features can be found in **Supplementary Materials 1** and **Supplementary Table 2**. The positions of the MM with respect to the SMA (x, y, and z) were also extracted, which we refer to as location features. These location features were used to approximate the established classification of the lymph node metastases stage ¹⁹. We included these location features since lesions more proximal to the origin of the SMA tend to be more often symptomatic ²⁰, bringing the total number of features to 1131.

To create a decision model from the features, the WORC toolbox was used, see **Fig. 1** ^{21,22}. In WORC, the decision model creation is divided in several steps, for example, feature selection, resampling and machine learning. For each step, a number of different methods are included. WORC performs an automated, exhaustive search among a variety of algorithms and their parameters to establish workflows that maximize performance

and determines which combination of algorithms maximizes the prediction performance on the training set.

Several models were created using different features to assess the predictive value of the various characteristics in predicting the development of symptomatic mesenteric mass: 1) age and sex; 2) baseline characteristics; 3) MM features; 4) SM features; 5) location features; 6) MM and SM features combined; 7) MM, SM and location features combined; 8) all features combined; and 9) similar to model₈, but excluding patients with positive enteric contrast. Model₁ and model₂ were created to assess whether simple, objective characteristics may provide information on symptom development. Model₉ was created to assess the impact of the usage of enteric contrast in the CT scans on the model performance. Even though the main area of interest is mesentery and not the bowel lumen, which is mostly affected by the contrast, the differences in appearance may influence the feature values and thus potentially bias the models. A schematic overview of the various models is given in **Table 1**. The code for both the feature extraction and creation of the decision models using WORC has been published open-source²³.

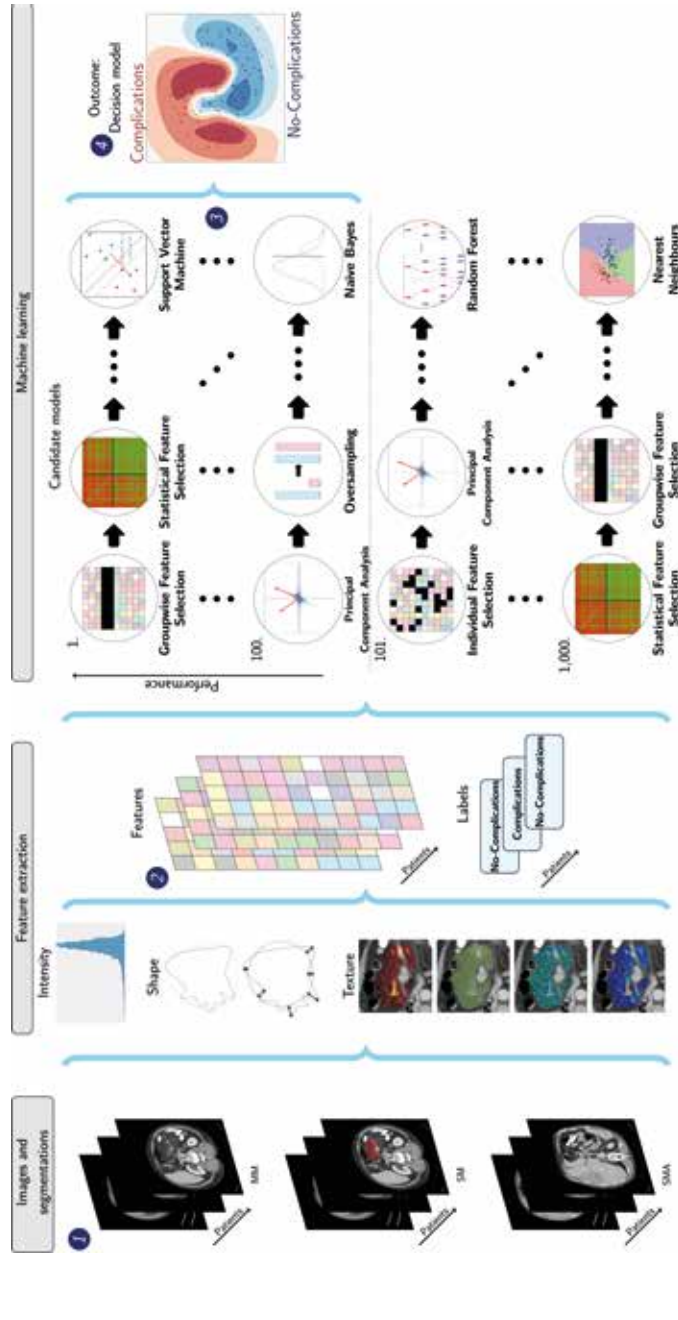
TABLE 1. Description of the nine models to assess the predictive value of various feature groups in predicting abdominal complications

Model	Enteric contrast	Radiomics features	Non-imaging features	Number of patients
Model ₁	Yes	None	Age, sex	68
Model ₂	Yes	None	All*	68
Model ₃	Yes	MM	None	68
Model ₄	Yes	SM	None	68
Model ₅	Yes	Location	None	68
Model ₆	Yes	MM, SM	None	68
Model ₇	Yes	MM, SM, Location	None	68
Model ₈	Yes	MM, SM, Location	All*	68
Model ₉	No	MM, SM, Location	All*	52

* Age, sex, tumor grade, ENETS disease stage, CgA, 5-HIAA.

CgA: serum chromogranin A, normal range < 94 µg/L; 5-HIAA: urinary 5-hydroxyindoleacetic acid excretion, normal range < 50 µmol /24 h, MM: mesenteric mass, SM: surrounding mesentery.

FIGURE 1. Schematic overview of the radiomics approach: adapted from (Vos, et al. 2019)



Processing steps include segmentation of the mesenteric mass (MM), surrounding mesentery (SM), and superior mesenteric artery (SMA) on the CT scan (1), feature extraction from the CT based on the segmentations (2), and the creation of a decision model (4), using an ensemble of the best 100 workflows from 1,000 candidate workflows (3), where the workflows are different combinations of the processing and analysis steps (e.g. the classifier used). Adapted, with permission, from Vos et al. (2019): the images under (1), texture features, numbers at (3), and output at (4) have been modified with respect to the original figure.

Comparison with clinical practice

In order to compare the performance of our model with current clinical practice, the CT scans were evaluated by the MTB from the Erasmus MC, an ENETS center of excellence. The MTB was asked to determine whether the patient was likely to develop intestinal complications due to the mesenteric mass and fibrosis within 1 year (yes / no), based on the same CT scan used for the radiomics analysis. The MTB assessed features such as bowel wall ischemia, edema, and severity of mesenteric fibrosis and vessel encasement. However, as there is no established method to use these features to guide decision-making, the features were simply assessed and expert opinion was used to determine if the patient is likely to develop intestinal complications, which resembles clinical practice.

Statistical analysis

Differences between the asymptomatic and symptomatic groups in baseline clinical characteristics were evaluated using SPSS software (version 21 for Windows, SPSS Inc.). Data were presented as the median and interquartile range (IQR; 25th–75th percentiles) or percentage with count. Continuous data were compared by using a Mann-Whitney U test. A Chi-square test was performed for the comparison of categorical data. A *P*-value of < 0.05 was considered statistically significant.

Agreement between the different raters in the systematic clinical evaluation was determined using Fleiss Kappa, where a value < 0.40 indicated poor agreement²⁴.

The statistics for the radiomics models were evaluated using the WORC software^{21,22}. To evaluate the significance of individual features, a Mann-Whitney U test was used. The *P*-values were corrected for multiple testing using the Bonferroni correction. A *P*-value of < 0.05 was considered statistically significant.

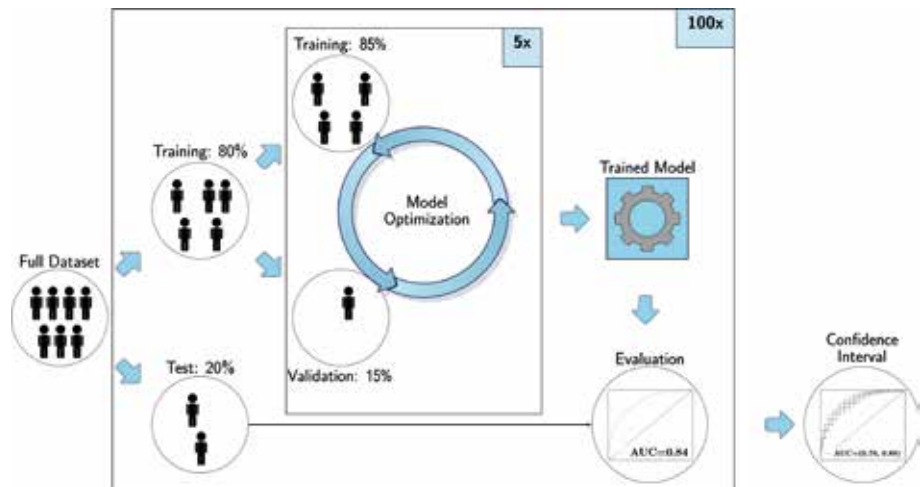
In all radiomics experiments, evaluation was implemented through a 100x random-split cross-validation, with 80% of the data used for training and 20% for independent testing, see **Fig. 2**. On the training set, another random-split cross-validation was performed, splitting the dataset in 85% for training and 15% for validation to be used for the model optimization. Hence, all optimization was done on the training dataset: the test dataset was only used for evaluation to prevent overfitting on the test dataset. In both

cross-validations, splitting was done in a stratified manner, to ensure that the balance between the asymptomatic and symptomatic groups was similar in training and test set.

To gain insight into the predictions of the model, patients were ranked from typical to atypical for both the asymptomatic and the symptomatic group, based on the model prediction consistency. This was determined by the number of times (percentage) that a patient was classified correctly when included in the test set. Typical examples for each class were defined as patients who were always classified correctly; atypical vice versa.

Performance was evaluated using the area under the receiver operating characteristic (ROC) curve (AUC), balanced classification accuracy (BCA), sensitivity, and specificity. For the radiomics models, 95% confidence intervals (CIs) on the average performance metrics over all 100 cross-validation iterations were constructed using the corrected resampled t-test, thereby taking into account that samples in the cross-validation splits are not statistically independent²⁵. ROC confidence bands were constructed using fixed-width bands²⁶. For the MTB, 95% CIs were constructed with Graphpad Software Prism using the modified Wald method. In all analyses, the symptomatic group was defined as the positive class.

FIGURE 2. Visualization of the 100x random-split cross-validation, including a second 5x random-split cross-validation within the training set in which the model optimization was conducted



Results

Dataset characteristics

A total of 68 patients was included, with 32 in the asymptomatic group and 36 in the symptomatic group. There were no significant differences between the groups in baseline clinical characteristics (**Table 2**). For the asymptomatic group, the median time between the CT scan and development of abdominal symptoms or end-of-follow-up was 70.5 months (IQR; 50 – 86 months). For the symptomatic group, the median time between CT scan and palliative surgery was 97 days (IQR; 49 – 140 days). In the symptomatic group, indications for surgery were respectively: obstruction ($n = 19$, 53%), pain ($n = 13$, 36%), ischemia ($n = 2$, 6%), and perforation ($n = 2$, 6%). For 32 patients, laparotomy findings revealed macroscopic signs of mesenteric fibrosis and, when acute pain was present preoperatively, signs of ischemia were present in 59% ($n = 19$). In the remaining four operated patients, documentation of findings during surgery was scarce.

The resulting multicenter CT dataset originated from 29 different scanners and thereby showed substantial heterogeneity in the imaging protocols (**Table 2**). Statistically significant differences in the distribution of the parameters between the CT scans of the symptomatic and the asymptomatic group were found for the use of enteric contrast, pixel spacing, tube current, and kilovoltage peak. However, the absolute differences were generally small, for example, 0.73 mm versus 0.75 mm in mean pixel spacing. Additionally, nine different reconstruction kernels were used.

Feature significance

After correcting for multiple testing, from the 1137 features (1128 imaging, 3 location, and 6 patient characteristics), 73 were found to have significant P -values (0.003 – 0.045), see **Supplementary Fig. 1**. These included only features extracted from the SM: a more detailed description of these features is given in **Supplementary Materials 2**. No shape features, thus also not the SM volume, were found to be significant.

TABLE 2. Baseline characteristics of the 68 patients. Numerical data are presented as median with inter-quartile range (IQR) in brackets. Categorical data are presented as percentages with count in brackets. *P*-values are calculated using a Mann-Whitney U test for numerical data, a Chi-square test for categorical data.

Characteristic	Symptomatic (n = 36)	Asymptomatic (n = 32)	<i>P</i> -value
Clinical			
Age	66 [55 - 74]	62 [54 - 72]	0.90
Male	56% (20)	78% (25)	0.072
CgA	343 [178 - 1057]	170 [72 - 415]	0.27
5-HIAA	163 [59 - 481]	126 [78 - 288]	0.46
Tumor grade			0.40
Grade I	56 % (20)	56 % (18)	
Grade II	31 % (11)	19 % (6)	
Unknown	14% (5)	25% (8)	
ENETS disease stage			0.15
Stage III	22% (8)	9% (3)	
Stage IV	78% (28)	91% (29)	
CT Imaging			
Enteric contrast	36% (13)	9% (3)	0.009
Pixel spacing (mm)	0.73 [0.70, 0.77]	0.75 [0.73, 0.79]	0.04
Slice thickness (mm)	3.0 [3.0, 3.25]	3.0 [3.0, 5.0]	0.19
Tube current (mA)	158 [99, 312]	271 [144, 346]	0.034
Kilovoltage peak	100 [100, 120]	120 [100, 120]	0.020
Manufacturer			0.55
Siemens	30	30	
Philips	2	1	
Toshiba	3	1	
Unknown	1	0	
Surgery indication			
Obstruction	53% (19)		
Pain	36% (13)		
Ischemia	6% (2)		
Perforation	6% (2)		

CgA: serum chromogranin A, normal range < 94 µg/L; 5-HIAA: urinary 5-hydroxyindoleacetic acid excretion, normal range < 50 µmol /24 h

Systematic evaluation by clinicians

The performance of the systematic clinical evaluation by the five raters is shown in **Table 3**; their ROC curves are shown in **Fig. 3**. While all clinicians performed better than guessing (0.5), their AUCs varied (radiologists: 0.85 and 0.76, nuclear physician: 0.71, surgeon: 0.82, endocrinologist: 0.62). Fleiss Kappa between the five clinicians on evaluating patients as asymptomatic or symptomatic was 0.15, indicating poor agreement. The agreement on the classification of the radiological features was also poor (0.06 – 0.35) (**Supplementary Table 1**).

TABLE 3. Performances of systematic evaluation by five raters and the radiomics models. The radiomics models are based on: age and gender (Model₁); all non-imaging features (Model₂); features extracted from the mesenteric mass (MM) (Model₃); features extracted from the surrounding mesentery (SM) (Model₄); only the location (Model₅); both MM and SM features (Model₆); MM, SM, and location features (Model₇); MM, SM, location, and non-imaging features (Model₈); similar to model₈ but excluding patients with positive enteric contrast (Model₉). Performance for the radiomics models was given as mean (95% CI).

Model	AUC	BCA	Specificity	Sensitivity
Radiologist 1	0.85	0.80	0.84	0.75
Radiologist 2	0.76	0.73	0.66	0.81
Nuclear physician	0.71	0.68	0.91	0.44
Surgeon	0.82	0.79	0.78	0.81
Endocrinologist	0.60	0.59	0.63	0.56
Model ₁	0.49 (0.34, 0.65)	0.50 (0.39, 0.61)	0.49 (0.23, 0.74)	0.52 (0.30, 0.73)
Model ₂	0.58 (0.44, 0.72)	0.58 (0.46, 0.70)	0.55 (0.34, 0.76)	0.61 (0.41, 0.80)
Model ₃	0.65 (0.52, 0.79)	0.61 (0.49, 0.73)	0.61 (0.43, 0.78)	0.61 (0.42, 0.81)
Model ₄	0.81 (0.72, 0.91)	0.72 (0.62, 0.82)	0.67 (0.49, 0.85)	0.78 (0.61, 0.94)
Model ₅	0.72 (0.60, 0.84)	0.63 (0.51, 0.75)	0.60 (0.41, 0.79)	0.67 (0.47, 0.87)
Model ₆	0.77 (0.64, 0.90)	0.71 (0.59, 0.83)	0.69 (0.50, 0.88)	0.73 (0.55, 0.90)
Model ₇	0.74 (0.62, 0.87)	0.68 (0.55, 0.81)	0.65 (0.45, 0.85)	0.70 (0.52, 0.88)
Model ₈	0.79 (0.66, 0.91)	0.72 (0.61, 0.82)	0.72 (0.54, 0.90)	0.71 (0.52, 0.89)
Model ₉	0.77 (0.63, 0.91)	0.69 (0.55, 0.84)	0.74 (0.54, 0.94)	0.64 (0.40, 0.88)

AUC: area under the receiver operating characteristic curve; BCA: balanced classification accuracy

Evaluation of radiomics models

The performance of the various radiomics models is shown in **Table 3**. Model₁, using only age and sex, had a poor performance (AUC of 0.49), indicating that age and sex are not related to the risk of developing intestinal complications. Inclusion of tumor grade according to WHO criteria, ENETS disease stage, CgA level, and urinary 5-HIAA excretion, that is, model₂, performed slightly better (AUC of 0.58). Among the models using radiomics features from a single ROI, model₄, including SM, had the best performance (AUC of 0.81, sensitivity of 0.78, specificity of 0.67). Interestingly, model₅, including only the location features of the MM also had fair predictive power (AUC of 0.72). Combining all imaging and location features, model₇, performed similarly (AUC of 0.74, sensitivity of 0.70, specificity of 0.65) to the model based solely on the SM. Inclusion of the patient characteristics (model₈, AUC of 0.79) did not improve the predictive power.

In our dataset, 24% ($n = 16$) of the CT scans were performed with enteric contrast. Of these patients, 18.6% ($n = 3$) were asymptomatic; hence the distribution of enteric contrast with respect to asymptomatic and symptomatic group was significantly different ($P < 0.05$, **Table 2**). Excluding these patients, that is, model₉, yielded a similar performance (AUC of 0.77).

Of the 68 patients, 35 patients (19 asymptomatic, 16 symptomatic) were always classified correctly, that is, in all 100 cross-validation iterations, by model₄, and are thus considered typical. Of these 32 typical patients, 13 patients (7 asymptomatic, 6 symptomatic) were also correctly classified by all five clinicians. Analogously, 6 patients (3 asymptomatic, 3 symptomatic) were always classified incorrectly, and thus considered atypical. In **Fig. 4**, four CT slices of such typical and atypical examples of asymptomatic and symptomatic patients are depicted. The patients with enteric contrast were both in the typical ($n = 7$) and atypical ($n = 1$) examples of both classes.

Comparison with multidisciplinary tumor board

The MTB prediction of developing intestinal complications had a specificity of 0.69 (95% CI; 0.51, 0.82), a sensitivity of 0.64 (95% CI; 0.48, 0.78), and an accuracy of 0.66 (95% CI; 0.54, 0.77). For the sake of brevity, only the ROC curves of the single-ROI model with the highest AUC, model₄, the five raters, and the MTB performance are

depicted in **Fig. 3**. The performance of the MTB was slightly below the ROC curve of the mean performance of the radiomics model over all cross-validations, but within the 95% CI.

FIGURE 3. Receiver operating characteristic curve of radiomics Model₄, based on the surrounding mesentery, and of evaluation by five clinical raters (radiologist 1 (blue), radiologist 2 (green), nuclear physician (purple), surgeon (magenta), and endocrinologist (cyan)). The performance of the multidisciplinary tumor board (MTB) is indicated by a red dot. For the radiomics model, the grey crosses identify the 95% CIs of the performance over the 100x random-split cross-validation iterations; the orange curve is fit through the mean of the CIs.

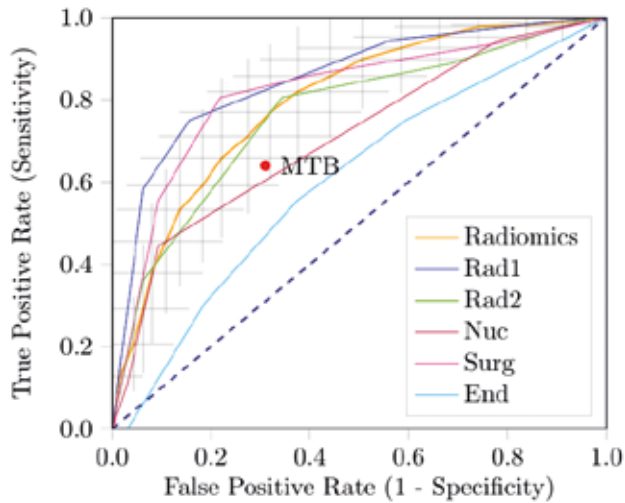
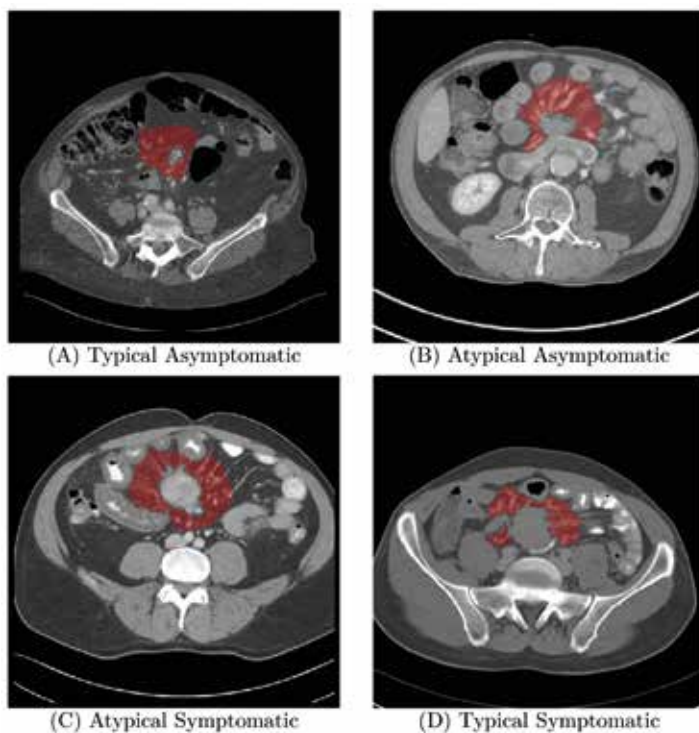


FIGURE 4. Examples of typical and atypical surrounding mesentery. The typical examples are two of the patients always classified correctly by Model₄; the atypical examples are two of the patients always classified incorrectly by Model₄.



Discussion

We evaluated both systematic clinical evaluation and a radiomics approach for reliably identifying patients who are prone to develop complications of the metastatic mesenteric mass and fibrosis, and thus may benefit from prophylactic surgery. Our results show that both the systematic clinical evaluation and our best performing radiomics model can identify these patients with a performance similar to a specialized MTB.

To date, there are no clear clinical or radiological predictors for the development of a symptomatic mesenteric mass^{7,8}. Therefore, we evaluated a wide array of clinical

characteristics and radiomics features. In contrast to other prognostic models in SI-NETs, we found that clinical characteristics such as age, sex, ENETS disease stage, tumor grade and markers had little to no predictive power for the development of a symptomatic mesenteric mass (model₁ and model₂)⁹⁻¹¹.

From the radiomics features, only SM features showed statistically significant differences between the asymptomatic and symptomatic patients. No MM or location features showed a statistically significant difference. This highlights the importance of the mesentery surrounding the metastatic mesenteric mass in the development of symptoms. In order to gain insight in the underlying profibrotic mechanisms, we analyzed the predictive features of the SM and found that most (93%) were texture features. Future detailed analysis of the relation between these features and clinical characteristics could elucidate the processes involved in the development of a symptomatic mesenteric mass and fibrosis and guide treatment development. The importance of the SM was also confirmed by the radiomics models, as the model solely using SM features (model₄) was one of the highest ranking models in terms of AUC and the performance was not improved by additional features (i.e. model₆ - model₈). Moreover, model₄ is clinically more feasible, as it only requires annotation of the surrounding mesentery. We will therefore further refer to model₄ as “the radiomics model”.

Systematic evaluation by clinicians resulted in similar discriminative power as the radiomics model. However, evaluation of the separate CT findings demonstrated poor inter-observer agreement, which is in line with findings in the literature²⁷. The relatively low degree of the overall agreement further limits the reliability of the prediction by the clinicians. The radiomics model, on the other hand, is independent of the observer and thus any personal training or experience, assuming the segmentation is reproducible. It could therefore be useful in clinics where there are no NET-specialists, to better identify patients that may benefit from prophylactic palliative surgery and refer these patients to a center of expertise. Moreover, reducing the bias in risk evaluation could aid assessment of treatment effectiveness for mesenteric metastases and fibrosis, and the development of clear guidelines for patient selection for prophylactic palliative surgery.

Some limitations to our study should be noted. *First*, although we used a multicenter imaging dataset and performed a rigorous cross-validation experiment strictly separating training from testing data, we did not validate our model on an independent, external

4

dataset. Moreover, even though our dataset was relatively large considering the rarity of SI-NETs, it was relatively small for a radiomics study²⁸, which may explain why our CIs are quite wide (e.g. the AUCs span between 20 – 30 % of the range). Additionally, testing for statistically significant differences of the AUCs through, for example, a DeLong test was not possible due to limited power. Expanding the size of the dataset may result in an increase in performance and increased statistical power. *Second*, in line with guidelines from the radiomics field²⁹, our study included CT scans over a time period of 10 years with variations in acquisition protocols. On one hand, this is a strength of our study, as the radiomics models had predictive value despite substantial acquisition variations. Moreover, as the models were trained on a wide variety of CT scanners and acquisition protocols, we expect the model to be able to accurately make predictions in a wide variety of (routine) settings. On the other hand, heterogeneity may have (negatively) affected our performance. Using a single-scanner study will limit the generalizability, but may positively impact the performance. Further research is required to evaluate the influence of acquisition parameters on the model performance. When expanding the dataset to include more patients, feature harmonization techniques such as ComBat may be employed³⁰. *Third*, our model relies on the manual annotation of the ROIs. Manual annotation can be time consuming and may lead to observer dependency of the model. Automation of the segmentation may help overcome these deficits.

To our knowledge, this is the first study that shows the potential of radiomics for the prediction of abdominal complications in SI-NETs. In our study, we used CT, as this was the preferred modality in routine clinical care³¹. Future research may investigate the potential value of other imaging modalities. The usage of magnetic resonance imaging (MRI) might be limited in this context as it holds similar information and is not routinely performed in SI-NETs³¹. On the other hand, use of nuclear imaging in SI-NETs is well-established, especially PET-CT using 68Ga-labeled somatostatin analogs³¹. Moreover, many new molecular imaging probes for the detection of fibrosis and fibrogenesis are being developed (e.g. fibroblast activation protein imaging)³²⁻³⁴. However, further research is required to evaluate the value of these imaging techniques in the context of this study, that is, for the prediction of abdominal complications in SI-NETs, potentially combined with radiomics.

Conclusion

This study used routinely acquired CT scans to identify SI-NET patients prone to the development of intestinal complications due to a metastatic mesenteric mass and fibrosis. The CT scans were analyzed by five clinicians with different levels of experience using systematic visual evaluation and a radiomics model. While all clinicians were able to identify patients at risk to some degree, the performance of the clinicians substantially varied and agreement was poor. The radiomics model is based on automatic feature extraction from contrast-enhanced CT scans and mainly driven by the appearance of the surrounding mesentery. The predictive power was similar to that of experienced clinicians and a specialized MTB. It could therefore aid in guiding the clinical decision on which patients should receive prophylactic palliative surgery.

Funding

Martijn Starmans acknowledges funding from the research program STRaTeGy (project number 14929-14930), which is (partly) financed by the Netherlands Organisation for Scientific Research (NWO). Anela Blazevic received funding from the Ipsen Fund via an unrestricted research fund. This work was carried out on the Dutch national e-infrastructure with the support of SURF Cooperative.

References

1. Wu L, Fu J, Wan L, et al. Survival outcomes and surgical intervention of small intestinal neuroendocrine tumors: a population based retrospective study. *Oncotarget*. Jan 17 2017;8(3):4935-4947.
2. Pavel M, O'Toole D, Costa F, et al. ENETS Consensus Guidelines Update for the Management of Distant Metastatic Disease of Intestinal, Pancreatic, Bronchial Neuroendocrine Neoplasms (NEN) and NEN of Unknown Primary Site. *Neuroendocrinology*. 2016;103(2):172-85.
3. Niederle B, Pape UF, Costa F, et al. ENETS Consensus Guidelines Update for Neuroendocrine Neoplasms of the Jejunum and Ileum. *Neuroendocrinology*. 2016;103(2):125-38.
4. Daskalakis K, Karakatsanis A, Hessman O, et al. Association of a prophylactic surgical approach to stage iv small intestinal neuroendocrine tumors with survival. doi: 10.1001/jamaoncol.2017.3326. *JAMA Oncol*. 2018;4(2):183-189.
5. Blazevic A, Zandee WT, Franssen GJH, et al. Mesenteric fibrosis and palliative surgery in small intestinal neuroendocrine tumours. *Endocr Relat Cancer*. Mar 2018;25(3):245-254.
6. Blažević A, Hofland J, Hofland LJ, Feelders RA, de Herder WW. Small intestinal neuroendocrine tumours and fibrosis: an entangled conundrum. *Endocr Relat Cancer*. Mar 2018;25(3):R115-R130.
7. Laskaratos F, Cox, Brian N., Woo, Wai Lok, Khalifa, M., Ewang, M., Navalkisoor, S., Quigley, A. M., Mandair, D., Caplin, M. and Toumpanakis, C. Assessment of Changes in Mesenteric Fibrosis (MF) after Peptide Receptor Radionuclide Therapy (PRRT) in Midgut Neuroendocrine Tumours (NETs). 2019:
8. Druce MR, Bharwani N, Akker SA, Drake WM, Rockall A, Grossman AB. Intra-abdominal fibrosis in a recent cohort of patients with neuroendocrine ('carcinoid') tumours of the small bowel. *QJM*. Mar 2010;103(3):177-85. doi:10.1093/qjmed/hcp191
9. Modlin IM, Gustafsson BI, Pavel M, Svejda B, Lawrence B, Kidd M. A nomogram to assess small-intestinal neuroendocrine tumor ('carcinoid') survival. *Neuroendocrinology*. 2010;92(3):143-57.
10. Fang C, Wang W, Feng X, et al. Nomogram individually predicts the overall survival of patients with gastroenteropancreatic neuroendocrine neoplasms. *Br J Cancer*. Nov 7 2017;117(10):1544-1550.

11. Pusceddu S, Barretta F, Trama A, et al. A classification prognostic score to predict OS in stage IV well-differentiated neuroendocrine tumors. *Endocr Relat Cancer*. Jun 2018;25(6):607-618.
12. Starmans MPA, Miclea RL, van der Voort SR, Niessen WJ, Thomeer MG, Klein S. Classification of malignant and benign liver tumors using a radiomics approach. presented at: SPIE Medical Imaging 2018: Image Processing; 2018;
13. Aerts HJWL, Velazquez ER, Leijenaar RTH, et al. Decoding tumour phenotype by noninvasive imaging using a quantitative radiomics approach. *Nature Communications*. 2014-6-3 2014;5doi:10.1038/ncomms5006
14. Karlo CA, Di Paolo PL, Chaim J, et al. Radiogenomics of clear cell renal cell carcinoma: associations between CT imaging features and mutations. *Radiology*. 2014 2014;270(2):464–471.
15. Yip SS, Aerts HJ. Applications and limitations of radiomics. *Phys Med Biol*. Jul 7 2016;61(13):R150-66. doi:10.1088/0031-9155/61/13/R150
16. Canellas R, Burk KS, Parakh A, Sahani DV. Prediction of Pancreatic Neuroendocrine Tumor Grade Based on CT Features and Texture Analysis. *AJR Am J Roentgenol*. Feb 2018;210(2):341-346. doi:10.2214/AJR.17.18417
17. Eisenhauer EA, Therasse P, Bogaerts J, et al. New response evaluation criteria in solid tumours: revised RECIST guideline (version 1.1). *Eur J Cancer*. Jan 2009;45(2):228-47.
18. Pantongrag-Brown L, Buetow PC, Carr NJ, Lichtenstein JE, Buck JL. Calcification and fibrosis in mesenteric carcinoid tumor: CT findings and pathologic correlation. *AM J ROENTGENOL*. 1995;164(2):387-391.
19. Öhrvall U, Eriksson B, Juhlin C, et al. Method for dissection of mesenteric metastases in mid-gut carcinoid tumors. *World J Surg*. 2000;24(11):1402-1408. doi:10.1007/s002680010232
20. Lardiere-Deguelte S, de Mestier L, Appere F, et al. Toward a Preoperative Classification of Lymph Node Metastases in Patients with Small Intestinal Neuroendocrine Tumors in the Era of Intestinal-Sparing Surgery. *Neuroendocrinology*. 2016;103(5):552-9. doi:10.1159/000441423
21. Starmans MPA. Workflow for Optimal Radiomics Classification (WORC). Accessed 17-10-2019, <https://github.com/MStarmans91/WORC>
22. Starmans MPA, van der Voort SR, Vos M, et al. Fully automatic construction of optimal radiomics workflows. In: *European Conference of Radiology (ECR) 2019*. Springer; 2019:S379.
23. Starmans MPA 2021 MesentericRadiomics. Zenodo. (available at: <https://github.com/MStarmans91/MesentericRadiomics>) (<https://doi.org/10.5281/zenodo.4916317>)

24. Bakeman R, Quera V. *Sequential Analysis and Observational Methods for the Behavioral Sciences*. Cambridge University Press; 2011.
25. Nadeau C, Bengio Y. Inference for the generalization error. 2000;307-313.
26. Macskassy SA, Provost F, Rosset S. ROC confidence bands: An empirical evaluation. *ACM*; 2005;537-544.
27. Jang HJ, Lim HK, Lee SJ, Lee WJ, Kim EY, Kim SH. Acute diverticulitis of the cecum and ascending colon: the value of thin-section helical CT findings in excluding colonic carcinoma. *AJR Am J Roentgenol*. May 2000;174(5):1397-402. doi:10.2214/ajr.174.5.1741397
28. Song J, Yin Y, Wang H, Chang Z, Liu Z, Cui L. A review of original articles published in the emerging field of radiomics. *European Journal of Radiology*. 2020/06/01/ 2020;127:108991. doi:https://doi.org/10.1016/j.ejrad.2020.108991
29. Traverso A, Wee L, Dekker A, Gillies R. Repeatability and Reproducibility of Radiomic Features: A Systematic Review. *International Journal of Radiation Oncology • Biology • Physics*. 2018/11/15 2018;102(4):1143-1158. doi:10.1016/j.ijrobp.2018.05.053
30. Fortin J-P, Parker D, Tunç B, et al. Harmonization of multi-site diffusion tensor imaging data. *NeuroImage*. 2017/11/01/ 2017;161:149-170. doi:10.1016/j.neuroimage.2017.08.047
31. Sundin A, Arnold R, Baudin E, et al. ENETS Consensus Guidelines for the Standards of Care in Neuroendocrine Tumors: Radiological, Nuclear Medicine and Hybrid Imaging. *Neuroendocrinology*. 2017;105(3):212-244. doi:10.1159/000471879
32. Montesi SB, Désogère P, Fuchs BC, Caravan P. Molecular imaging of fibrosis: recent advances and future directions. *The Journal of Clinical Investigation*. 2019;129(1):24-33. doi:10.1172/jci122132
33. Schmidkonz C, Rauber S, Atzinger A, et al. Disentangling inflammatory from fibrotic disease activity by fibroblast activation protein imaging. *Annals of the Rheumatic Diseases*. 2020;79(11):1485-1491. doi:10.1136/annrheumdis-2020-217408
34. Kratochwil C, Flechsig P, Lindner T, et al. ⁶⁸Ga-FAPI PET/CT: Tracer Uptake in 28 Different Kinds of Cancer. *Journal of Nuclear Medicine*. 2019;60(6):801-805. doi:10.2967/jnumed.119.227967

Appendix

Supplementary Material 1: Radiomics feature extraction

This supplementary material is similar to previous published studies ^{1,2}, but details relevant for the current study are highlighted.

A total of 564 radiomics features per region of interest (ROI) were used in this study. An overview of all features is provided in **Supplementary Table 2**. All features were extracted using the defaults for CT scans from the Workflow for Optimal Radiomics Classification (WORC) toolbox ³, which internally uses the PREDICT ⁴ and PyRadiomics ⁵ feature extraction toolboxes. The code to extract the features for this specific study has been published open-source ⁶. For details on the mathematical formulation of the features, we refer the reader to Zwanenburg et al. (2020) ⁷. More details on the extracted features can be found in the documentation of the respective toolboxes, mainly the WORC documentation ⁸.

Intensity features were extracted using the histogram of all intensity values within the ROIs and included several first-order statistics such as the mean, standard deviation and kurtosis. Shape features were extracted based only on the ROI, i.e. not using the image, and included shape descriptions such as the compactness, roundness and circular variance. Additionally, the volume and orientation of the ROIs were used. Texture features were extracted using the Gabor filters, Laplacian of Gaussian filters, Vessel filters ⁹, local phase filters ^{10,11}, Local Binary Patterns ¹², the Gray Level Co-occurrence Matrix ⁷, the Gray Level Size Zone Matrix ⁷, the Gray Level Run Length Matrix ⁷, the Neighbourhood Grey Tone Difference Matrix ⁷, and the Gray Level Difference Matrix ⁷.

Most of the features include parameters to be set for the extraction. Beforehand, the values of the parameters that will result in features with the highest discriminative power for the asymptomatic/symptomatic classification task are not known. Including these parameters in the workflow optimization would lead to repeated computation of the features, resulting in a redundant increase in computation time. Therefore, alternatively, these features are extracted at a range of parameters as is default in WORC. The hypothesis is that the features with high discriminative power will be selected by the feature selection methods and/or the machine learning methods. The parameters used are described in **Supplementary Table 2**.

The imaging data used in this study is multi-center, and therefore heterogeneous in terms of acquisition protocols. Especially the variations in slice thickness may cause feature values to be highly dependent on the acquisition protocol. Hence, extracting robust 3D features may be hampered by these variations, especially for low resolutions. The images were not resampled, as this would result in interpolation errors. To overcome this issue, all features were extracted per 2D axial slice and aggregated over all slices. Afterwards, several first-order statistics over the feature distributions were evaluated and used in the machine learning approach. Additionally, before feature extraction, all images were scaled to Hounsfield Units. As all images had the same unit, no additional normalization was applied.

Supplementary Table 1. Criteria for systematic evaluation whether patients with SI-NETs are symptomatic or asymptomatic. Agreement of the criteria between the five clinicians on the dataset used in this study consisting of 68 patients is indicated using Fleiss Kappa.

Characteristic	Ratings	Fleiss Kappa
Fibrosis (ordinal)	1	Grade 1
	2	Grade 2
	3	Grade 3
		0.31
Encasement of vessels (ordinal)	1	Yes
	2	Unsure
	3	No
		0.06
Lymph node location (categorical)	1	Stage I
	2	Stage II
	3	Stage III
	4	Stage IV
		0.02
Bowel wall edema (ordinal)	1	Yes
	2	Unsure
	3	No
		0.35
Bowel wall ischemia (ordinal)	1	Yes
	2	Unsure
	3	No
		0.17
Asymptomatic (ordinal)	1	Strongly disagree
	2	Disagree
	3	Neither agree or disagree
	4	Agree
	5	Strongly agree
		0.15

Supplementary Material 2: Significant features

After Bonferroni correction, 73 features had a statistically significant distribution ($P < 0.05$ in Mann-Whitney U test) in the asymptomatic and symptomatic group. The P -values and names of these features are depicted in **Supplementary Figure 1**. Several groups of features which quantify similar visual appearances in the images can be identified.

All statistically significant features were extracted from the surrounding mesentery (SM): no features from the mesenteric mass, neither the location or patient characteristics were found to be significant. Out of the 73 statistically significant features, 68 (93%) were texture features, as indicated by the blue bars. Thus, the differences between the symptomatic and asymptomatic patients are mostly explained by texture related characteristics of the surrounding mesentery, and not by characteristics of the CT intensity distribution or the shape and volume of the mesentery.

A total 64 (88%) of the statistically significant features is based on the Gray Level Co-occurrence Matrix (GLCM). In the GLCM, after discretizing the image in a fixed number of values, the co-occurrences of specific values between two pixels are counted. For counting the co-occurrences, different directions (e.g. horizontal, vertical) and spacings (e.g. one pixel, ten pixels) can be used. From the resulting GLCM matrix, several features can be computed, such as the homogeneity (uniform spreading of the counts among the different values), the dissimilarity (two values occur less equal to each other in one configuration (e.g. left low gray value – right high gray value) than the opposite (e.g. right low gray value – left high gray value), and the energy (more instances of intensity value pairs in the image that neighbor each other at higher frequencies). Using different combinations of the angle and the distance, 16 (22%) GLCM homogeneity features were significant, of which nine had the lowest P -values of all features. Hence, for the classification it seemed important whether only specific gray level values occurred often next to each other (low GLCM homogeneity), e.g. homogeneous ROI or very distinct patterns, or whether a wide variety of gray levels occurred often next to each other (high GLCM homogeneity), e.g. heterogeneous ROI or random patterns. Inspection of the distributions of these features showed that; 1) the average of the GLCM homogeneity was generally lower for the symptomatic group, indicating that generally these SMs are more homogeneous; and 2) the outliers of the GLCM homogeneity generally consisted of the asymptomatic group, indicating that symptomatic SMs generally were not extremely heterogeneous or homogeneous but rather in between.

It should be noted that the P -values presented here are not necessarily representative of which feature contribute most to the predictions made by the radiomics models. The combination of methods in the WORC toolbox allows for high order, non-linear combinations of multiple features. Hence, while a feature may have a low value in univariate testing, a multivariate combination of features (with lower univariate predictive value) may result in a better performance. Additionally, the combination of 50 workflows in the final model in WORC serves as a form of regularization to prevent the focus on a single feature (group). In this final model when using the SM features (Model 4), all feature groups as defined in Supplementary Materials 1 were approximately equally often used.

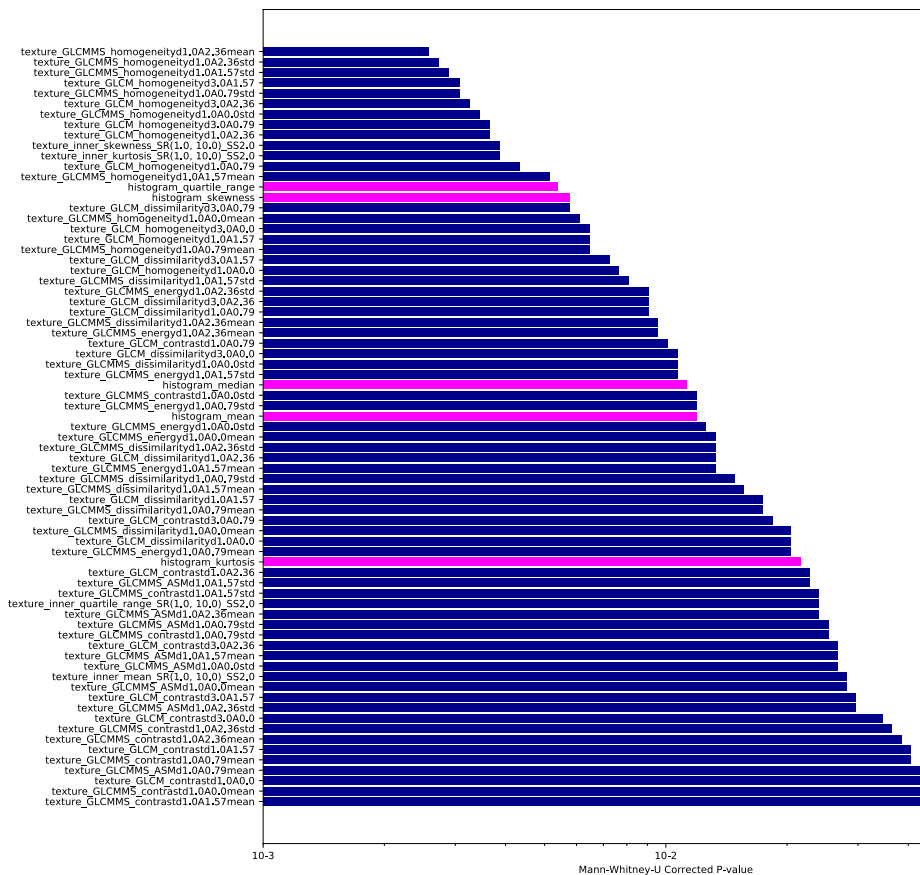
Thus, while the P -values of univariate statistical testing may give us information about the differences between asymptomatic and symptomatic patients in terms of appearance, a different combination of features may result in a better predictive performance than simply selecting the univariate most significant features.

SUPPLEMENTAL TABLE 2. Overview of the 564 features used in this study. GLCM features were calculated in four different directions (0, 45, 90, 135 degrees) using 16 gray levels and pixel distances of 1 and 3. LBP features were calculated using the following three parameter combinations: 1 pixel radius and 8 neighbours, 2 pixel radius and 12 neighbours, and 3 pixel radius and 16 neighbours. Gabor features were calculated using three different frequencies (0.05, 0.2, 0.5) and four different angles (0, 45, 90, 135 degrees). LoG features were calculated using three different widths of the Gaussian (1, 5 and 10 pixels). Vessel features were calculated using the full mask, the edge, and the inner region. Local phase features were calculated on the monogenic phase, phase congruency and phase symmetry.

Histogram (13 features)	LoG (13*3=39 features)	Vessel (12*3=39 features)	GLCM (MS) (6*3*4*2=144 features)	Gabor (13*4*3=156 features)	NGTDM (5 features)	LBP (13*3=39 features)
min	min	min	contrast (normal, MS mean + std)	min	busyness	min
max	max	max	dissimilarity (normal, MS mean + std)	max	coarseness	max
mean	mean	mean	homogeneity(normal, MS mean + std)	mean	complexity	mean
median	median	median	angular second moment (ASM) (normal, MS mean + std)	median	contrast	median
std	std	std	energy (normal, MS mean + std)	std	strength	std
skewness	skewness	skewness	correlation (normal, MS mean + std)	skewness		skewness
kurtosis	kurtosis	kurtosis		kurtosis		kurtosis
peak	peak	peak		peak		peak
peak position	peak position	peak position		peak position		peak position
range	range	range		range		range
energy	energy	energy		energy		energy
quartile	quartile	quartile		quartile range		quartile range
range	entropy	entropy		entropy		entropy
GLSZM (16 features)	GLRM (16 features)	GLDM (14 features)	Shape (35 features)	Orientation (9 features)	Local phase (13*3=39 features)	
Gray Level Non Uniformity	Gray Level Non Uniformity	Dependence Entropy	compactness (mean + std)	theta_x	min	
Gray Level Variance	Gray Level Variance	Dependence Non-Uniformity	radial distance (mean + std)	theta_y	max	
High Gray Level Zone Emphasis	High Gray Level Run Emphasis	Normalized	roughness (mean + std)	theta_z	mean	
Large Area Emphasis	Long Run Emphasis	Dependence Variance	convexity (mean + std)	COM index x	median	
Large Area High Gray Level Emphasis	Long Run High Gray Level Emphasis	Gray Level Non-Uniformity	circular variance (mean + std)	COM index y	std	
Large Area Low Gray Level Emphasis	Long Run Low Gray Level Emphasis	High Gray Level Variance	principal axes ratio (mean + std)	COM index z	skewness	
Low Gray Level Zone Emphasis	Low Gray Level Run Emphasis	High Gray Level Emphasis	elliptic variance (mean + std)	COM x	kurtosis	
SizeZoneNonUniformity	RunEntropy	Large Dependence Emphasis	solidity (mean + std)	COM y	peak	
SizeZoneNonUniformityNormalized	RunLengthNonUniformity	Large Dependence High Gray Level Emphasis	area (mean, std, min + max)	COM z	peak position	
SmallAreaEmphasis	RunLengthNonUniformityNormalized	Emphasis	volume (total, mesh, volume)		range	
SmallAreaHighGrayLevelEmphasis	RunPercentage	Large Dependence Low Gray Level Emphasis	elongation		energy	
SmallAreaLowGrayLevelEmphasis	RunVariance	Emphasis	flatness		quartile	
ZonePercentage	ShortRunEmphasis	Low Gray Level Emphasis	least axis length		entropy	
ZoneVariance	ShortRunHighGrayLevelEmphasis	Small Dependence Emphasis	major axis length			
	ShortRunLowGrayLevelEmphasis	Small Dependence High Gray Level Emphasis	minor axis length			
		Emphasis	maximum diameter 3D			
		Small Dependence Low Gray Level Emphasis	maximum diameter 2D (rows, columns, slices)			
		Emphasis	sphericity			
			surface area			
			surface volume ratio			

*Abbreviations: COM: center of mass; GLCM: gray level co-occurrence matrix; MS: multi slice; NGTDM: neighborhood gray tone difference matrix; GLSZM: gray level size zone matrix; GLRLM: gray level run length matrix; LBP: local binary patterns; LoG: Laplacian of Gaussian; std: standard deviation.

SUPPLEMENTARY FIGURE 1. Significant features



4

Supplementary References

1. Vos M, Starmans MPA, Timbergen MJM, et al. Radiomics approach to distinguish between well differentiated liposarcomas and lipomas on MRI. *The British Journal of Surgery*. 2019-12 2019;106(13):1800-1809. doi:10.1002/bjs.11410
2. Timbergen MJM, Starmans MPA, Padmos GA, et al. Differential diagnosis and mutation stratification of desmoid-type fibromatosis on MRI using radiomics. *European Journal of Radiology*. 01-10-2020 2020;131:109266. doi:10.1016/j.ejrad.2020.109266
3. Starmans MPA, Van der Voort SR, Phil T, Klein S. Workflow for Optimal Radiomics Classification (WORC). Zenodo. Accessed 12-01-2021, <https://github.com/MStarmans91/WORC>
4. van der Voort SR, Starmans MPA. Predict a Radiomics Extensive Differentiable Interchangeable Classification Toolkit (PREDICT). Zenodo. Accessed 18-11-2020, <https://github.com/Svdvoort/PREDICTFastr>
5. van Griethuysen JJM, Fedorov A, Parmar C, et al. Computational Radiomics System to Decode the Radiographic Phenotype. *Cancer Research*. 2017-11-01 2017;77(21):e104-e107. doi:10.1158/0008-5472.CAN-17-0339
6. Starmans MPA 2021 MesentericRadiomics. Zenodo. (available at: <https://github.com/MStarmans91/MesentericRadiomics>) (<https://doi.org/10.5281/zenodo.4916317>)
7. Zwanenburg A, Vallières M, Abdalah M, et al. The Image Biomarker Standardization Initiative: Standardized Quantitative Radiomics for High-Throughput Image-based Phenotyping. *Radiology*. 03/10 2020;295:191145. doi:10.1148/radiol.2020191145
8. Starmans MPA. Workflow for Optimal Radiomics Classification (WORC) Documentation. Accessed 17-07-2020, <https://worc.readthedocs.io>
9. Frangi AF, Niessen WJ, Vincken KL, Viergever MA. Multiscale vessel enhancement filtering. Springer Berlin Heidelberg; 1998:130-137.
10. Kovese P. Phase congruency detects corners and edges. 2003:
11. Kovese P. Symmetry and asymmetry from local phase. Citeseer; 1997:2-4.
12. Ojala T, Pietikainen M, Maenpaa T. Multiresolution gray-scale and rotation invariant texture classification with local binary patterns. *IEEE Transactions on Pattern Analysis and Machine Intelligence*. 2002;24(7):971-987. doi:10.1109/TPAMI.2002.1017623



Chapter 5

Sexual dimorphism in small-intestinal neuroendocrine tumors: lower prevalence of mesenteric disease in premenopausal women

5

Anela Blažević, Anand M. Iyer, Marie-Louise F. van Velthuysen, Johannes Hofland, Lindsey Oudijk, Wouter W. de Herder, Leo J. Hofland and Richard A. Feelders

J Clin Endocrinol Metab 2022, 107(5):e1969-e1975

Abstract

Context: Small intestinal neuroendocrine tumors (SI-NETs) have a modest but significantly higher prevalence and worse prognosis in male patients.

Objective: This work aims to increase understanding of this sexual dimorphism in SI-NETs.

Patients and Methods: Retrospectively, SI-NET patients treated in a single tertiary center were included and analyzed for disease characteristics. Estrogen receptor 1 (*ESR1*) and 2 (*ESR2*), progesterone receptor (*PGR*) and androgen receptor (*AR*) messenger RNA (mRNA) expression was assessed in primary tumors and healthy intestine. Estrogen receptor alpha (ER α) and AR protein expression were analyzed by immunohistochemistry in primary tumors and mesenteric metastases.

Results: Of the 559 patients, 47% were female. Mesenteric metastasis/fibrosis was more prevalent in men (71% / 46%) than women (58% / 37%, $P = 0.001$ and $P = 0.027$, respectively). In women, prevalence of mesenteric metastases increased gradually with age from 41.1% in women <50 years to 71.7% in women >70 years. Increased expression of *ESR1* and *AR* mRNA was observed in primary tumors compared to healthy intestine (both $P < 0.001$). ER α staining was observed in tumor cells and stroma with a strong correlation between tumor cells of primary tumors and mesenteric metastases ($\rho = 0.831$, $P = 0.02$), but not in stroma ($\rho = -0.037$, $P = 0.91$). AR expression was only found in stroma.

Conclusion: Sexual dimorphism in SI-NETs was most pronounced in mesenteric disease and the risk of mesenteric metastasis in women increased around menopause. The combination of increased ER α and AR expression in the SI-NET microenvironment suggests a modulating role of sex steroids in the development of the characteristic SI-NET mesenteric metastasis and associated fibrosis.

Introduction

Small intestinal neuroendocrine tumors (SI-NETs) arise from the enterochromaffin cells in the intestinal tract and have an incidence of approximately 1 per 100 000¹. SI-NETs predominantly metastasize to the liver and mesenteric lymph nodes². SI-NET mesenteric metastases are distinct as they are often surrounded by hallmark mesenteric fibrosis, which can cause severe complications such as bowel obstruction and ischemia. These mesenteric metastases are generally slow-growing and it's difficult to identify patients at risk for progressive mesenteric disease. However, our group has recently shown that sex is an important factor in predicting growth in SI-NET mesenteric metastases³.

While biological sex differences affecting incidence, prognosis and therapeutic response are well established in many cancer types, sex disparities have been scarcely investigated in NETs. However, there is accumulating data on the presence of relevant sex differences in prevalence and prognosis of NETs. Women are more likely to have a primary NET in the lung or stomach, whereas men are more likely to have a primary tumor in the small intestine or pancreas^{4,5}. Men are also more likely to present with metastasized disease at diagnosis and have a worse prognosis, even after correction for age and disease characteristics such as type of primary tumor, tumor grade and disease stage^{4,5}.

In addition to sexual dimorphism in prevalence and prognosis, hormonal influences on SI-NETs are further suggested by the studies showing efficacy of tamoxifen in SI-NETs⁶⁻⁹. Tamoxifen is a synthetic nonsteroidal selective estrogen receptor modulator primarily used in the treatment of breast cancer. Moreover, due to its antifibrotic effect it is also used in fibrotic diseases such as retroperitoneal fibrosis¹⁰. In SI-NETs, tumor growth control and amelioration of carcinoid syndrome symptoms has been described after treatment with tamoxifen⁶⁻⁹. However, these results were not replicated in a larger case series¹¹. These discrepancies could be due to variable hormone receptor expression in tumor cells and tumor microenvironment^{6,7}. Unfortunately, little is known about sex hormone receptor expression in SI-NETs. Most studies analyzing sex hormone receptor expression in NETs focused on immunohistochemical expression of estrogen receptor alpha (ER α) or progesterone receptor (PR) in pancreatic NETs, although some studies

include a subset of SI-NET patients. These studies showed that SI-NETs can express ER α , while PR expression was minimal or absent^{12,13}.

The objectives of this study were to: (1) assess sex differences in SI-NET disease characteristics such as tumor grade, age and tumor stage at diagnosis, metastatic pattern and mesenteric fibrosis and (2) evaluate expression of sex steroid hormone receptors in SI-NET primary tumors and mesenteric metastases, both in tumor cells and the surrounding tumor microenvironment.

Methods and Materials

Patients

Patients were included if they were treated at our center between 1993 and 2016 with a histologically proven SI-NET and had at least 2 contrast-enhanced computed tomography (CT) scans. The study was performed retrospectively and did not require approval from an ethics committee in the Netherlands according to the Central Committee on Research involving Human Subjects (CCMO) guidelines. Age, sex, tumor grade, tumor stage, presence of hepatic and/or mesenteric metastases and associated fibrosis and serum chromogranin A (CgA, upper limit of normal, 94 $\mu\text{g/L}$) were recorded at the time of diagnosis or at the first available moment. For correlation with mRNA expression levels, urinary 5-hydroxyindoleacetic acid (5-HIAA) excretion (upper limit of normal, 50 $\mu\text{mol/24 h}$) was recorded at the time of resection and collection of the tissue sample. Urinary 5-HIAA excretion was determined by measuring the mean urinary 5-HIAA levels in two 24-hour urine samples. Tumor grading and staging was performed in accordance with the European Neuroendocrine Tumor Society (ENETS) guideline¹⁴.

Imaging

Radiological features of mesenteric disease were assessed on routinely performed contrast-enhanced CT scans in accordance with RECIST 1.1 criteria¹⁵. A mesenteric node of ≥ 10 mm on the short axis was considered a pathological mesenteric metastases. Mesenteric fibrosis was defined as radiating strands of soft tissue in the mesentery¹⁶.

Gene Expression of Sex Steroid Receptors

Frozen tissue of 24 primary SI-NETs and adjacent normal intestine was obtained from the Erasmus MC Tissue Bank. Tissue samples were included if the tumor sample consisted of at least 80% tumor tissue and normal intestine sample contained no tumor cells or necrosis. **Table 1** shows clinical data of patients included ($n = 24$)

TABLE 1. Clinical information patients included for gene expression (messenger RNA) analysis.

	All patients ($n = 24$)
Median age, years	65 (53 – 76)
Female	12 (50 %)
Tumor grade	
Grade 1	17 (71 %)
Grade 2	7 (29 %)
Median urinary 5-HIAA, $\mu\text{mol}/24\text{h}$	190 (54 – 602)

Data are given as median (interquartile range) or n (%).

Abbreviations: 5-HIAA, urinary 5-hydroxyindoleacetic acid excretion; IQR, interquartile range

RNA was extracted from 20 cryostat sections of 20 μm . For histological confirmation of the inclusion criteria, hematoxylin-eosin staining was performed on a sequential 5 μm section. Total RNA was isolated from the specimens using the High Pure RNA Tissue Kit (Roche) according to the manufacturer's protocol. To synthesize complimentary DNA (cDNA), the RevertAid First Strand cDNA Synthesis Kit (ThermoFisher Scientific, The Netherlands) was used according to manufacturer's protocol with 500 ng of input RNA. The samples were analyzed using Taqman gene expression assays (Applied Biosystems) for expression of sex hormone receptor genes: estrogen receptor 1 (*ESR1*, gene coding for ER α), estrogen receptor 2 (*ESR2*, gene coding for ER β), progesterone receptor (*PGR*), and androgen receptor (*AR*), and 3 reference genes [hypoxanthine phosphoribosyl transferase (*HPRT1*), β -Actin (*ACTB*), and β -glucuronidase (*GUSB*)] (**Table 2**). For each sample, quantitative polymerase chain reaction (qPCR) was performed in duplicates in a 384-well plate with 4 μL cDNA, 0.5 μL Taqman primers (45 nM final concentration,

both forward and reverse) and probes (12.5 nM final concentration), and 5 mL TaqMan Universal PCR Master Mix (Applied Biosystems) in a total reaction volume of 10 μ l. The qPCR reaction was performed in a QuantStudio 7 Flex real time PCR system thermocycler (Applied Biosystems, Foster City, CA, USA). The expression of the genes of interest was normalized using the geometric mean of the expression of the 3 reference genes ¹⁷.

TABLE 2. Primers and probes used for real-time quantitative polymerase chain reaction

Gene	Assay ID	EF
<i>ACTB</i>	Hs01060665_g1	1.96
<i>AR</i>	Hs00171172_m1	1.98
<i>ERS1</i>	Hs01046816_m1	1.95
<i>ESR2</i>	Hs01100353_m1	2.51
<i>GUSB</i>	Hs00939627_m1	1.95
<i>HPRT1</i>	Hs02800695_m1	1.92
<i>PGR</i>	Hs01556702_m1	2.00

All used primers are commercially available (Thermo Fisher Scientific, Breda, The Netherlands). Abbreviations: *ACTB*: Beta-actin; *AR*: androgen receptor, *EF*: efficiency factor, *ESR1*: estrogen receptor 1, *ESR2*: estrogen receptor 2, *GUSB*: glucuronidase beta, *HPRT*: hypoxanthine phosphoribosyltransferase 1, *PGR*: progesterone receptor.

Immunohistochemistry of ER α and AR

Immunohistochemistry (IHC) for ER α and AR was performed on formalin-fixed, paraffin-embedded whole sections of primary SI-NETs and paired mesenteric metastases obtained from the Erasmus MC Tissue Bank. Samples were selected based on histopathologic review of the mesenteric metastases. Using hematoxylin-eosin-stained sections of the mesenteric metastases, the degree of fibrosis was graded based on the width of intratumoral fibrous tissue bands: no fibrosis (< 1 mm), intermediate (1-2 mm), severe (> 2 mm) ¹⁶. Patients were included if there was no mesenteric fibrosis ($n = 6$) or severe fibrosis ($n = 6$) (**Table 3**). Sequential 4 μ m thick formalin-fixed, paraffin-embedded

sections were stained for ER α (antibody ID: AB_2335977, rabbit monoclonal, dilution 1 $\mu\text{g}/\text{ml}$, clone SP1, Ventana) and AR (antibody ID:AB_2893478, rabbit monoclonal, dilution 1.55 $\mu\text{g}/\text{ml}$, clone SP107, Cell Marque) by automated IHC using the Ventana Benchmark ULTRA (Ventana Medical Systems Inc.). In brief, following deparaffinization and heat-induced antigen retrieval with CC1 (no. 950-500, Ventana) for 64 minutes the tissue samples were incubated with the antibody of interest for 32 minutes at 37°C. The staining was developed using Optiview universal DAB detection Kit (no. 760-700, Ventana), followed by hematoxylin II counterstain for 8 minutes and then a blue coloring reagent for 8 minutes according to the manufacturer's instructions (Ventana). Positive controls were used on every slide. Sections were scored independently by 2 experienced pathologists (M.F.V., L.O.). The mean percentage of staining positive cells was used for analysis. In case of a discrepancy of $\geq 25\%$, a consensus score was reached.

TABLE 3. Clinical information patients included for protein expression (immunohistochemistry) analysis.

	Mesenteric fibrosis (n = 6)	No mesenteric fibrosis (n = 6)	P-value
Median age, years	56 (49 - 65)	56 (49 - 61)	0.99
Female	3 (50 %)	3 (50 %)	1.00
Tumor grade 1	6 (100 %)	6 (100 %)	1.00
Median urinary 5-HIAA, $\mu\text{mol}/24$ hour	150 (68 - 1299)	60 (49 - 103)	0.57
ENETS disease stage			0.25
Stage III	2 (33 %)	4 (67 %)	
Stage IV	4 (67 %)	2 (33 %)	
Preoperative treatment			0.22
None	3 (50 %)	5 (83 %)	
SSA	3 (50 %)	1 (17 %)	

Data are given as median (interquartile range) or n (%).

Abbreviations: 5-HIAA, urinary 5-hydroxyindoleacetic acid excretion, normal range $<50 \mu\text{mol}/24$ hour; ENETS, European Neuroendocrine Tumor Society; SSA, somatostatin analogue.

Statistics

SPSS software (version 21 for Windows, SPSS Inc.) was used for statistical analysis. Data were presented as median and interquartile range (IQR; 25th–75th percentiles) or count with percentage. Continuous data were compared by using a Mann-Whitney U test or Wilcoxon signed-rank test for paired data. For correlation analysis, the Spearman correlation coefficient was calculated. A Chi-square test was performed for comparison of categorical data. Odds ratios (OR) for development of mesenteric metastases and fibrosis were determined by logistic regression and shown with 95% CIs. Significant predictors were further analyzed in multinomial logistic regression with interaction terms. To aid interpretation of the interaction term, we divided our patient cohort in 5 equally large age categories, with group 1, <50 years; group 2, 50 – 57 years; group 3, 57 – 63 years; group 4, 63 – 70 years; group 5, >70 years. A *P*-value of < 0.05 was considered statistically significant.

Results

Patient Characteristics

A total of 559 SI-NET patients were included, of which 47% female. As shown in **Table 4**, there were no statistically significant differences between male and female patients in tumor grade, CgA level, or ENETS disease stage. At baseline, the majority of included patients had a SI-NET grade 1 (48%) and metastatic disease (ENETS disease stage IV, 76%). There was no difference in the percentage of patients with hepatic metastases (72% in male vs. 70% in female patients). Men more frequently had mesenteric metastases (71%) and fibrosis (46%) compared to women (58% and 37%, respectively). In case of mesenteric metastases, the dominant mesenteric metastases was larger in men (median diameter of 30 mm; IQR: 24 - 40 mm) than in women (median diameter of 27 mm; IQR 20 – 36 mm). Finally, men had a higher baseline 24-hour urinary 5-HIAA excretion (median 142 $\mu\text{mol}/24\text{h}$ versus median 97 $\mu\text{mol}/24\text{h}$ in female patients, *P* = 0.001) and more often had a 24-hour urinary 5-HIAA excretion above the upper limit of normal (78% versus 71% in female patients, *P* = 0.037).

TABLE 4. Baseline characteristics

Characteristic	Men (n = 296)	Women (n = 263)	P-value
Median age, years	61 (52 – 68)	60 (52 – 69)	0.93
Age groups, years			0.41
< 50 years	57 (50%)	56 (50%)	
50 – 57 years	59 (52%)	54 (48%)	
57 – 63 years	66 (59%)	46 (41%)	
63 – 70 years	61 (56%)	48 (44%)	
> 70 years	53 (47%)	60 (53%)	
Tumor grade			0.69
Grade 1	137 (46%)	134 (51%)	
Grade II	79 (27%)	66 (25%)	
Grade III	7 (2%)	8 (3%)	
Unknown	73 (25%)	55 (21%)	
ENETS disease stage			0.29
Stage I/II	6 (2%)	13 (5%)	
Stage III	60 (20%)	53 (20%)	
Stage IV	229 (78%)	198 (75%)	
Hepatic metastases	216 (72%)	185 (70%)	0.525
Mesenteric metastases	212 (71%)	153 (58%)	0.001
Median size of largest mesenteric metastasis, mm	30 (24 – 40)	27 (20 – 36)	0.005
Mesenteric fibrosis	135 (46%)	97 (37%)	0.027
Median CgA, µg/L	215 (94 – 763)	206 (79 – 825)	0.516
Median 5-HIAA, µmol /24 hour	142 (53 – 549)	97 (36 – 373)	0.001

Data are presented as median (interquartile range) or n (%).

Abbreviations: 5-HIAA: urinary 5-HIAA excretion, normal range <50 µmol/24 hour; CgA, serum chromogranin A, normal range <94 µg/L; ENETS, European Neuroendocrine Tumor Society

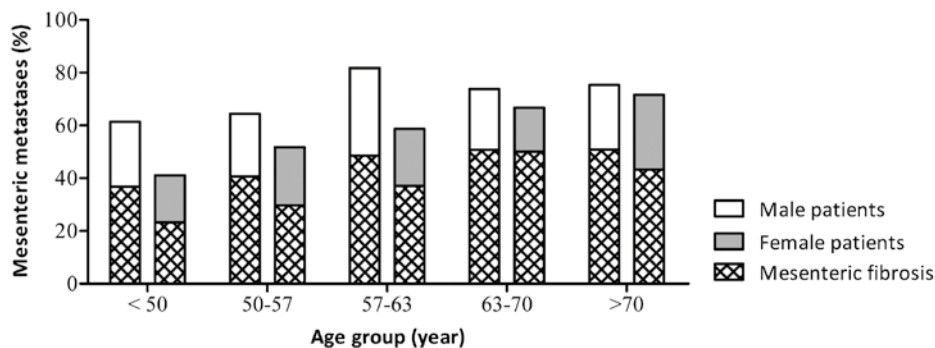
Sexual Dimorphism in Mesenteric Metastasis and Fibrosis

Male patients had an increased risk for mesenteric metastasis (OR 1.83, [95% CI: 1.29 - 2.59]) and mesenteric fibrosis (OR 1.47, [95% CI: 1.05 - 2.06]). Next, we analyzed whether the sex difference in prevalence of mesenteric metastases and fibrosis was influenced by other clinical characteristics. We performed univariate analysis for age, tumor grade, CgA serum level and 5-HIAA urinary excretion. Significant predictors for the presence of mesenteric metastases were age (OR 1.04, [95% CI: 1.03 - 1.06]) and urinary 5-HIAA excretion (OR per 100 $\mu\text{mol/l}$ 1.06, [95% CI: 1.02 - 1.10]). For the presence of mesenteric fibrosis, significant predictors were also age (OR 1.03, [95% CI: 1.01 - 1.05]) and urinary 5-HIAA excretion (OR per 100 $\mu\text{mol/l}$ 1.04, [95% CI: 1.01 - 1.07]). Tumor grade and CgA serum level were not significant predictors for mesenteric metastases or fibrosis.

When age, sex and 5-HIAA were added to a multinomial regression model, only the interaction term for female sex and age remained a significant predictor for mesenteric metastases (OR 1.04, [95% CI: 1.02 - 1.07]) and fibrosis (OR 1.04, [95% CI: 1.02 - 1.07]). To aid interpretation of the interaction term, we divided our patient cohort in 5 equally large age groups and used these age groups to show the prevalence of mesenteric metastasis and fibrosis (**Fig. 1**). In men, there is no significant difference between the age groups in prevalence of mesenteric metastases ($P = 0.80$) or fibrosis ($P = 0.428$). In contrast, in women, there is a significant difference between the age groups in the prevalence of mesenteric metastases ($P = 0.009$) and fibrosis ($P = 0.035$) with an increase of both in older patients.

Next, we focused on mesenteric fibrosis in patients with mesenteric metastases. The percentage of patients with mesenteric metastases that develop mesenteric fibrosis was not influenced by age or sex. Mesenteric fibrosis was present in 61.3% ($n = 130$) of men with mesenteric metastases and this was equal to the percentage of mesenteric fibrosis (60.1%, $n = 92$, $P = 0.82$) in women with mesenteric metastases. When assessed across the 5 age groups, there was no significant difference in the percentage of mesenteric fibrosis in patients with mesenteric metastases neither in men ($P = 0.874$) or women ($P = 0.539$), as can be appreciated in **Figure 1**.

FIGURE 1. Sexual dimorphism in prevalence of mesenteric metastases in small-intestinal neuroendocrine tumors.



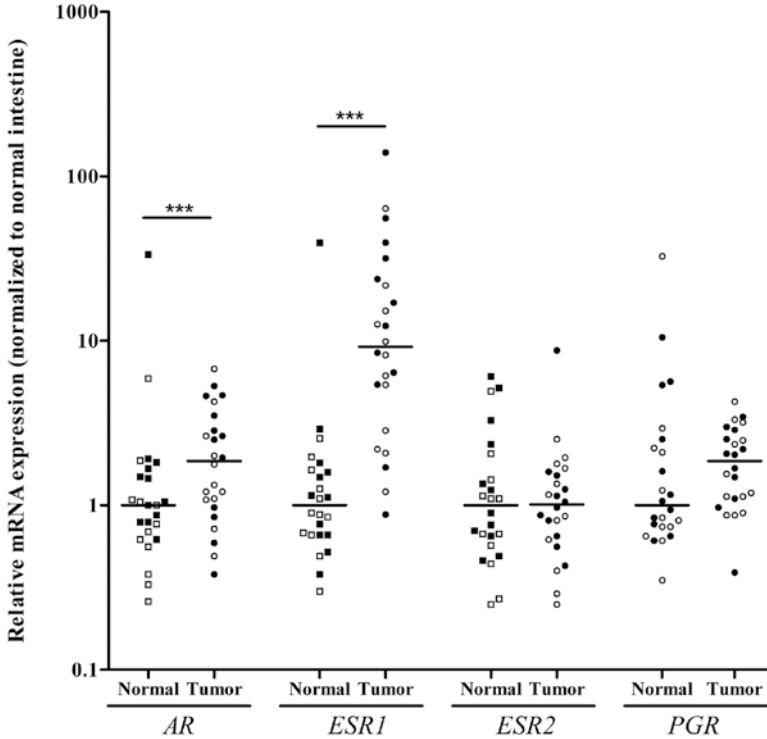
The patient cohort ($n = 559$) was divided into 5 equal age groups: <50 years, 50-57 years, 57-63 years, 63-70 years, and >70 years.

Expression of Sex Steroid Hormone Receptors in SI-NETs

As there was a sex difference in metastatic pattern of SI-NETs, we analyzed gene expression of four sex steroid hormone receptors *AR*, *ESR1*, *ESR2*, and *PGR* in 24 primary SI-NETs and in adjacent normal intestine (**Fig. 2**). There was an equal distribution of male ($n = 12$) and female patients ($n = 12$). Tumors were classified as grade 1 (71%, $n = 17$) or grade 2 (29%, $n = 7$). All 4 receptors (*AR*, *ESR1*, *ESR2* and *PGR*) were expressed in primary SI-NET and normal intestine. Expression levels did not differ between men and women or between tumor grade 1 and grade 2. *ESR1* and *AR* showed a significantly increased mRNA expression in primary SI-NETs compared to adjacent normal intestinal tissue.

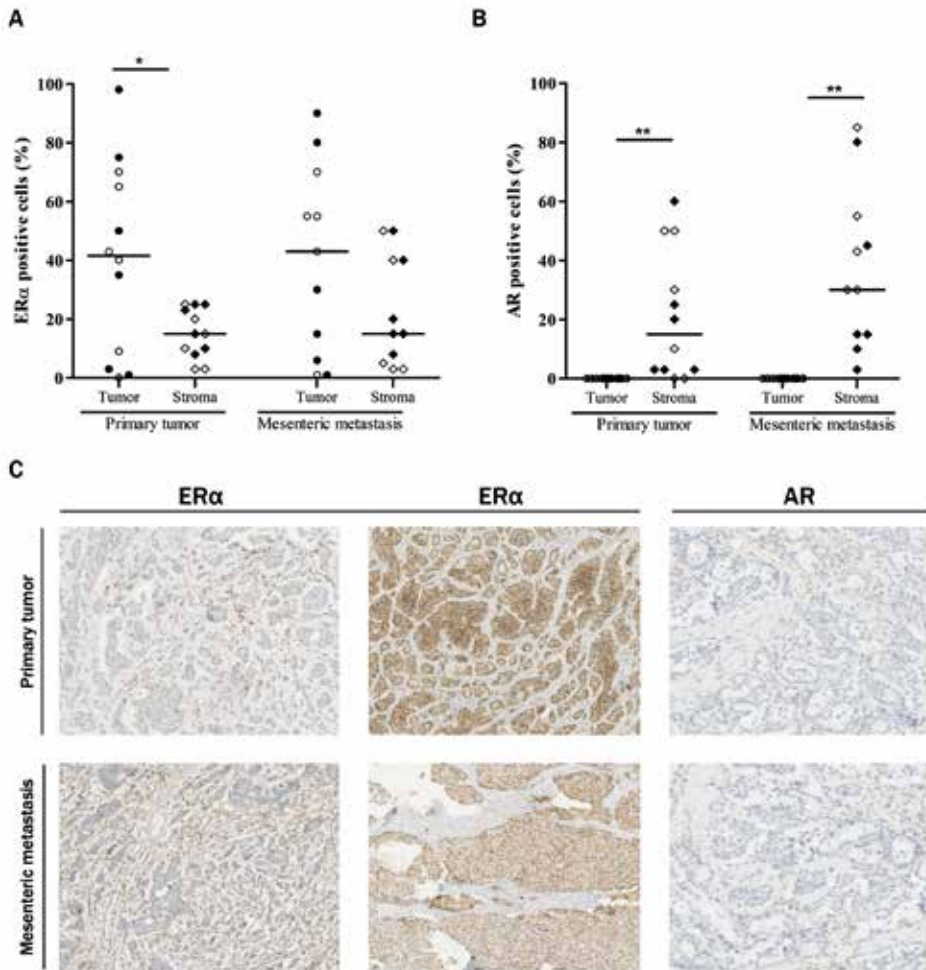
As urinary 5-HIAA excretion was significantly different between male and female patients (**Table 4**), we analyzed whether there was a correlation with *ESR1* and *AR* expression and found no correlation between urinary 5-HIAA excretion and expression of *ESR1* ($\rho = 0.179$, $P = 0.44$), nor *AR* ($\rho = 0.305$, $P = 0.18$). Finally, we assessed the ratio of *ESR1* and *AR* expression and found no differences between men and women or between tumor grade or degree of fibrosis. There was also no correlation between *ESR1/AR* ratio and urinary 5-HIAA excretion ($\rho = -0.003$, $P = 0.99$).

FIGURE 2. *AR*, *ESR1*, *ESR2*, and *PGR* messenger RNA expression in 24 primary small-intestinal neuroendocrine tumors (SI-NETs; tumor) and adjacent normal intestinal tissue (normal).



Scatter plot with individual data points shown with median (line). Clear symbols represent male patients; black symbols female patients. *** $P < 0.001$, primary SI-NET vs normal intestinal tissue.

FIGURE 3. Immunohistochemical analysis of estrogen receptor alpha (ER α) and androgen receptor (AR) expression in primary tumors and paired mesenteric metastases.



Percentage of ER α (A) and AR (B) positive tumor and stromal cells is shown by scatter plot of individual data points with median (line). Clear symbols represent male patients; black symbols represent female patients. * $P < 0.05$, ** $P < 0.01$, tumor vs stromal cells. (C) Photomicrographs of representative tissue slides of immunohistochemical staining for ER α and AR. Upper row shows primary tumors; lower row shows mesenteric metastases. The columns show, respectively, high ER α expression in stromal cells, high ER α expression in tumor cells, and AR expression in stromal cells.

Immunohistochemistry

As *ESR1* and *AR* showed significantly increased mRNA expression in primary SI-NETs, ER α and AR expression was further analyzed by IHC. IHC was performed on 12 primary tumors and paired mesenteric metastases. All primary tumors were classified as tumor grade 1, and there was an equal distribution of male ($n = 6$) and female ($n = 6$) patients. The results are shown in **Figure 3**. ER α expression was found both in tumor and stromal cells. Especially in tumor cells, there was a large variability in ER α expression level as can be appreciated in **Figure 3**. There was a strong correlation between ER α expression in tumor cells of primary tumors and tumor cells of the paired mesenteric metastases ($\rho = 0.769$, $P = 0.006$). In contrast, there was no correlation between ER α expression in the stromal compartment of primary tumors and of the paired mesenteric metastases ($\rho = -0.198$, $P = 0.56$). Generally, ER α expression tended to be higher in tumor cells than in stromal cells. In primary tumors, ER α expression was significantly higher in tumor cells compared to stromal cells (**Fig. 3A**, $P = 0.03$). The same trend could be observed in the mesenteric metastases ($P = 0.12$). There were no sex differences in ER α expression in primary tumors (tumor cells: $P = 0.82$, stromal cells: $P = 0.33$), nor in mesenteric metastases (tumor cells: $P = 0.79$, stromal cells: $P = 0.43$).

In contrast to ER α , AR expression was only found in stromal cells (**Fig. 3B**). Tumor cells showed no AR positivity. To understand the significant higher mRNA expression in primary SI-NETs compared to healthy intestine (**Fig. 2**), we also assessed the healthy intestine and found no AR expression in glandular cells and sparse AR positivity in stromal cells. The level of stromal AR expression in primary tumors did not correlate with stromal AR expression of paired mesenteric metastases ($\rho = -0.187$, $P = 0.58$). Seven primary tumors and 10 mesenteric metastases had $\geq 10\%$ AR-positive stromal cells. However, there was no significant difference between stromal AR expression in primary tumors and paired mesenteric metastases ($P = 0.18$). Also, there was no sex difference in AR expression in primary tumors ($P = 0.74$) or in mesenteric metastases ($P = 0.24$).

Discussion

It has been demonstrated that SI-NETs have a modest but significantly higher prevalence and worse prognosis in male patients ^{4,5}. In this study, we aimed to examine this sexual dimorphism in greater detail. In our cohort of SI-NET patients, we also found a slight predominance of men. However, there were no sex differences in tumor grade and disease stage, the two most established prognostic factors for SI-NETs ¹⁴. There was a sexual dimorphism in the metastatic pattern. SI-NETs predominantly metastasize to the liver and mesentery, and while there was no sex difference in percentage of hepatic metastases, men significantly more often had mesenteric metastases. As mesenteric metastases are associated with a worse prognosis, even independently from the presence of mesenteric fibrosis, this could contribute to the worse prognosis in male SI-NET patients ¹⁸. Interestingly, the protective effect of female sex was most pronounced in women younger than 50 years and dissipated with increasing age. As this is in line with sex hormone changes during the lifetime of women, it might suggest a mesentery-specific effect of sex hormones, particularly estradiol.

To gain insight in the possible underlying mechanism of the sexual dimorphism in mesenteric metastatic risk, we assessed sex steroid hormone receptor expression. In accordance with previous studies, we found that SI-NETs have a highly variable ER α expression in tumor cells that strongly correlates between primary tumor and metastases ^{12,13}. The role of ER α signaling on tumor growth and fibrogenesis in SI-NETs is scarcely investigated. However, earlier studies showing clinical effect of tamoxifen on tumor growth and hormonal secretion symptoms suggest involvement of ER α signaling in these processes. Moreover, the highly variable expression of ER α in SI-NETs could explain the inconsistent results of tamoxifen treatment in SI-NET ^{6-9,11}.

However, to understand the sexual dimorphism in mesenteric metastatic potential, we also need to look at the tumor microenvironment. The tumor microenvironment is essential for supporting tumor growth and metastasis, and can contribute to treatment efficiency or resistance ¹⁹. We found ER α and AR protein expression in stromal cells of SI-NETs. The effect of ER α and AR on the tumor microenvironment and risk of developing metastasis is most studied in cancers of the reproductive system such as breast and prostate cancer. In general, ER α signaling attenuates metastatic potential by reducing

epithelial-to-mesenchymal transition (EMT). This is effected by inhibition of regulators such as transforming growth factor beta (TGF- β), which is also an important proliferative and profibrotic growth factor in SI-NETs^{20,21}. On the other hand, AR signalling is known to stimulate metastatic potential by inducing EMT and stimulating angiogenesis²²⁻²⁴. It might be hypothesized that the ratio of ER α and AR activation, determined by exposure to estrogens and androgens, may in part explain sex differences in mesenteric metastatic potential.

Interestingly, in stromal cells of SI-NETs, the expression levels of both ER α and AR are not correlated between primary tumors and paired mesenteric metastases. There was a trend to increased expression of both receptors in the stromal cells of mesenteric metastases. This may suggest that the mesentery is more sensitive to differences in sex hormone levels than other organs, making the protective effects of ER α signaling on SI-NET metastasis most noticeable in the mesentery. The gradual increase in prevalence of mesenteric metastases over the years in women, instead of a sharp increase after menopause shown in this study, may be explained by the very slow growth rate of mesenteric metastases³.

The sexual dimorphism in metastatic pattern and the reduced rate of mesenteric metastases in premenopausal women with SI-NETs are important findings as it could help understand sex-specific risk and guide personalized treatment management. However, this study has several limitations. The study is based on data from a single tertiary center. Therefore, validation in other cohorts is needed. Further, the number of tumor samples used for IHC analysis was limited, affecting the observation of possible significant differences. Therefore, further research is necessary to determine the effects of estrogen and androgen signaling in tumorigenic processes and the potential of hormonal treatments such as tamoxifen in SI-NETs.

Conclusion

In this study we examined sex differences between SI-NET patients and found a pronounced difference in mesenteric disease. Women have a lower risk of mesenteric metastases, and this difference is most pronounced in premenopausal women. There was no sex difference in the prevalence of hepatic metastases or in the overall percentage of metastasized disease. Nor was there a sex difference in prevalence of mesenteric fibrosis in patients with mesenteric metastases. We showed that SI-NETs have increased *ESR1* and *AR* gene expression compared to healthy intestinal tissue. SI-NET tumor cells only had ER α protein expression, while in stromal cells both ER α and AR protein expression was found. The expression level of ER α and AR in stroma of mesenteric metastases tended to be higher and did not correlate to expression in the primary tumor. This suggests that sex hormone signaling pathways might be new and important players involved in modulating metastatic processes in SI-NETs.

References

1. Hofland J, Kaltsas G, de Herder WW. Advances in the Diagnosis and Management of Well-Differentiated Neuroendocrine Neoplasms. *Endocr Rev.* Apr 1 2020;41(2):371-403.
2. Pavel M, O'Toole D, Costa F, et al. ENETS Consensus Guidelines Update for the Management of Distant Metastatic Disease of Intestinal, Pancreatic, Bronchial Neuroendocrine Neoplasms (NEN) and NEN of Unknown Primary Site. *Neuroendocrinology.* 2016;103(2):172-85.
3. Blažević A, Brabander T, Zandee WT, et al. Evolution of the Mesenteric Mass in Small Intestinal Neuroendocrine Tumours. *Cancers.* 2021;13(3):443.
4. Yao JC, Hassan M, Phan A, et al. One Hundred Years After "Carcinoid": Epidemiology of and Prognostic Factors for Neuroendocrine Tumors in 35,825 Cases in the United States. *Journal of Clinical Oncology.* 2008;26(18):3063-3072. doi:10.1200/jco.2007.15.4377
5. Hallet J, Law CHL, Cukier M, Saskin R, Liu N, Singh S. Exploring the rising incidence of neuroendocrine tumors: A population-based analysis of epidemiology, metastatic presentation, and outcomes. *Cancer.* 2015;121(4):589-597. doi:10.1002/cncr.29099
6. Biasco E, Antonuzzo A, Galli L, et al. Small-Bowel Neuroendocrine Tumor and Retroperitoneal Fibrosis: Efficacy of Octreotide and Tamoxifen. *Tumori Journal.* 2015;101(1):e24-e28. doi:10.5301/tj.5000259
7. Arganini M, Spinelli C, Cecchini GM, Miccoli P. Long term treatment with tamoxifen for metastatic carcinoid tumor. *Acta Chir Belg.* 1989 Jul-Aug 1989;89(4):209-211.
8. Myers CF, Ershler WB, Tannenbaum MA, Barth R. Tamoxifen and Carcinoid Tumor. doi: 10.7326/0003-4819-96-3-383_1. *Annals of Internal Medicine.* 1982/03/01 1982;96(3):383-383. doi:10.7326/0003-4819-96-3-383_1
9. Stathopoulos GP, Karvountzis GG, Yiotis J. Tamoxifen in carcinoid syndrome. *N Engl J Med.* Jul 2 1981;305(1):52.
10. van Bommel EF, Hendriks TR, Huiskes AW, Zeegers AG. Brief communication: tamoxifen therapy for nonmalignant retroperitoneal fibrosis. *Ann Intern Med.* Jan 17 2006;144(2):101-6.
11. Moertel CG, Engstrom PF, Schutt AJ. Tamoxifen Therapy for Metastatic Carcinoid Tumor: A Negative Study. doi: 10.7326/0003-4819-100-4-531. *Annals of Internal Medicine.* 1984/04/01 1984;100(4):531-532. doi:10.7326/0003-4819-100-4-531
12. Zimmermann N, Lazar-Karsten P, Keck T, et al. Expression Pattern of CDX2, Estrogen and Progesterone Receptors in Primary Gastroenteropancreatic Neuroendocrine Tumors and Metastases. *Anticancer Res.* Mar 2016;36(3):921-4.

13. Arnason T, Sapp HL, Barnes PJ, Drewniak M, Abdolell M, Rayson D. Immunohistochemical expression and prognostic value of ER, PR and HER2/neu in pancreatic and small intestinal neuroendocrine tumors. *Neuroendocrinology*. 2011;93(4):249-58.
14. Niederle B, Pape UF, Costa F, et al. ENETS Consensus Guidelines Update for Neuroendocrine Neoplasms of the Jejunum and Ileum. *Neuroendocrinology*. 2016;103(2):125-38.
15. Eisenhauer EA, Therasse P, Bogaerts J, et al. New response evaluation criteria in solid tumours: revised RECIST guideline (version 1.1). *Eur J Cancer*. Jan 2009;45(2):228-47.
16. Pantongrag-Brown L, Buetow PC, Carr NJ, Lichtenstein JE, Buck JL. Calcification and fibrosis in mesenteric carcinoid tumor: CT findings and pathologic correlation. *AJR Am J Roentgenol*. Feb 1995;164(2):387-91.
17. Vandesompele J, De Preter K, Pattyn F, et al. Accurate normalization of real-time quantitative RT-PCR data by geometric averaging of multiple internal control genes. *Genome Biol*. Jun 18 2002;3(7):RESEARCH0034.
18. Laskaratos FM, Diamantopoulos L, Walker M, et al. Prognostic Factors for Survival among Patients with Small Bowel Neuroendocrine Tumours Associated with Mesenteric Desmoplasia. *Neuroendocrinology*. 2018;106(4):366-380. doi:10.1159/000486097
19. Cuny T, de Herder W, Barlier A, Hofland LJ. Role of the tumor microenvironment in digestive neuroendocrine tumors. *Endocr Relat Cancer*. Nov 1 2018;25(11):R519-R544.
20. Piperigkou Z, Karamanos NK. Estrogen receptor-mediated targeting of the extracellular matrix network in cancer. *Semin Cancer Biol*. May 2020;62:116-124.
21. Blažević A, Hofland J, Hofland LJ, Feelders RA, de Herder WW. Small intestinal neuroendocrine tumours and fibrosis: an entangled conundrum. *Endocr Relat Cancer*. Mar 2018;25(3):R115-R130.
22. Zhu ML, Kyprianou N. Role of androgens and the androgen receptor in epithelial-mesenchymal transition and invasion of prostate cancer cells. *FASEB J*. Mar 2010;24(3):769-77.
23. Cai J, Hong Y, Weng C, Tan C, Imperato-McGinley J, Zhu YS. Androgen stimulates endothelial cell proliferation via an androgen receptor/VEGF/cyclin A-mediated mechanism. *Am J Physiol Heart Circ Physiol*. Apr 2011;300(4):H1210-21.
24. Yoshida S, Aihara K, Ikeda Y, et al. Androgen receptor promotes sex-independent angiogenesis in response to ischemia and is required for activation of vascular endothelial growth factor receptor signaling. *Circulation*. Jul 2 2013;128(1):60-71.

6



Chapter 6

Aberrant tryptophan metabolism in stromal cells is associated with mesenteric fibrosis in small intestinal neuroendocrine tumors

Anela Blažević, Anand M. Iyer, Marie-Louise F. van Velthuysen, Johannes Hofland, Peter M. van Koestveld, Gaston J. H. Franssen, Richard A. Feelders, Marina Zajec, Theo M. Luiders, Wouter W. de Herder and Leo J. Hofland

Abstract

Background: Increased levels of serotonin secretion are associated with mesenteric fibrosis (MF) in small intestinal neuroendocrine tumors (SI-NETs). However, the profibrotic potential of serotonin differs between patients and in this study, we aimed to gain an understanding of the mechanisms underlying this variability. To this end, we analyzed the proteins involved in tryptophan metabolism in SI-NETs.

Methods: Proteomes of tumor and stroma from primary SI-NETs and paired mesenteric metastases of patients with MF ($n = 6$) and without MF ($n = 6$) were identified by liquid chromatography-mass spectrometry (LC-MS). The differential expression of proteins involved in tryptophan metabolism between patients with and without MF was analyzed. Concurrently, monoamine oxidase A (MAO-A) expression was analyzed in the tumor and stromal compartment by immunohistochemistry (IHC) and reported as intensity over area (I/A).

Results: Of the 42 proteins involved in tryptophan metabolism, 20 were detected by LC-MS. Lower abundance of ten proteins was found in the mesenteric metastases stroma in patients with MF. No differential expression was found in primary SI-NETs. In patients with MF, IHC showed lower MAO-A expression in the stroma of the primary SI-NETs (median 4.2 I/A vs. 6.5 I/A in patients without MF, $P = 0.003$) and mesenteric metastases (median 2.1 I/A vs. 2.8 I/A in patients without MF, $P = 0.019$).

Conclusion: We found a decreased expression of tryptophan and serotonin-metabolizing enzymes in the stroma in patients with MF, most notably in the mesenteric stroma. This might result in an increased profibrotic potential of serotonin and explain the variability in the development of SI-NET-associated fibrotic complications.

Introduction

Small intestinal neuroendocrine tumors (SI-NETs) are accompanied by specific clinical pathology, most notable carcinoid syndrome and fibrotic complications such as carcinoid heart disease and mesenteric fibrosis (MF) ¹. There is a lack of medical treatment options to prevent or reduce symptoms, in particular, for the fibrotic complications². Increased understanding of the pathobiology of these fibrotic complications is key to develop effective treatment options.

It is well established that SI-NETs secrete a wide array of bioactive molecules, with a central role for the bioamine serotonin ^{2,3}. Serotonin signaling is involved in various biological processes. Importantly, it can promote fibrosis development in various tissues ⁴. Serotonin production by SI-NETs is often measured on a systemic level by the urinary excretion of 5-hydroxyindoleacetic acid (5-HIAA), the main serotonin metabolite ⁵. Increased 5-HIAA urinary excretion in SI-NETs is associated with fibrotic complications. However, even though serotonin seems to be an important driver of SI-NET-associated fibrotic complications, several questions remain unanswered. First, it is unclear why certain locations, that is heart valves and mesentery, are more susceptible to the profibrotic effect of serotonin. Second, contrary to carcinoid heart disease, increased 5-HIAA excretion levels are a poor predictor for the individual risk of mesenteric fibrosis development ^{2,6}. Since 5-HIAA excretion levels do not necessarily correspond with local serotonin levels, this suggests an important role for paracrine serotonin signaling in SI-NET-associated mesenteric fibrosis ⁴.

We hypothesize that individual susceptibility for mesenteric fibrosis could be influenced by the local tumor microenvironment. Tryptophan metabolism is involved in the synthesis and catabolism of serotonin⁷. Individual differences in this process could explain the variable risk for mesenteric fibrosis, as a decreased serotonin catabolism would result in increased serotonin signaling in the tumor microenvironment ⁸. To investigate this further, we analyzed the proteome of SI-NETs and their microenvironment in patients with and without MF for proteins involved in the tryptophan metabolism by liquid chromatography–mass spectrometry (LC-MS).

Methods

Sample selection

Patients were included from the Erasmus Medical Center NET database. The study was performed retrospectively, and, according to the guidelines of the Central Committee on Research involving Human Subjects, this does not require approval from an ethics committee in the Netherlands. Patients were selected for inclusion if they underwent a resection of a pathologically proven primary SI-NET with metastasectomy of the dominant mesenteric node at the Erasmus Medical Center between 2008 and 2016¹. The dominant mesenteric node needed to be ≥ 10 mm on the short axis on a preoperative contrast-enhanced CT scan.

This group of 72 patients was assessed for mesenteric fibrosis on the preoperative CT scan and on 4- μ m thick formalin-fixed, paraffin-embedded (FFPE), hematoxylin and eosin (HE)-stained sections of the largest mesenteric metastasis. Radiological MF was defined as the presence of radiating soft tissue strands in the mesentery and no radiological MF was defined as no radiating strands of soft tissue visible on CT scan. Histological assessment classified mesenteric metastases with intratumoral fibrous bands > 2 mm as severe MF while those with intratumoral fibrous bands < 0.5 mm were classified as no-MF⁹. Patients were included in the MF group ($n = 6$) if there was radiological evidence for MF and severe MF on histological assessment. As sex is correlated with the risk of mesenteric disease, we selected an equal number of male and female patients¹⁰. The non-MF group consisted of matched patients (age, sex and tumor grade according to World Health Organization, $n = 6$) without MF on radiological and histological assessment.

Sample collection and data acquisition

FFPE tissue samples of the primary tumor and mesenteric metastasis from the first intestinal resection with mesenteric metastectomy were selected. Sections of 10 μ m were attached to a polyethylene naphthalate slide (Carl Zeiss MicroImaging, Munich, Germany) and HE stained. The tissue samples were collected as described previously¹¹. Briefly, the tissue samples were separated by laser capture microdissection in tumor and stromal components using Zeiss PALM MicroBeam IV LCM microscope (Carl Zeiss MicroImaging, GmbH). This resulted in four samples for each patient: tumor cells of

primary tumor, tumor cells of mesenteric metastasis, stromal cells of primary tumor and stromal cells of mesenteric metastasis. For each sample, an area of $\sim 2 \text{ mm}^2$ that corresponds to $\sim 20,000$ cells was collected in a 0.5 mL opaque AdhesiveCap tube (Carl Zeiss MicroImaging). Following collection, the microdissected samples were dissolved in 20 μL of 0.1% RapiGest SF (Waters, Milford, MA, USA) and transferred into LoBind Eppendorf tubes (Eppendorf AG, Hamburg, Germany) and were digested with trypsin. LC-MS measurements were performed on an RSLC nano LC system (Thermo Fisher Scientific) coupled to an Orbitrap Fusion Tribrid Mass Spectrometer (Thermo Fisher Scientific) as described previously¹². Briefly, 10 μL of digest was loaded onto a trap column (C18 PepM¹²ap, 300 μm ID x 5 mm, 5 μm , 100 \AA) and desalted for 10 min using 0.1% TFA at a flow rate of 20 $\mu\text{L}/\text{min}$. Trap column was switched in-line with an analytical column (PepMap C18, 75 μm ID x 250 mm, 2 μm , 100 \AA) and peptides were eluted using a binary 90' gradient increasing solvent B from 4 to 38%, whereby solvent A was 0.1% formic acid, solvent B 80% acetonitrile and 0.08% formic acid, flow rate 300 nL/min and column temperature 40°C. For electrospray ionization, nano ESI emitter (New Objective) was used and a spray voltage of 1.7 kV was applied. A data-dependent acquisition MS method was used with an orbitrap survey scan (range 375 - 1500 m/z, 120,000 resolution, AGC target 400,000), followed by consecutive isolation, fragmentation (HCD, 30% NCE) and detection (ion trap, AGC 10,000) of the peptide precursors detected in the survey scan until a duty cycle time of 3" was exceeded ('Top Speed' method). Precursor masses that were selected once for MS/MS were excluded for subsequent fragmentation for 60". Acquired data has been made publicly available through the ProteomeXchange Consortium using the PRIDE identifier PXD029979¹³. MS/MS spectra from the raw data files of each sample were converted into MGF files using ProteoWizard (version 3.0). MGF peak list files were used to carry out searches using Mascot (version 2.3.02) against the Uniprot database (selected for *Homo sapiens*, downloaded 15 November 2015, 20,194 entries). Carbamidomethylation (+57 Da) of cysteine was set as the fixed modification and hydroxylations (+16 Da) of proline, lysine, and methionine were included as variable modifications. Mascot search results were further analyzed in Scaffold (v4.6.2, Portland, OR, USA) with protein confidence levels set to a 1% false discovery rate (FDR), at least two peptides per protein, and a 1% FDR at the peptide level. FDRs were estimated by inclusion of a decoy database

search generated by Mascot. A Protein Report exported from Scaffold was used for data analysis. To analyze the components of tryptophan metabolism, the identified proteins were cross-referenced with genes from the tryptophan metabolism pathway hsa00380 of the Kyoto Encyclopedia of Genes and Genomes (KEGG) pathway database (<http://www.genome.jp/kegg/pathway.html>).

Validation of monoamine oxidase A expression

Immunohistochemistry (IHC) for monoamine oxidase A (MAO-A) was performed on FFPE whole sections of all the analyzed primary tumors and mesenteric metastases. Sequential 4 μm thick FFPE sections were stained for MAO-A (EPR7101, ab126751, 1:3200, Abcam) by automated IHC using the Ventana Benchmark ULTRA (Ventana Medical Systems Inc.). In brief, following deparaffinization and heat-induced antigen retrieval with CC1 (no. 950-500, Ventana) for 64 min the tissue samples were incubated with the antibody of interest for 32 min at 37°C. The staining was developed using Optiview universal DAB detection Kit (no. 760-700, Ventana), followed by hematoxylin II counterstain for 8 min and then a blue coloring reagent for 8 min according to the manufacturer's instructions (Ventana). Positive controls were used on every slide.

Immunohistochemically stained samples were digitalized and four fields of view were representatively selected. Each field of view was exported as an image file on a 10x magnification scale and contained both tumor cells and stroma. The exported images were analyzed using the CellProfiler software (version 3.0, www.cellprofiler.org)¹⁴. Each image was manually segmented into the tumor and stromal compartments and the average intensity of DAB staining of the segmented area (I/A) was noted.

Statistics

Baseline patient characteristics and IHC data were presented as a median with interquartile range (IQR; 25th–75th percentiles) or as a percentage with count. Differential protein expression between MF and non-MF samples of the four groups (tumor cells of primary tumor, tumor cells of mesenteric metastasis, stromal cells of primary tumor and stromal cells of mesenteric metastasis) was determined using the spectral index (SpI) calculation. SpI is a metric calculated by the abundance of spectral

counts in each group relative to the number of samples in which it is detectable. We have used SpI as it has a higher sensitivity to detect differential protein expression compared to several other methods¹⁵. The significance of a given SpI is determined by permutation testing of the whole dataset¹⁵. In our study, an FDR of 1% corresponded with the absolute SpI threshold of 0.60. Continuous data were compared by using a Mann-Whitney U test or Wilcoxon signed-rank test for paired data. A *P*-value of < 0.05 was considered statistically significant.

Results

Dataset characteristics

For this study, 12 SI-NET patients were included. The baseline characteristics are shown in **Table 1**. There were no significant differences between the MF and non-MF patients with respect to age, sex, tumor grade, urinary 5-HIAA excretion, ENETS disease stage or preoperative medical treatment.

TABLE 1. Baseline characteristics

	MF (n = 6)	Non-MF (n = 6)	<i>P</i> -value
Median age (IQR) – years	56 (49 – 65)	56 (49 – 61)	0.99
Female, n (%)	3 (50 %)	3 (50 %)	1.00
Tumor grade 1, n (%)	6 (100 %)	6 (100 %)	1.00
Median urinary 5-HIAA (IQR), μmol/24h	150 (68 – 1299)	60 (49 – 103)	0.57
ENETS disease stage, n (%)			0.25
Stage III	2 (33 %)	4 (67 %)	
Stage IV	4 (67 %)	2 (33 %)	
Preoperative treatment, n (%)			0.22
None	3 (50 %)	5 (83 %)	
SSA	3 (50 %)	1 (17 %)	
Surgery indication, n (%)			0.26
Curative	1 (17%)	4 (67%)	
Palliative - prophylactic	3 (50%)	2 (33%)	
Palliative – symptomatic	2 (33%)	N/A	

5-HIAA: urinary 5- hydroxyindoleacetic acid excretion, normal range < 50 μmol /24 h,
SSA: somatostatin analogue

TABLE 2. Results of spectral index analysis comparing fibrotic and non-fibrotic samples

Protein	Gene	Primary tumor		Mesenteric metastasis	
		Tumor	Stroma	Tumor	Stroma
Acetyl-CoA acetyltransferase, mitochondrial	<i>ACAT1</i>	0.01	0.29	-0.08	-0.74
Acetyl-CoA acetyltransferase, cytosolic	<i>ACAT2</i>	0.39	N/A	0.17	N/A
Aldehyde dehydrogenase X, mitochondrial	<i>ALDH1B1</i>	-0.27	0.14	-0.53	-0.33
Aldehyde dehydrogenase, mitochondrial	<i>ALDH2</i>	0.02	0.07	0.04	-0.36
Aldehyde dehydrogenase family 3 member A2	<i>ALDH3A2</i>	0.57	N/A	0.06	N/A
Alpha-aminoadipic semialdehyde dehydrogenase	<i>ALDH7A1</i>	0.13	-0.26	-0.08	-0.50
4-trimethylaminobutyraldehyde dehydrogenase	<i>ALDH9A1</i>	-0.02	-0.17	0.09	-0.58
Amiloride-sensitive amine oxidase	<i>AOC1</i>	0.32	-0.11	0.48	-0.59
Catalase	<i>CAT</i>	0.19	-0.36	0.12	-0.83
Aromatic-L-amino-acid decarboxylase	<i>DDC</i>	0.03	-0.05	-0.11	-0.52
Dihydropolyl dehydrogenase	<i>DLD</i>	0.14	0.15	-0.13	-0.50
Dihydropolyllysine-residue succinyltransferase component	<i>DLST</i>	0.02	0.16	0.16	-0.83
Enoyl-CoA hydratase, mitochondrial	<i>ECHS1</i>	0.12	-0.14	-0.04	-0.67
3-hydroxyanthranilate 3,4-dioxygenase	<i>HAAO</i>	0.26	0.48	-0.63	-0.61
Hydroxyacyl-coenzyme A dehydrogenase, mitochondrial	<i>HADH</i>	0.19	-0.33	0.00	-0.17
Trifunctional enzyme subunit alpha, mitochondrial	<i>HADHA</i>	0.21	0.03	0.03	-0.95
Monoamine oxidase A	<i>MAOA</i>	0.29	-0.15	-0.04	-0.67
Monoamine oxidase B	<i>MAOB</i>	0.17	0.19	0.00	-0.60
2-oxoglutarate dehydrogenase, mitochondria	<i>OGDH</i>	0.31	0.33	0.12	-0.83
2-oxoglutarate dehydrogenase-like, mitochondrial.	<i>OGDHL</i>	0.41	0.23	0.15	-0.67

Spectral index is calculated by the abundance of spectral counts in fibrotic samples and non-fibrotic samples (MF vs non-MF) relative to the number of samples in which it is detectable. A false discovery rate (FDR) of 1% corresponded with the absolute Spl threshold of 0.60.

Values of ≤ -0.60 or ≥ 0.60 were considered significantly differentially expressed (bold).

LC-MS analysis of proteins involved in the tryptophan metabolism pathway

Proteomics analysis was performed on four samples of each patient, resulting in four groups: tumor cells of primary tumor, stroma of primary tumor, tumor cells of mesenteric metastasis and stroma of mesenteric metastasis. In the overall dataset, 2988 individual proteins could be identified. When compared to the 42 genes of the KEGG tryptophan metabolism pathway, we found 20 genes that coded for the proteins in our dataset (**Supplementary Table 1**, see section on supplementary materials at the end of this chapter). Differential expression of proteins between MF and non-MF samples in each group was determined by SpI and yielded 10 differentially expressed proteins (**Table 2**).

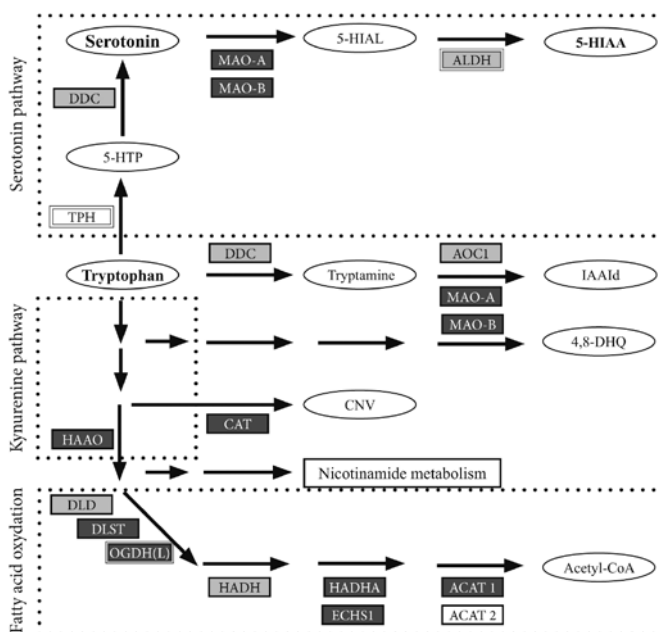
The differentially expressed proteins were mostly found in the tryptophan – serotonin metabolism and the fatty acid oxidation arm of the tryptophan metabolism pathway. In the kynurenine metabolism arm, only 3-hydroxyanthranilate 3,4-dioxygenase (HAAO) could be detected. All the differentially expressed proteins showed significantly lower abundance in fibrotic mesenteric stroma compared to non-fibrotic mesenteric stroma. Additionally, HAAO had a significantly lower abundance in fibrotic mesenteric tumor cells compared to non-fibrotic mesenteric tumor cells. No significant differential expression of the 20 selected proteins was observed between MF and non-MF samples in the primary tumor and stroma groups. **Figure 1** shows a simplified diagram of the tryptophan metabolism pathway annotated with the identified and differentially expressed proteins in the mesenteric stroma samples.

Immunohistochemical analysis of monoamine oxidase A protein expression

We validated, by IHC staining, the expression of MAO-A, a key enzyme responsible for serotonin metabolism. Cytoplasmic staining was present in all primary tumors and mesenteric metastases, both in tumor cells and surrounding stroma. In the stromal compartment, MAO-A staining was predominantly expressed by fibroblasts (**Fig. 2A**). In primary tumors, the stromal compartment had a significantly lower staining score of MAO-A compared to tumor cells (median 5.5 I/A vs 28.3 I/A, respectively, $P < 0.001$). Similarly, in mesenteric metastases, the stromal MAO-A staining score was lower than in

tumor cells (median 2.6 I/A vs 27.5 I/A, respectively, $P < 0.001$). Comparing the stromal compartments, MAO-A expression was lower in mesenteric metastases than in primary tumors (median 2.6 I/A vs 5.5 I/A, respectively, $P < 0.001$).

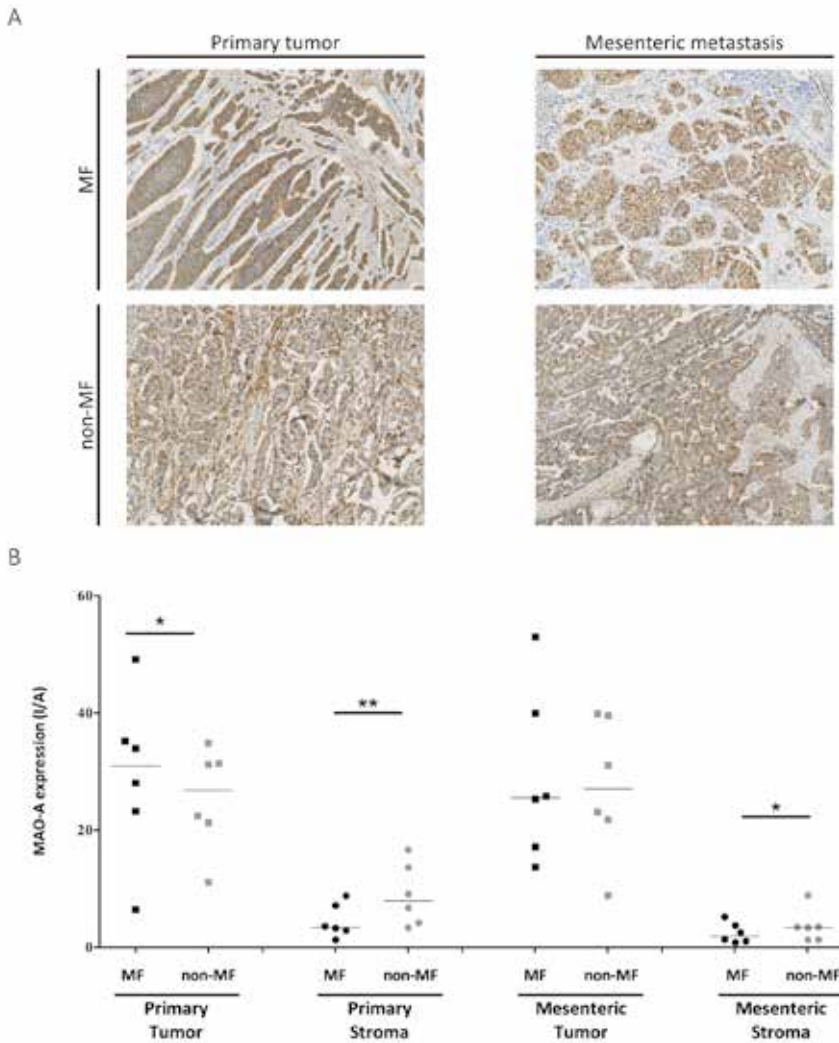
FIGURE 1. Simplified tryptophan metabolism pathway in mesenteric metastases stroma



Metabolites are shown as ellipses and enzymes as rectangles. Gray rectangles represent identified proteins and dark gray rectangles represent enzymes with significantly lower abundance in mesenteric metastases stroma of patients with mesenteric fibrosis.

Abbreviations; 4,8-DHG: 4,8-dihydroxy-quinoline, 5-HTP: 5-hydroxy- L-Tryptophan, 5-HIAL: 5-hydroxyindole- acetylaldehyde, 5-HIAA: 5-hydroxyindoleacetic acid, ACAT1: acetyl-CoA acetyltransferase (mitochondrial), ACAT2: acetyl-CoA acetyltransferase (cytosolic), ALDH (multiple enzymes): aldehyde dehydrogenase X (mitochondrial), aldehyde dehydrogenase (mitochondrial), aldehyde dehydrogenase family 3 member A2, alpha-aminoacidic semialdehyde dehydrogenase and 4-trimethylaminobutyraldehyde dehydrogenase, AOC1: amiloride-sensitive amine oxidase, CAT: catalase, CNV: cinnavalininate, DDC: aromatic-L-amino-acid decarboxylase, DLD: dihydrolipoyl dehydrogenase (mitochondrial), DLST: dihydrolipoyllysine-residue succinyltransferase component of 2-oxoglutarate dehydrogenase complex (mitochondrial), ECHS1: enoyl-CoA hydratase (mitochondrial), HAAO: 3-hydroxyanthranilate 3,4-dioxygenase, HADH: hydroxyacyl-coenzyme A dehydrogenase (mitochondrial), HADHA: Trifunctional enzyme subunit alpha (mitochondrial), IAAld: indole-3-acetaldehyde, MAO-A: Monoamine oxidase A, MAO-B: Monoamine oxidase B, OGDH(L): 2-oxoglutarate dehydrogenase and 2-oxoglutarate dehydrogenase-like (mitochondrial), TPH: Tryptophan 5-hydroxylase 1 and 2.

FIGURE 2. IHC analysis of MAO-A expression



A. Photomicrographs of representative IHC staining for MAO-A. The left panel shows primary tumor tissue, the right panel shows mesenteric metastasis tissue. The upper panels show tissue of MF patients, the lower panels show tissue of non-MF patients. **B.** Median MAO-A expression in MF ($n = 6$) and non-MF ($n = 6$) SI-NET in primary tumor tumor cells, primary tumor stroma, mesenteric metastasis tumor cells and mesenteric metastasis stroma. MAO-A expression is scored as DAB intensity in segmented area (I/A). Each dot represents one individual patient with overall median indicated by the horizontal line. * $P < 0.05$, ** $P < 0.01$ MF vs non-MF.

Abbreviations: IHC, immunohistochemical; MF, mesenteric fibrosis; MAO-A, monoamine oxidase A; non-MF, no mesenteric fibrosis, SI-NET, small intestinal neuroendocrine tumors.

Next, we compared patients with and without mesenteric fibrosis (MF vs non-MF) (**Fig. 2B**). In primary tumors, patients with MF had higher MAO-A staining score in tumor cells (median 33.5 I/A vs 25.8 I/A in non-MF, $P = 0.03$). On the other hand, in the stromal compartment of primary tumors, the MAO-A staining score was lower in patients with MF (median 4.2 I/A vs 6.5 I/A in non-MF, $P = 0.003$). In mesenteric metastases, there was no difference in MAO-A staining score in MF and non-MF tumors cells (median 25.8 I/A vs 27.6 I/A, respectively, $P = 0.92$). Similar to the findings in primary tumors, MAO-A staining score in the stromal compartment of mesenteric metastases was lower in the MF samples (median 2.1 I/A vs 2.8 I/A in non-MF, $P = 0.019$). As more patients with MF received SSA treatment preoperatively compared to non-MF patients (**Table 1**, $P = 0.22$), we analyzed if this affected MAO-A expression and found no significant differences between SSA treated and naive patients within the four tissue groups.

Discussion

We have studied the protein expression of metabolizing enzymes within the tryptophan pathway in primary SI-NETs and paired mesenteric metastases and found most notably a decreased expression of serotonin-metabolizing enzymes in the stroma of fibrotic mesenteric metastases.

Serotonin production outside the central nervous system is limited to enterochromaffin cells and in extension to SI-NETs, in case of malignant transformation. In other tissues, serotonin levels are regulated by serotonin-metabolizing enzymes¹⁶. Serotonin is a well-established profibrotic factor and increased paracrine serotonin signaling is known to induce tissue fibrosis and tumor cell proliferation^{3,4}. Lower levels of serotonin-metabolizing enzymes result in an increase of local serotonin levels¹⁶. This could also explain the observation that urinary 5-HIAA excretion, a marker for systemic serotonin production, is a poor predictor for mesenteric fibrosis as it may not reflect local serotonin activity^{6,17}. The lower abundance of serotonin-metabolizing enzymes found in this study could be a major factor contributing to the increased risk of mesenteric fibrosis in some SI-NET patients. Interestingly, we found lower levels of MAO-A, the primary catabolizing enzyme of serotonin, in stroma of mesenteric metastases compared to primary tumors.

This may represent an important mechanism in the predisposition of SI-NET-associated fibrosis in specific locations such as the mesentery.

MAO-A expression can be regulated via various mechanisms. It is well established that *MAO-A* gene and promotor polymorphism can result in lower transcription efficiency and increased serotonin levels. However, MAO-A expression can also be affected by environmental and epigenetic events¹⁸. Downregulation of MAO-A by epigenetic methylation and histone acetylation has been demonstrated in cholangiocarcinoma and hepatocellular carcinoma and was associated with increased invasiveness, low tumor differentiation and poor prognosis^{19,20}. However, studies on the role of MAO-A in tumorigenesis have not been consistent. In contrast to hepatocellular and cholangiocarcinoma, increased expression of MAO-A in stromal fibroblasts in prostate cancer promotes tumorigenesis *in vitro* and *in vivo*²¹. Furthermore, increased MAO-A expression was suggested to play a role in non-small cell lung cancer by promoting epithelial to mesenchymal transition²². These results suggest that the function of MAO-A varies in different cancer types warranting caution in the development of therapies targeting MAO-A.

Therapeutic targeting of MAO-A has predominantly focussed on the use of small molecule MAO inhibitors (MAOI), especially in the treatment of psychiatric and neurological disorders²³. Recent studies have demonstrated interesting novel effects of MAOI in cancer models. Inhibition of MAO-A activity by MAOI resulted in tumor suppression in preclinical mouse syngeneic and human xenograft tumor models. The antitumor effect was enhanced when MAOI was used in combination with immune checkpoint anti-PD-1 treatment²⁴. Also, MAO-A promotes tumor associated macrophages' immunosuppressive functions via upregulation of oxidative stress which could be regulated by the use of MAOI resulting in enhanced antitumor immunity²⁵. However, relatively fewer options are as yet available to increase MAO-A expression or activity. Valproic acid (VPA), an anticonvulsant, was found to be an inducer of MAO-A activity through the Akt/FoxO1 signaling pathway²⁶. VPA may thus be a potential therapeutic option in regulating serotonin-mediated fibrosis in SI-NET. An additional benefit of VPA is its activity as a potent histone deacetylase inhibitor that has been demonstrated in NET cell lines to increase expression of somatostatin receptor 2 and have a cytotoxic effect^{27,28}. However, the consequences of MAO-A inhibition vs. induction on SI-NET tumor progression and fibrogenesis need to be investigated further.

Next to the proteins involved in the conversion to and degradation of serotonin, the tryptophan pathway consists of enzymes involved in the kynurenine metabolism and fatty acid oxidation. In the kynurenine pathway tryptophan is metabolized to nicotinamide adenosine dinucleotide and is involved in the pathogenesis of many inflammatory and malignant diseases²⁹. Kynurenine metabolites have an immune suppressive effect resulting in a decreased antitumor immune response²⁹. On the other hand, this immunosuppressive effect has also been shown to attenuate fibrosis³⁰. In our study, we could only identify HAAO as part of the kynurenine pathway. Although this enzyme had a lower expression in both the fibrotic mesenteric tumor and stromal compartment, it is difficult to speculate the effect this could have on kynurenine metabolites and fibrogenesis in the SI-NET tumor microenvironment as most of the pathway could not be assessed.

On analyzing the arm of the tryptophan metabolism pathway involved in fatty acid oxidation, we were able to detect eight enzymes. These enzymes had a lower abundance in patients with mesenteric fibrosis, especially in the stroma of mesenteric metastases. Dysregulation of fatty acid metabolism is a common feature in cancer cells. Elevated exogenous uptake of fatty acids and subsequent oxidation allows for a valuable source of ATP and other molecules needed for proliferation in times of metabolic stress, such as hypoxia³¹. Decreased fatty acid oxidation could result in increased reactive oxidative species production that results in profibrotic changes such as induction of myofibroblastic differentiation and increased transforming growth factor β (TGF- β) signaling³².

This study has some limitations that may affect the conclusions drawn. As we have used a label-free proteomics approach not all proteins involved in the tryptophan metabolism could be detected. Notably, tryptophan hydroxylase 1, the rate-limiting enzyme for peripheral serotonin synthesis, was not detected. Secondly, using this approach the estimation of the abundance of the detected proteins is semi-quantitative. To overcome this limitation, we validated the expression of the main serotonin-inactivating enzyme, MAO-A using IHC and found an identical pattern of decreased expression in mesenteric stroma as with the proteomics analysis. Thirdly, the small sample size is a major limitation of this study. Hence an in-depth investigation of the potential association of protein expression with disease characteristics was not possible. However, the altered expression of the enzymes involved in tryptophan metabolism demonstrated in this study may represent an important mechanism involved in mesenteric fibrosis in SI-NETs and

warrants further research. Further in-depth studies involving larger sample populations could validate potential targets to develop effective treatment options for SI-NET-associated mesenteric fibrosis.

In conclusion, we found lower expression of enzymes involved in the tryptophan metabolism, especially serotonin-degrading enzymes, in the stroma of fibrotic mesenteric metastases. Differential expression of these enzymes might be important factor underlying the risk of development of SI-NET-associated mesenteric fibrosis.

References

1. Niederle B, Pape UF, Costa F, et al. ENETS Consensus Guidelines Update for Neuroendocrine Neoplasms of the Jejunum and Ileum. *Neuroendocrinology*. 2016;103(2):125-38.
2. Koumariou A, Alexandraki KI, Wallin G, Kaltsas G, Daskalakis K. Pathogenesis and Clinical Management of Mesenteric Fibrosis in Small Intestinal Neuroendocrine Neoplasms: A Systematic Review. *J Clin Med*. Jun 8 2020;9(6)
3. Blažević A, Hofland J, Hofland LJ, Feelders RA, de Herder WW. Small intestinal neuroendocrine tumours and fibrosis: an entangled conundrum. *Endocr Relat Cancer*. Mar 2018;25(3):R115-R130.
4. Mann DA, Oakley F. Serotonin paracrine signaling in tissue fibrosis. *Biochimica et Biophysica Acta (BBA) - Molecular Basis of Disease*. 2013/07/01/ 2013;1832(7):905-910. doi:https://doi.org/10.1016/j.bbadis.2012.09.009
5. Hofland J, Zandee WT, de Herder WW. Role of biomarker tests for diagnosis of neuroendocrine tumours. *Nature Reviews Endocrinology*. 2018/11/01 2018;14(11):656-669. doi:10.1038/s41574-018-0082-5
6. Blažević A, Zandee WT, Franssen GJH, et al. Mesenteric fibrosis and palliative surgery in small intestinal neuroendocrine tumours. *Endocr Relat Cancer*. Mar 2018;25(3):245-254.
7. Roth W, Zadeh K, Vekariya R, Ge Y, Mohamadzadeh M. Tryptophan Metabolism and Gut-Brain Homeostasis. *International Journal of Molecular Sciences*. 2021;22(6):2973.
8. Shih JC, Chen K, Ridd MJ. Monoamine oxidase: from genes to behavior. *Annu Rev Neurosci*. 1999;22:197-217. doi:10.1146/annurev.neuro.22.1.197
9. Pantongrag-Brown L, Buetow PC, Carr NJ, Lichtenstein JE, Buck JL. Calcification and fibrosis in mesenteric carcinoid tumor: CT findings and pathologic correlation. *AM J ROENTGENOL*. 1995;164(2):387-391.
10. Blažević A, Iyer AM, van Velthuysen M-LF, et al. Sexual Dimorphism in Small-intestinal Neuroendocrine Tumors: Lower Prevalence of Mesenteric Disease in Premenopausal Women. *The Journal of Clinical Endocrinology & Metabolism*. 2022;doi:10.1210/clinem/dgac001
11. Zajec M, Kros JM, Dekker-Nijholt DAT, et al. Identification of Blood-Brain Barrier-Associated Proteins in the Human Brain. *J Proteome Res*. Jan 1 2021;20(1):531-537.
12. van der Ende EL, Meeter LH, Stingl C, et al. Novel CSF biomarkers in genetic frontotemporal dementia identified by proteomics. *Ann Clin Transl Neurol*. Apr 2019;6(4):698-707.

13. Vizcaíno JA, Côté RG, Csordas A, et al. The PRoteomics IDentifications (PRIDE) database and associated tools: status in 2013. *Nucleic Acids Res.* Jan 2013;41(Database issue):D1063-9.
14. Carpenter AE, Jones TR, Lamprecht MR, et al. CellProfiler: image analysis software for identifying and quantifying cell phenotypes. *Genome Biol.* 2006;7(10):R100.
15. Fu X, Gharib SA, Green PS, et al. Spectral index for assessment of differential protein expression in shotgun proteomics. *J Proteome Res.* Mar 2008;7(3):845-54.
16. Mohammad-Zadeh LF, Moses L, Gwaltney-Brant SM. Serotonin: a review. *J Vet Pharmacol Ther.* Jun 2008;31(3):187-99.
17. Laskaratos FM, Diamantopoulos L, Walker M, et al. Prognostic Factors for Survival among Patients with Small Bowel Neuroendocrine Tumours Associated with Mesenteric Desmoplasia. *Neuroendocrinology.* 2018;106(4):366-380. doi:10.1159/000486097
18. Naoi M, Riederer P, Maruyama W. Modulation of monoamine oxidase (MAO) expression in neuropsychiatric disorders: genetic and environmental factors involved in type A MAO expression. *Journal of Neural Transmission.* 2016/02/01 2016;123(2):91-106. doi:10.1007/s00702-014-1362-4
19. Li J, Yang X-M, Wang Y-H, et al. Monoamine oxidase A suppresses hepatocellular carcinoma metastasis by inhibiting the adrenergic system and its transactivation of EGFR signaling. *Journal of Hepatology.* 2014/06/01/ 2014;60(6):1225-1234. doi:https://doi.org/10.1016/j.jhep.2014.02.025
20. Huang L, Frampton G, Rao A, et al. Monoamine oxidase A expression is suppressed in human cholangiocarcinoma via coordinated epigenetic and IL-6-driven events. *Lab Invest.* 2012;92(10):1451-1460. doi:10.1038/labinvest.2012.110
21. Li J, Pu T, Yin L, Li Q, Liao C-P, Wu BJ. MAOA-mediated reprogramming of stromal fibroblasts promotes prostate tumorigenesis and cancer stemness. *Oncogene.* 2020/04/01 2020;39(16):3305-3321. doi:10.1038/s41388-020-1217-4
22. Liu F, Hu L, Ma Y, et al. Increased expression of monoamine oxidase A is associated with epithelial to mesenchymal transition and clinicopathological features in non-small cell lung cancer. *Oncol Lett.* Mar 2018;15(3):3245-3251.
23. Finberg JPM, Rabey JM. Inhibitors of MAO-A and MAO-B in Psychiatry and Neurology. 10.3389/fphar.2016.00340. *Frontiers in Pharmacology.* 2016;7:340.
24. Wang X, Li B, Kim Yu J, et al. Targeting monoamine oxidase A for T cell-based cancer immunotherapy. *Science Immunology.* 2021/05/14 2021;6(59):eabh2383. doi:10.1126/sciimmunol.abh2383

25. Wang Y-C, Wang X, Yu J, et al. Targeting monoamine oxidase A-regulated tumor-associated macrophage polarization for cancer immunotherapy. *Nature Communications*. 2021/06/10 2021;12(1):3530. doi:10.1038/s41467-021-23164-2
26. Wu JB, Shih JC. Valproic acid induces monoamine oxidase A via Akt/forkhead box O1 activation. *Mol Pharmacol*. Oct 2011;80(4):714-23.
27. Veenstra MJ, van Koetsveld PM, Dogan F, et al. Epidrug-induced upregulation of functional somatostatin type 2 receptors in human pancreatic neuroendocrine tumor cells. *Oncotarget*. Mar 13 2018;9(19):14791-14802.
28. Arvidsson Y, Johanson V, Pfragner R, Wängberg B, Nilsson O. Cytotoxic Effects of Valproic Acid on Neuroendocrine Tumour Cells. *Neuroendocrinology*. 2016;103(5):578-591. doi:10.1159/000441849
29. Chen Y, Guillemin GJ. Kynurenine pathway metabolites in humans: disease and healthy States. *Int J Tryptophan Res*. 2009;2:1-19.
30. Dolivo DM, Larson SA, Dominko T. Tryptophan metabolites kynurenine and serotonin regulate fibroblast activation and fibrosis. *Cellular and Molecular Life Sciences*. 2018/10/01 2018;75(20):3663-3681. doi:10.1007/s00018-018-2880-2
31. Koundouros N, Poulogiannis G. Reprogramming of fatty acid metabolism in cancer. *British Journal of Cancer*. 2020/01/01 2020;122(1):4-22. doi:10.1038/s41416-019-0650-z
32. Li X, Zhang W, Cao Q, et al. Mitochondrial dysfunction in fibrotic diseases. *Cell Death Discovery*. 2020/09/05 2020;6(1):80. doi:10.1038/s41420-020-00316-9

Appendix

Supplementary materials

The first two columns show the protein name (protein) and gene identifier (gene) of the 20 proteins involved in tryptophan metabolism pathway that were identified in the 48 SI-NET tissue samples. The next columns show the total spectrum count for each protein (spectrum count) and the number of samples in which the protein could be detected (positive samples) in the six samples of each tissue group; tumor cells of primary tumors of patients with mesenteric fibrosis (MF, $n = 6$) and patients without fibrosis (non-MF, $n = 6$), stromal cells of primary tumors of patients with MF ($n = 6$) and non-MF ($n = 6$), tumor cells of mesenteric metastases of patients with MF ($n = 6$) and non-MF ($n = 6$) and stromal cells of mesenteric metastases of patients with MF ($n = 6$) and non-MF ($n = 6$). The total spectrum count and number of positive samples was extracted from a Protein Report export from Scaffold.

SUPPLEMENTARY TABLE 1. Proteins involved in the tryptophan metabolism pathway identified in SI-NET tissue

Protein	Gene	Mesenteric metastases (n = 12)															
		Primary tumors (n = 12)				Stromal cells				Tumor cells							
		Tumor cells		Stromal cells		Tumor cells		Stroma cells		MF (n = 6)		non-MF (n = 6)		MF (n = 6)		non-MF (n = 6)	
Acetyl-CoA acetyltransferase, mitochondrial	ACAT1	35	6	34	6	8	6	6	4	33	6	39	6	1	1	10	5
Acetyl-CoA acetyltransferase, cytosolic	ACAT2	5	3	1	1	0	0	0	0	2	2	1	1	0	0	0	0
Aldehyde dehydrogenase X, mitochondrial	ALDH1B1	10	5	15	6	41	6	31	6	4	4	16	5	8	6	16	6
Aldehyde dehydrogenase, mitochondrial	ALDH2	49	6	47	6	37	6	32	6	50	6	46	6	14	6	30	6
Aldehyde dehydrogenase family 3 member A2	ALDH3A2	7	5	2	2	0	0	0	0	5	3	4	3	0	0	0	0
Alpha-aminoacidic semialdehyde dehydrogenase	ALDH7A1	26	6	20	6	2	2	5	3	18	6	21	6	0	0	11	3
4-trimethylaminobutyl-aldehyde dehydrogenase	ALDH9A1	47	6	49	6	7	4	7	6	49	6	41	6	7	4	21	6
Amiloride-sensitive amine oxidase	AOC1	7	4	3	3	7	4	14	3	9	4	2	2	8	3	36	5
Catalase	CAT	10	6	8	5	7	6	15	6	13	6	12	5	3	1	17	6
Aromatic-L-amino-acid decarboxylase	DDC	161	6	153	6	38	6	42	6	137	6	172	6	24	5	67	6
Dihydrolipoyl dehydrogenase	DLD	36	6	27	6	6	5	5	4	27	6	35	6	0	0	5	3
Dihydrolysinine-residue succinyltransferase component	DLST	29	6	28	6	18	6	13	6	26	6	19	6	0	0	8	5
Enoyl-CoA hydratase, mitochondrial	ECHS1	43	6	34	6	8	5	9	6	36	6	39	6	0	0	8	4
3-hydroxyanthranilate 3,4-dioxygenase	HAO	10	6	8	4	7	4	2	1	3	3	9	6	2	1	7	5
Hydroxyacyl-coenzyme A dehydrogenase, mitochondrial	HADH	19	6	13	6	0	0	2	2	10	5	10	5	0	0	1	1
Trifunctional enzyme subunit alpha, mitochondrial	HADHA	71	6	46	6	15	6	17	5	59	6	56	6	1	1	24	6
Monoamine oxidase A	MAOA	16	5	9	4	4	3	5	4	7	4	8	4	0	0	7	4
Monoamine oxidase B	MAOB	10	4	6	4	14	6	11	5	4	3	4	3	1	1	11	4
2-oxoglutarate dehydrogenase, mitochondrial	OGDH	38	6	20	6	8	5	4	4	33	6	26	6	0	0	7	5
2-oxoglutarate dehydrogenase-like, mitochondrial	OGDHL	22	6	12	4	5	4	3	3	27	6	20	6	0	0	5	4

7



Chapter 7

Proteomic analysis of small intestinal neuroendocrine tumors and mesenteric fibrosis

Anela Blažević, Anand M. Iyer, Marie-Louise F. van Velthuysen, Johannes Hofland, Gaston J. H. Franssen, Richard A. Feelders, Marina Zajec, Theo M. Luider, Wouter W. de Herder and Leo J. Hofland

Submitted for publication

Abstract

Mesenteric metastases in small intestinal neuroendocrine tumors (SI-NETs) are associated with mesenteric fibrosis (MF) in a proportion of patients. MF can induce severe abdominal complications and an effective preventive treatment is lacking. To elucidate possible novel therapeutic targets, we performed a proteomics-based analysis of MF. The tumor cell and stromal compartment of primary tumors and paired mesenteric metastases of SI-NET patients with MF ($n = 6$) and without MF ($n = 6$) was analyzed by liquid chromatography-mass spectrometry-based proteomics. Analysis of differential protein abundance was performed. Collagen alpha-1(XII) (COL12A1) and complement C9 (C9) expression was evaluated by immunohistochemistry (IHC) in mesenteric metastases.

A total of 2988 proteins was identified. Unsupervised hierarchical clustering showed close clustering of paired primary and mesenteric tumor cell samples. Comparing MF to non-MF samples, we detected differentially protein abundance solely in the mesenteric metastasis stroma group. There was no differential abundance of proteins in tumor cell samples or primary tumor stroma samples. Analysis of the differentially abundant proteins ($n = 36$) revealed higher abundance in MF samples of C9, various collagens and proteoglycans associated with profibrotic extracellular matrix dysregulation and signaling pathways. Proteins involved in fatty acid oxidation showed a lower abundance. COL12A1 and C9 were confirmed by IHC to have significantly higher expression in MF mesenteric metastases compared to non-MF.

In conclusion, proteome profiles of SI-NETs with and without MF differ primarily in the stromal compartment of mesenteric metastases. Analysis of differentially abundant proteins revealed possible new signaling pathways involved in mesenteric fibrosis development.

Introduction

Small intestinal neuroendocrine tumors (SI-NETs) are rare neoplasms originating from the enterochromaffin cells of the intestine¹⁻³. In recent decades there has been significant progress in treatment options resulting in prolonged survival and improvement of the clinical symptoms of carcinoid syndrome^{4,5}. However, the SI-NET-associated mesenteric fibrosis (MF), another hallmark of SI-NETs, remains without effective medical treatment^{4,6}. MF is known to develop around a metastatic mesenteric mass and can induce severe abdominal complications such as intestinal obstruction, ischaemia and perforation^{7,8}.

In order to find therapeutic options, it is paramount to improve our knowledge of the processes involved in MF development^{9,10}. SI-NETs seem to be prone to the development of fibrosis through secretion of serotonin in combination with various other profibrotic growth factors such as transforming growth factor beta (TGF β)¹⁰. TGF β signalling can induce myofibroblastic differentiation in stromal cells. This stimulates profibrotic tissue remodelling by inducing the production and deposition of extracellular matrix components such as various collagens¹⁰. The remodelling of extracellular matrix stimulates tumor growth and migration and also results in increased secretion of profibrotic growth factors resulting in a positive profibrotic feedback loop^{10,11}. However, little is known about the specific composition and changes in the extracellular matrix during metastasis and fibrosis in SI-NETs.

Also, even though most patients with mesenteric SI-NET metastasis have an increased serotonin production, MF occurs only in approximately 50% of these patients^{6,12}. The previous studies examining profibrotic factors in SI-NET focus on tumor cells and do not address the predisposition of the mesentery for fibrosis development. Better understanding of the underlying mechanisms of the difference in MF susceptibility between tissues and individuals is essential for the development of targeted therapies for MF. To this end, we have studied the proteome of SI-NETs in both tumor cells and the stromal compartment.

In this study, we have used label-free liquid chromatography-mass spectrometry (LC-MS) proteomics to analyse the tumor and stromal compartment of the primary SI-NETs and the paired mesenteric metastases in patients with and without MF. Using this method, we have previously found differences in the tryptophan and serotonin metabolizing

proteins between patients with and without SI-NET-associated mesenteric fibrosis¹³. In this study, we aimed to elucidate new pathways involved in SI-NET fibrogenesis using a discovery driven approach of proteomics analysis.

Methods

Sample selection

Patients were included from the Erasmus University Medical Center NET database, which encompassed at time of inclusion all NET patients treated between January 1993 and December 2017 in the Erasmus MC, Rotterdam, the Netherlands. The study was performed retrospectively with anonymized data, and, according to the guidelines of the Central Committee on Research involving Human Subjects (CCMO), this does not require approval from an ethics committee in the Netherlands. Patients were eligible for inclusion if they underwent a resection of a pathologically proven primary SI-NET with metastasectomy of the dominant mesenteric node¹⁴.

In these patients, MF was assessed by both radiological and histopathological parameters. Radiological MF was defined as radiating soft tissue strands in the mesentery surrounding a mesenteric node of ≥ 10 mm on a preoperative contrast-enhanced computed tomography (CT) scan. The stage of the mesenteric metastases was classified as following in every patient on preoperative imaging: stage I mesenteric metastases are located close to the intestine, stage II involves arterial branches close to the origin in the mesenteric artery, stage III mesenteric metastases extend along, without encircling, the superior mesenteric artery trunk, stage IV grows around the mesenteric artery and involves the origin of proximal jejunal arteries or extend retroperitoneally, behind or above the pancreas¹⁵.

Histopathological assessment of MF was performed with hematoxylin and eosin (HE) stained sections of the resected mesenteric metastases. MF was classified according to the presence of intratumoral fibrous bands. Mesenteric metastases with intratumoral fibrous bands < 0.5 mm were classified as no MF, while those with fibrous bands > 2 mm were classified as severe MF⁸. Patients were included in non-MF group ($n = 6$) if there was no radiological or histopathological evidence of MF. The MF group ($n = 6$) consisted of age,

sex and tumor grade matched patients with radiological evidence of MF in combination with severe MF on histopathology. All the included patients had mesenteric metastases synchronous with the primary tumor.

Sample collection and data acquisition

Formalin-fixed paraffin-embedded (FFPE) tissue samples of the primary tumor and mesenteric metastasis from the first intestinal resection with mesenteric metastasectomy were selected. Sections of 10 μm were attached to a polyethylene naphthalate slide (Carl Zeiss MicroImaging, Munich, Germany) and HE stained. The tissue samples were collected as described previously^{13,16}. Briefly, the tissue samples were separated in tumor and stromal components by laser-capture microdissection (LCM) using Zeiss PALM MicroBeam IV LCM microscope (Carl Zeiss MicroImaging, GmbH, Munich, Germany). LCM allows to reduce bias when analyzing heterogeneous tumors¹⁷. This collection resulted 4 samples for each patient: tumor cells of the primary tumor, and mesenteric metastasis, stromal cells of the primary tumor and mesenteric metastasis. For each sample, we collected tissue from the infiltration border as this is known to be the localization of most profibrotic changes in the SI-NET microenvironment¹⁰. To account for tumor heterogeneity, tissue was collected from multiple areas (ranging from 20 to 50 locations) within one tissue sample. A total area of $\sim 2 \text{ mm}^2$ was collected for each sample in a 0.5 ml opaque AdhesiveCap tube (Carl Zeiss MicroImaging, Munich, Germany). Following collection, the microdissected samples were dissolved in 20 μL of 0.1% RapiGest SF (Waters, Milford, MA) and transferred into LoBind Eppendorf tubes (Eppendorf AG, Hamburg, Germany) and digested with high-grade trypsin (Promega). LC-MS measurements were performed on an RSLC nano LC system (Thermo Fisher Scientific, Germering, Germany) coupled to an Orbitrap Fusion Tribrid Mass Spectrometer (Thermo Fischer Scientific, San Jose, CA, USA) as described previously^{13,18}. Acquired data have been made publicly available through the ProteomeXchange Consortium using the PRIDE identifier PXD029979¹⁹. MS/MS spectra from the raw data files of each sample were converted into MGF files using ProteoWizard (version 3.0). MGF peak list files were used to carry out searches using Mascot (version 2.3.02) against the Uniprot database (selected for *Homo sapiens*, downloaded Nov 15, 2015, 20,194 entries). Carbamidomethylating (+57 Da) of cysteine was set as a fixed modification and hydroxylations (+16 Da) of proline,

lysine, and methionine were included as variable modifications. Mascot search results were further analyzed in Scaffold (v4.6.2, Portland, OR, USA) with protein confidence levels set to a 1% false discovery rate (FDR), at least 2 peptides per protein, and a 1% FDR at the peptide level. FDRs were estimated by inclusion of a decoy database search generated by Mascot. A Protein Report exported from Scaffold was used for data analysis.

Immunohistochemistry

Immunohistochemistry (IHC) was performed for validation of the differential abundance analysis on FFPE whole sections of the mesenteric metastases tissue samples used for proteomics analysis ($n = 12$). Possible targets were selected by reviewing literature available on Pubmed. A search for studies that performed IHC was carried out for each differentially abundant protein (see **Table 2**). If there were at least two studies showing photomicrographs of human tissue stained with an antibody for a differentially abundant protein, the antibody was assessed for availability and performance on SI-NET tissue samples. This resulted in two antibodies, complement component C9 (C9) and collagen alpha-1(XII) chain (COL12A1), which had a reliable performance. IHC was performed on sequential 4 μm thick FFPE sections that were stained for C9 (ab173302, 1:19200, Abcam) and COL12A1 (ab121304, 1:100, Abcam) by automated IHC using the Ventana Benchmark ULTRA (Ventana Medical Systems Inc.). In brief, following deparaffinization and heat-induced antigen retrieval with CC1 (no. 950-500, Ventana) for 64 minutes the tissue samples were incubated with the antibody of interest for 32 minutes at 37°C. The staining was developed using Optiview universal DAB detection Kit (no. 760-700, Ventana), followed by hematoxylin II counter stain for 8 minutes and then a blue coloring reagent for 8 minutes according to the manufacturer's instructions (Ventana). Positive controls were used on every slide. The cytoplasmic staining was scored semi-quantitatively by an experienced pathologist (MFV) using the immunoreactive score (IRS)²⁰. The IRS is calculated by multiplication of the percentage of positive cells (0, 0%; 1, < 10%; 2, 10-50%; 3, 51-80%; 4, >80%) and the intensity of the staining (0, no staining; 1, mild; 2, moderate; 3, strong). This results in IRS scores between 0 and 12. Based on the IRS scores, the samples were classified in four IHC score categories: 0, IRS score 0-1; 1, IRS score 2-3; 2, IRS score 4-8 and 3, IRS score 9-12.

Statistics

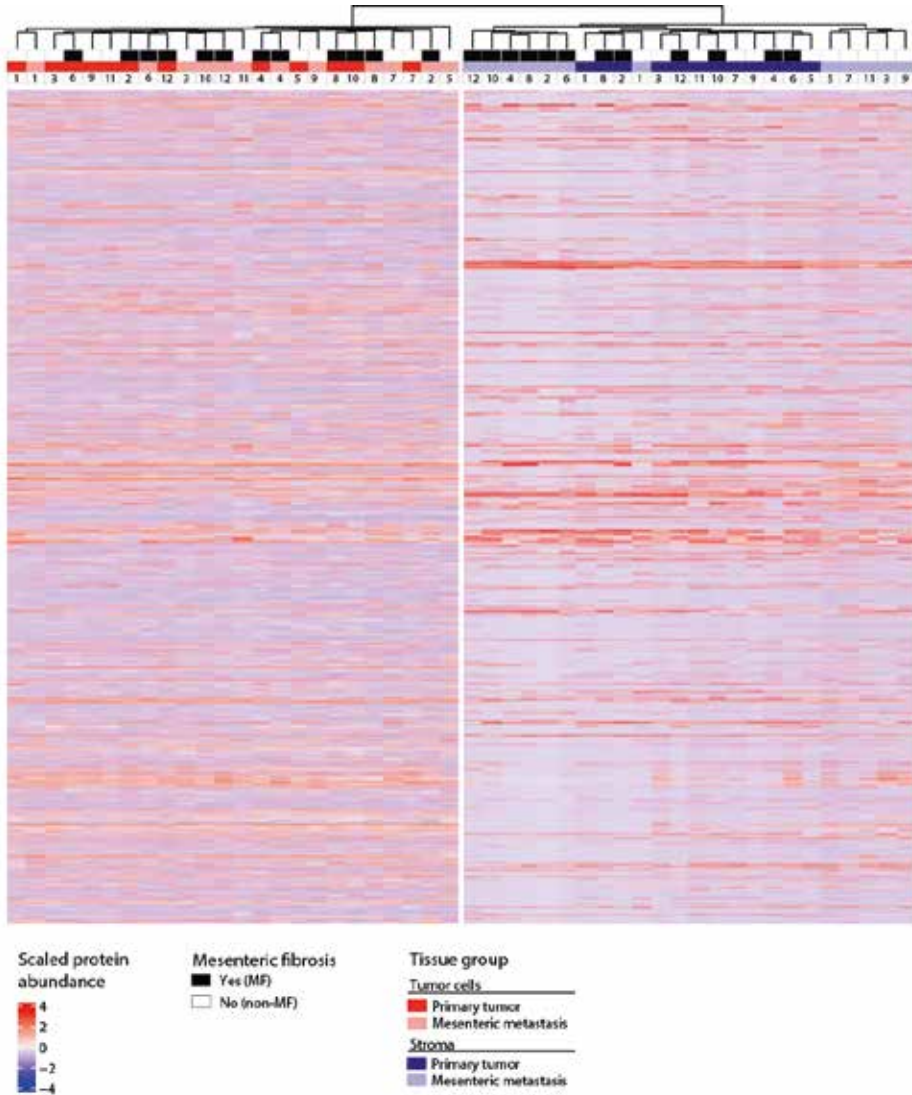
Patient characteristic and IHC data were analyzed using SPSS software (version 21 for Windows, SPSS Inc.). Data were presented as median and interquartile range (IQR; 25th–75th percentiles) or count with percentage. Continuous data were compared by using a Mann-Whitney U test or Wilcoxon signed-rank test for paired data. Proteomics data was analyzed using R software version 4.1.2 (<http://www.r-project.org/>). ComplexHeatmap package was used for the heatmap visualization with unsupervised hierarchical clustering²¹. Differential protein abundance between MF and non-MF samples was determined using two different methods: spectral index (SpI) method and DESeq2^{22,23}. SpI is a metric that calculates the protein abundance in each group relative to the number of samples with detectable peptide. The significance of a given SpI is determined by permutation testing of the whole dataset²². In our study, a false discovery rate (FDR) of 1% corresponded with the absolute SpI threshold of 0.60. DESeq2 tests differential expression using a negative binomial model based on estimates of variance-mean dependence and was implemented using the DESeq2 Bioconductor package²³. A Benjamini-Hochberg FDR correction for multiple testing was applied.

QIAGEN Ingenuity Pathway Analysis was used to interpret the biological processes²⁴. A data set consisting of the protein identifiers and spectral counts of the detected proteins was uploaded into the application. Each identifier was mapped to its corresponding object in QIAGEN's Knowledge Base. Differentially abundant proteins were identified as Network Eligible Molecules. These molecules were overlaid onto a global molecular network developed from information contained in the QIAGEN Knowledge Base. Networks of Network Eligible Molecules were then algorithmically generated based on their connectivity.

Results

Protein identification by proteomics

In this study, we have explored the protein profiles of primary tumors and the paired mesenteric metastases of MF patients ($n = 6$) and matched non-MF patients $n = 6$) using LC-MS proteomics. The baseline characteristics of the included patients are shown in **Table 1**. All included tumors were grade 1 according to WHO classification and there was an equal distribution of male and female patients¹⁴. A total of 2988 proteins were identified in the 48 samples. The highest number of proteins could be identified in the tumor cell group; 2048 proteins [range: 2128 – 2455] in primary tumor tissue and 2068 proteins [range: 2115 – 2479] in mesenteric metastasis tissue. In the stromal compartment, 1571 proteins [range: 1311– 1768] were identified in the primary tumor stroma tissue and 1638 proteins [range: 1086 – 1895] in the mesenteric metastasis stroma tissue. As shown in **Figure 1**, unsupervised hierarchical clustering revealed a strict dichotomy in protein expression between the tumor and stromal samples. The tumor samples from the primary tumor and mesenteric metastasis of each patient tended to cluster close to each other and there was no clustering according to MF status (MF vs non-MF). The stromal samples did not show this pairwise clustering. The stromal samples revealed 3 large clusters: MF mesenteric metastases, primary tumors and non-MF mesenteric metastases. There was no evident dichotomy between MF and non-MF stromal samples of primary tumors.

FIGURE 1. Clustering analysis of proteomics data

Heatmap showing unsupervised hierarchical clustering of all proteins detected ($n = 2988$). Each column represents one sample ($n = 48$). First row indicates the presence of MF: yes (black) or no (white). Second row indicates the sample group: tumor cells from primary tumor ($n = 12$, dark red) and mesenteric metastases ($n = 12$, light red), stroma from primary tumor ($n = 12$, dark blue) and mesenteric metastases ($n = 12$, light blue). The third row indicates the patient ID number. The key color bar indicates scaled protein abundance (dark red indicates relatively higher expression; dark blue indicates relatively lower expression).

TABLE 1. Baseline characteristics included SI-NET patients

	MF (n = 6)	Non-MF (n = 6)	P- value
Age - years	56 (49 – 65)	56 (49 – 61)	0.985
Female	3 (50 %)	3 (50 %)	1.00
Tumor grade I	6 (100 %)	6 (100 %)	1.00
5- HIAA	150 (68 – 1299)	60 (49 – 103)	0.567
ENETS disease stage			0.248
Stage III	2 (33 %)	4 (67 %)	
Stage IV	4 (67 %)	2 (33 %)	
Mesenteric metastases stage			1.00
Stage I	2 (33 %)	2 (33%)	
Stage II	2 (33%)	2 (33 %)	
Stage III	2 (33 %)	2 (33 %)	
Surgery indication			0.223
Curative	1 (17 %)	3 (50 %)	
Symptomatic	2 (33 %)		
Preventive	3 (50 %)	3 (50 %)	
Time from diagnosis to surgery - months	3.7 (1.9 – 21.5)	2.8 (1.9 – 10.9)	0.818

Continuous data are shown as median with interquartile range (IQR; 25th–75th percentiles) in brackets. Categorical data are count with percentages in brackets. Continuous data were compared using a Mann-Whitney U test. A Chi-square test was performed for comparison of categorical data. A *P*-value of < 0.05 was considered statistically significant.

5-HIAA: urinary 5-HIAA excretion, normal range < 50 $\mu\text{mol}/24\text{ h}$, MF: mesenteric fibrosis, non-MF: no mesenteric fibrosis.

Analysis of differentially protein abundance

Using SpI and DESeq2 analysis, differential protein abundance between the MF and the non-MF samples in every tissue group was identified. SpI analysis found the most differentially abundant proteins ($n = 452$) in the mesenteric metastasis stroma samples. In the mesenteric metastasis stroma samples, 25 of these proteins were more abundant in the MF group, while 427 were more abundant in the non-MF group. Analysis by DESeq2 of differential protein abundance between MF and non-MF samples per tissue

group, revealed 80 differentially abundant proteins. The differential abundance of these proteins was all detected in the mesenteric metastasis stroma tissue. There was no differential protein abundance in primary tumors (tumor and stroma samples) nor in mesenteric metastasis tumor samples using DESeq2 analysis.

To increase the precision of our analysis, we have combined the results of the SpI and DESeq2 differential abundance analysis. Proteins that showed significant differential abundance using both methods ($n = 36$) were all detected in mesenteric metastasis stroma samples and are shown in **Table 2**.

Next, we used IPA to gain further insight in the function of these differentially abundant proteins and to generate relational networks. The top three molecular and cellular functions of the differentially abundant proteins were cellular movement (P -value range: $8.12e-03 - 2.12e-06$), cellular assembly and organization (P -value range: $8.12e-03 - 9.83e-05$) and cellular function and maintenance (P -value range: $8.12e-03 - 9.35e-05$). The IPA Network generation yielded 3 networks consisting of respectively 18, 11 and 7 of the differentially abundant proteins (**Figure 2**). The proteins within the first network included the differentially expressed collagens and revealed an interaction with phosphoinositide 3-kinase/Akt (PI3K/Akt), mitogen-activated protein kinase/extracellular signal-regulated kinase (MAPK/ERK), platelet-derived growth growth factor (PDGF) and vascular endothelial growth factor (VEGF) signaling (**Figure 2A**). The second network included mostly proteins that were less abundant in the MF mesenteric metastasis stroma tissue. These proteins were associated with the fatty acid oxidation. However, two more abundant proteins, C9 and sushi repeat-containing protein SRPX2 (SRPX2), are associated with the complement cascade and inflammation. Also, this second network showed an interaction with the nuclear factor kappa B (NF- κ B) complex signaling (**Figure 2B**). The third network included 7 differentially abundant proteins of which 6 were more abundant in MF mesenteric stroma. These proteins were mostly part of the extracellular matrix and showed an interaction with TGF β signaling pathway.

TABLE 2. Proteins with differential abundance in fibrotic (MF) versus non-fibrotic (non-MF) stromal samples of mesenteric metastases

Gene	Protein	Spl ⁱ	P-value ⁱⁱ	Location
ASPN	Asporin	0.66	0.037	Extracellular space
ATP1A1	Sodium/potassium-transporting ATPase subunit alpha-1	-0.96	0.015	Plasma membrane
ATP6V1A	V-type proton ATPase catalytic subunit A	-0.8	0.013	Cytoplasm
C9	Complement C9	1	0.017	Extracellular space / plasma membrane
CAND1	Cullin-associated NEDD8-dissociated protein 1	-1	0.03	Cytoplasm / extracellular space
CLEC11A	C-type lectin domain family 11 member A	0.83	0.046	Extracellular space
COL10A1	Collagen alpha-1(X) chain	0.77	0.008	Extracellular space
COL11A1	Collagen alpha-1(XI) chain	0.69	0.014	Extracellular space
COL12A1	Collagen alpha-1(XII) chain	0.67	0.014	Extracellular space
COL8A2	Collagen alpha-2(VIII) chain	0.83	0.016	Extracellular space
DBNL	Drebrin-like protein	-1	<0.001	Cytoskeleton
DPP7	Dipeptidyl peptidase 2	-0.83	0.015	Cytoplasm / extracellular space
DYNC1H1	Cytoplasmic dynein 1 heavy chain 1	-0.84	0.012	Cytoskeleton
EPB41L2	Band 4.1-like protein 2	-0.89	<0.001	Cytoskeleton
FMOD	Fibromodulin	0.74	<0.001	Extracellular space
HADHA	Trifunctional enzyme subunit alpha, mitochondrial	-0.95	0.007	Mitochondrion
HADHB	Trifunctional enzyme subunit beta, mitochondrial	-0.96	0.008	Mitochondrion
HSP90AB1	Heat shock protein HSP 90-beta	-0.65	0.002	Cytoplasm / extracellular space
HSPA9	Stress-70 protein, mitochondrial	-0.88	<0.001	Mitochondrion
HTRA1	Serine protease HTRA1	0.63	0.001	Extracellular space
ILF3	Interleukin enhancer-binding factor 3	-0.96	<0.001	Cytoplasm / extracellular space
KRT80	Keratin, type II cytoskeletal 80	0.66	0.003	Cytoplasm
MAP4	Microtubule-associated protein 4	-0.92	<0.001	Cytoskeleton
MARCKS	Myristoylated alanine-rich C-kinase substrate	-0.96	<0.001	Cytoskeleton

MFAP4	Microfibril-associated glycoprotein 4	0,63	0,016	Extracellular space
MFGES8	Lactadherin	1	<0,001	Extracellular space
NUCKS1	Nuclear ubiquitous casein and cyclin-dependent kinase substrate 1	-1	0,008	Nucleus
PCOLCE	Procollagen C-endopeptidase enhancer 1	0,79	0,002	Extracellular space
PDIA4	Protein disulfide-isomerase A4	-0,83	0,001	Cytoplasm
RPS4X	40S ribosomal protein S4, X isoform	-1	0,008	Cytoplasm / extracellular space
SERPINF1	Pigment epithelium-derived factor	0,74	<0,001	Extracellular space
SRPX	Sushi repeat-containing protein SRPX	0,76	0,039	Extracellular space / plasma membrane
SRPX2	Sushi repeat-containing protein SRPX2	0,83	<0,001	Extracellular space / plasma membrane
TCP1	T-complex protein 1 subunit alpha	-1	<0,001	Cytoskeleton
THBS1	Thrombospondin-1	0,73	0,018	Extracellular space
TNS1	Tensin-1	-0,68	0,015	Cytoskeleton

ⁱSpectral index (Spl) values of ≤ -0.60 or ≥ 0.60 were considered significantly differentially expressed. A value > 0 indicates a higher abundance in MF samples and a value < 0 indicates a lower abundance in MF samples. ⁱⁱAdjusted *P*-value derived from DESeq2 analysis.

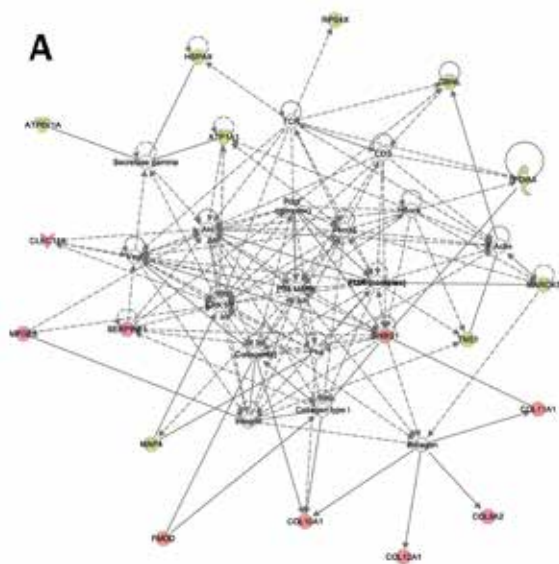
Validation of differentially abundant proteins

Based on previous literature, we selected two proteins, C9 and COL12A1, out of the 36 differentially expressed proteins for validation in mesenteric metastases. COL12A1 was one of the proteins in IPA generated network 1 and C9 was one of the proteins in network 2 (**Figure 2**). Both proteins had higher abundance in the stroma of mesenteric metastases of patients with MF, analyzed by LC-MS (**Table 2**). The proteomic analysis of the tumor samples detected no C9 expression, while COL12A1 was detected only in 2 mesenteric tumor samples (1 MF and 1 non-MF sample).

Immunohistochemical staining showed C9 and COL12A1 positive staining on tumor cells and in the stromal compartment of mesenteric metastases (**Figure 3**). C9 staining was very heterogeneous in both compartments. In tumor cells, most C9 staining was seen on the infiltrative border and the outer cells of tumor nests (**Figure 3A**). In the

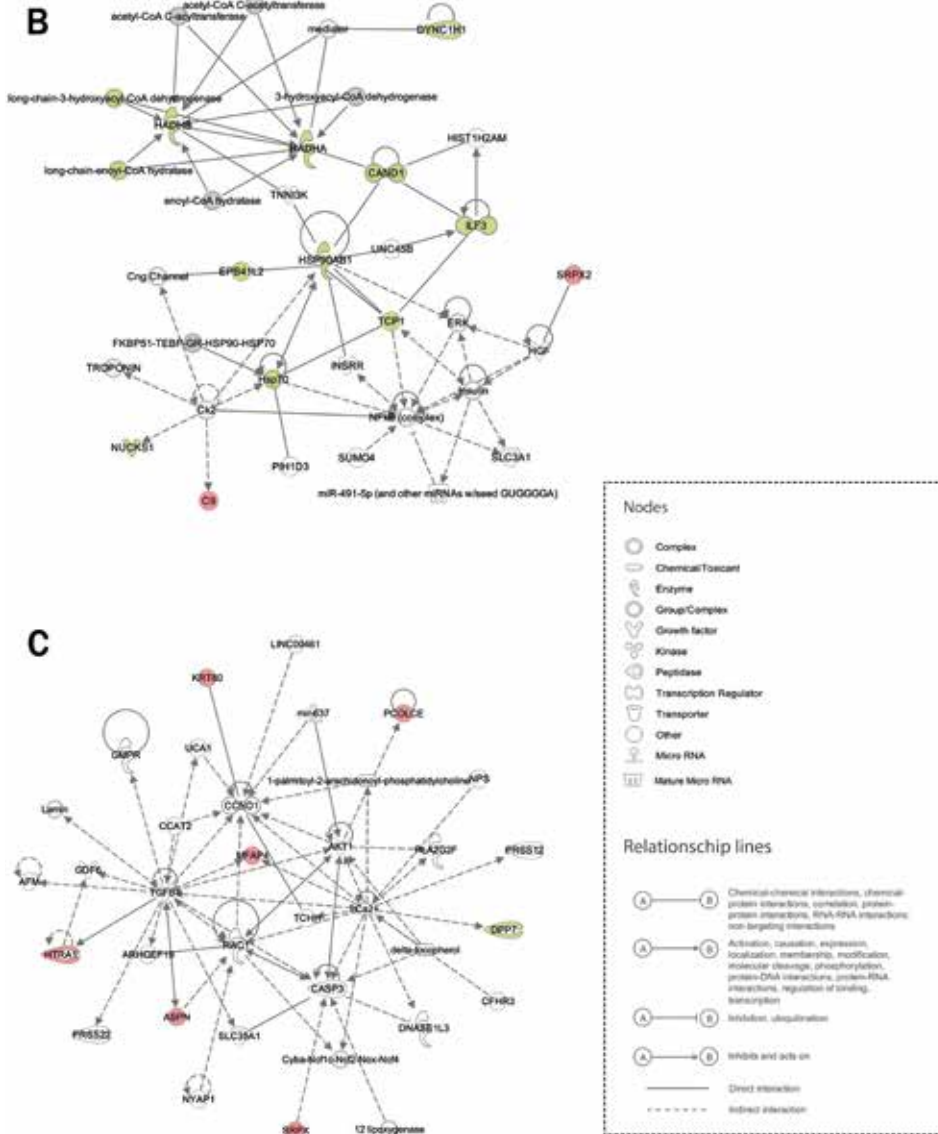
stromal compartment, there was no evident association between the heterogeneous expression and the infiltrative border. In comparison to non-MF patients, MF patients had a significantly higher expression of C9 in tumor cells and stroma (**Figure 3C**). COL12A1 expression was also seen on tumor cells and the stromal compartment of mesenteric metastases and was expressed at a significantly higher level in patients with MF (**Figure 3D**). In concordance with C9 staining, COL12A1 positive cells were mostly seen at the infiltrative border and the outer cells of tumor nests. Stromal COL12A1 staining was very heterogeneous with some fibrotic areas showing strong staining (**Figure 3B**). These areas were not otherwise distinct e.g., had no higher level of vascularization, immune or tumor cell infiltration.

FIGURE 2. Network analysis of differentially abundant proteins in mesenteric stroma



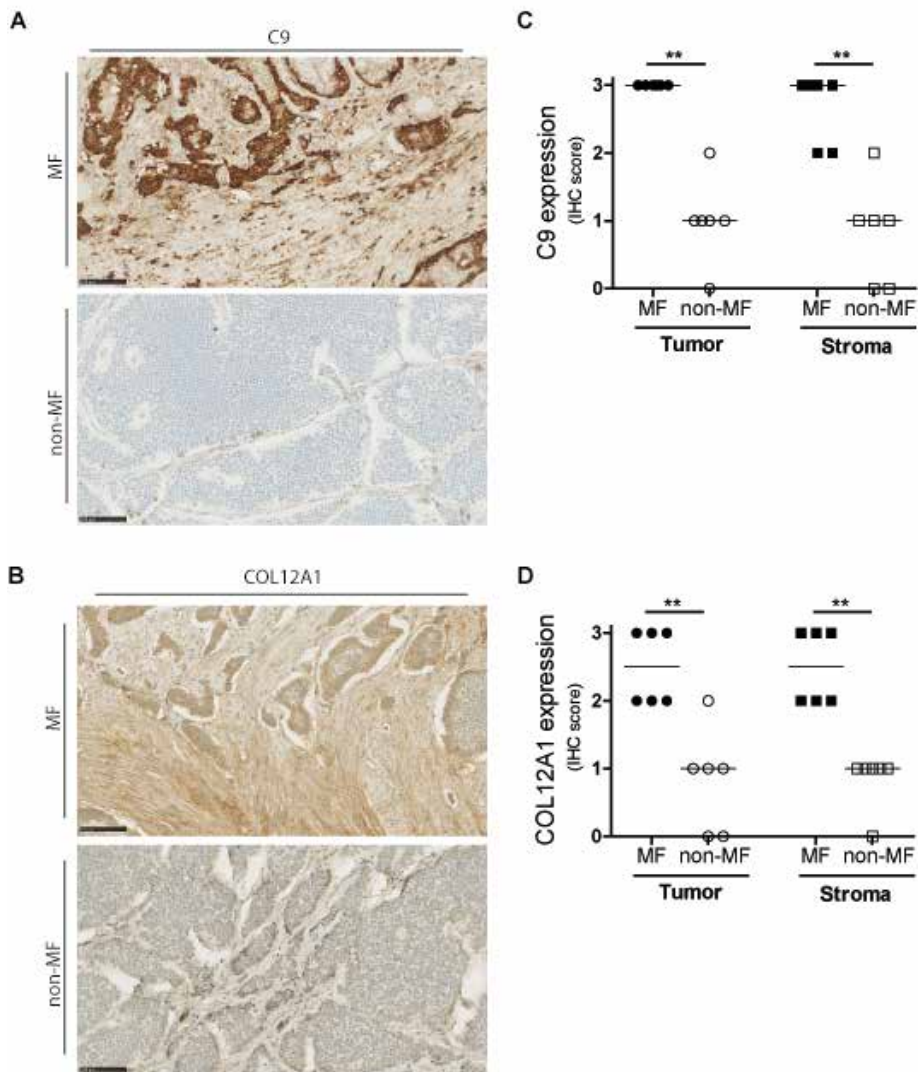
Molecules highlighted red had a higher abundance in MF mesenteric stroma and molecules highlighted green had a lower abundance in MF mesenteric stroma. Uncolored molecules were integrated based on IPA Network generation algorithm.

FIGURE 2. Network analysis of differentially abundant proteins in mesenteric stroma



Molecules highlighted red had a higher abundance in MF mesenteric stroma and molecules highlighted green had a lower abundance in MF mesenteric stroma. Uncolored molecules were integrated based on IPA Network generation algorithm.

FIGURE 3. Immunohistochemical analysis of C9 and COL12A1 expression A-B



Photomicrographs of representative immunohistochemical (IHC) staining for C9 (A) and COL12A1 (B). The upper panel shows MF mesenteric metastasis tissue, the lower panel shows non-MF mesenteric metastasis tissue. Original magnification: 200x (scale 1 μ m). C-D. IHC score of C9 (C) and COL12A1 (D) on tumor cells and stromal compartment of MF mesenteric metastases ($n = 6$) and non-MF mesenteric metastases ($n = 6$). Each dot and square represent one individual patient with overall median indicated by the horizontal line. ** $P < 0.01$ MF vs non-MF.

Discussion

As there are limited therapeutical options for MF, it is of paramount importance to gain knowledge about the processes involved the profibrotic deregulation of the SI-NET tumor microenvironment to find effective therapies^{10,25}. To this end, we studied primary SI-NETs and paired mesenteric metastases using an unbiased, label-free LC-MS proteomics approach. This resulted in new insights in the proteins associated with MF that can assist in guiding further research and treatment development.

Analysis of the detected proteomes of all samples revealed close clustering of the primary and mesenteric tumor samples of individual patients, suggesting a similarity between the samples and therefore relative limited transformation within a patient of the proteome of tumor cells during the metastatic process. On the other hand, unsupervised clustering of the stromal samples showed clear clustering of the fibrotic mesenteric metastasis stroma samples away from primary tumor stroma samples and non-fibrotic mesenteric metastasis stroma samples. This clustering suggests a specific protein fingerprint is associated with the presence of MF in mesenteric metastasis samples. Analysis of differential protein abundance confirmed the findings from the clustering analysis, as solely in mesenteric metastasis stroma samples, we detected differentially abundant proteins when comparing MF samples and non-MF samples. Network analysis of these differentially abundant proteins revealed multiple new pathways possibly involved in mesenteric fibrosis, next to conforming the involvement of known profibrotic factors such as TGF β .

The first network included multiple collagen subtypes that had a higher abundance in MF mesenteric metastases stroma. These collagens are associated with extracellular matrix dysregulation towards myofibroblastic differentiation, invasion and desmoplasia²⁶⁻²⁹. By IHC staining for COL12A1, we confirmed the higher expression in MF mesenteric metastases. Interestingly, most COL12A1 was found on the invasion front suggesting that also in SI-NETs it is involved in ECM dysregulation towards invasion. Based on IPA network analysis, these changes in collagen expression might be linked with VEGF signaling and the PI3K/Akt pathway. VEGF induced PI3K/Akt signaling has been linked to fibrosis development and regulation of TGF β expression^{30,31}. While overexpression of VEGF is well established in NETs and activation of Akt has been shown previously in

SI-NETs, it was not previously linked to MF development^{32,33}. Interestingly, pirfenidone, a novel anti-fibrotic drug, has been shown to suppress fibrogenesis in intestinal fibroblasts by inhibition of PI3K/Akt signalling pathway and more anti-fibrotic drugs targeting PI3K signaling are being developed^{31,34}.

The second IPA network included proteins involved in the fatty acid oxidation and inflammation. The proteins that were associated with mitochondrial fatty acid oxidation had a lower abundance in the MF mesenteric stroma suggesting mitochondrial dysfunction. Mitochondrial dysfunction leads to higher levels of reactive oxygen species (ROS) production which cause inflammation and induces fibrogenesis^{35,36}. ROS have also been shown to result in complement activation³⁷. This link between the decreased fatty acid oxidation and increased inflammation is further suggested by the increased abundance of C9 and SRPX2 in patients with mesenteric fibrosis. Using IHC, the strongest staining with C9 was seen on the border between tumor cells and stroma in mesenteric tissue from patients with MF. While to date there are no effective drugs targeting excessive ROS production or complement activation in fibrosis or cancer, the generated network offers interesting potential targets such as nuclear factor κ B (NF- κ B). NF- κ B is one of the molecules that links inflammation to cancer and fibrosis and novel drugs are being developed to alter NF- κ B³⁸. To date, NF- κ B in NETs is scarcely studied and its role in MF is unknown^{39,40}. However, as it has an important regulatory role in other cancers and fibrotic diseases with possible therapeutic options, it is an interesting target for further research^{38,41}.

The third IPA network that we have described consisted of various proteins that were mostly more abundant in MF mesenteric stroma. Many of these proteins are proteoglycans, such as asporin (ASPN) and microfibrillar-associated protein 4 (MFAP4), which are important constituents of the extracellular matrix. These proteins are essential for the correct balance between collagen synthesis and degradation. The increased abundance of these proteins in the mesenteric stroma of patients with mesenteric fibrosis is in line with a shift to more collagen synthesis. This results in change of the mechanic properties of the extracellular matrix, disrupting the matrix-mediated intercellular mechanocommunications which can result in increased secretion of profibrotic factors such as TGF β ⁴²⁻⁴⁴. A slight disruption in the balance of extracellular matrix remodelling

can therefore create a profibrotic feedback loop as both fibroblasts and SI-NET cells are mechanosensing⁴⁵. It is therefore interestingly to investigate the proteins in this network in greater detail as they could be the links between the extensive fibrogenesis seen in some patients and the known profibrotic factors secreted by SI-NETs.

It is important to also note the limitations of this study. We have used a label-free LC-MS proteomics method to identify proteins with differential abundance in MF and non-MF samples. This method permits to search hypothesis-free for proteins and pathways involved in MF. However, using this method only the relative high abundant proteins are detected. This can explain the discrepancy between the proteomics and IHC analysis in detecting COL12A1 and C9 expression in SI-NET tumor cells. In our study, more individual proteins were identified in tumor cell samples than in stroma samples. The signal from COL12A1 and C9 could therefore been overshadowed by other more abundant proteins in tumor cell samples. This example therefore elucidates the discovery driven nature of this study and demonstrates the importance of further validation of these results using targeted methods. Moreover, our study had a discovery driven design and it is important to further explore these pathways in a larger population with a more mechanistical approach. Recently, significant advances have been made in the development of SI-NET organoids and spheroids^{46,47}. Development of these new tumor models enables researchers to embed SI-NETs cells in 3D multicellular models that can also have various compositions of the extracellular matrix¹¹. Differences in collagen types and abundance can alter spheroid mechanics and influence pathways involved in tumor invasion and tissue remodelling and could be used to assess the involvement of the pathways identified in this study in mesenteric fibrosis and tumor invasion¹¹. Finally, it is important to note that we included only grade 1 SI-NETs to reduce potential bias in the proteomics analysis. The majority of cases with mesenteric fibrosis are SI-NET grade 1^{6,48}. However, to be certain that the same pathological mechanisms underlay mesenteric fibrosis in higher grade SI-NETs, it is important to include higher grade SI-NETs in validation studies.

In conclusion, we found that the proteome profiles of primary SI-NETs and paired mesenteric metastases differ primarily in the stromal compartment and a specific fibrotic fingerprint could be detected in mesenteric metastases stroma samples. Among the more

abundant proteins in MF mesenteric stroma were COL12A1 and C9. Further analysis of the differentially abundant proteins in mesenteric stroma and the associated networks could possibly lead to identification of therapeutic targets in MF.

Acknowledgements

The authors thank the Erasmus MC department for Pathology and especially dr. Thierry P.P. Van den Bosch for technological advice and performing the IHC staining.

References

1. Patel N, Benipal B. Incidence of Neuroendocrine Tumors in the United States from 2001-2015: A United States Cancer Statistics Analysis of 50 States. *Cureus*. Mar 26 2019;11(3):e4322.
2. Dasari A, Shen C, Halperin D, et al. Trends in the Incidence, Prevalence, and Survival Outcomes in Patients With Neuroendocrine Tumors in the United States. *JAMA Oncol*. Oct 1 2017;3(10):1335-1342.
3. Leoncini E, Boffetta P, Shafir M, Aleksavska K, Boccia S, Rindi G. Increased incidence trend of low-grade and high-grade neuroendocrine neoplasms. *Endocrine*. Nov 2017;58(2):368-379.
4. Pavel M, O'Toole D, Costa F, et al. ENETS Consensus Guidelines Update for the Management of Distant Metastatic Disease of Intestinal, Pancreatic, Bronchial Neuroendocrine Neoplasms (NEN) and NEN of Unknown Primary Site. *Neuroendocrinology*. 2016;103(2):172-85.
5. Pavel M, Gross DJ, Benavent M, et al. Telotristat ethyl in carcinoid syndrome: safety and efficacy in the TELECAST phase 3 trial. *Endocrine-Related Cancer*. 2018;25(3):309-322. doi:10.1530/erc-17-0455
6. Blazevic A, Zandee WT, Franssen GJH, et al. Mesenteric fibrosis and palliative surgery in small intestinal neuroendocrine tumours. *Endocr Relat Cancer*. Mar 2018;25(3):245-254.
7. Makridis C, Rastad J, Oberg K, Akerström G. Progression of metastases and symptom improvement from laparotomy in midgut carcinoid tumors. *World J Surg*. Sep 1996;20(7):900-6; discussion 907.
8. Pantongrag-Brown L, Buetow PC, Carr NJ, Lichtenstein JE, Buck JL. Calcification and fibrosis in mesenteric carcinoid tumor: CT findings and pathologic correlation. *AM J ROENTGENOL*. 1995;164(2):387-391.
9. Modlin IM, Moss SF, Chung DC, Jensen RT, Snyderwine E. Priorities for improving the management of gastroenteropancreatic neuroendocrine tumors. *J Natl Cancer Inst*. 2008;100(18):1282-1289. doi:10.1093/jnci/djn275
10. Blažević A, Hofland J, Hofland LJ, Feelders RA, de Herder WW. Small intestinal neuroendocrine tumours and fibrosis: an entangled conundrum. *Endocr Relat Cancer*. Mar 2018;25(3):R115-R130.
11. Boot RC, Koenderink GH, Boukany PE. Spheroid mechanics and implications for cell invasion. doi: 10.1080/23746149.2021.1978316. *Advances in Physics: X*. 2021/01/01 2021;6(1):1978316. doi:10.1080/23746149.2021.1978316

12. Laskaratos FM, Walker M, Wilkins D, et al. Evaluation of Clinical Prognostic Factors and Further Delineation of the Effect of Mesenteric Fibrosis on Survival in Advanced Midgut Neuroendocrine Tumours. *Neuroendocrinology*. 2018;107(3):292-304.
13. Blazevic A, Iyer AM, van Velthuysen MF, et al. Aberrant tryptophan metabolism in stromal cells is associated with mesenteric fibrosis in small intestinal neuroendocrine tumors. *Endocr Connect*. Mar 1 2022;
14. Niederle B, Pape UF, Costa F, et al. ENETS Consensus Guidelines Update for Neuroendocrine Neoplasms of the Jejunum and Ileum. *Neuroendocrinology*. 2016;103(2):125-38.
15. Ohrvall U, Eriksson B, Juhlin C, et al. Method for dissection of mesenteric metastases in mid-gut carcinoid tumors. *World J Surg*. Nov 2000;24(11):1402-8.
16. Zajec M, Kros JM, Dekker-Nijholt DAT, et al. Identification of Blood-Brain Barrier-Associated Proteins in the Human Brain. *J Proteome Res*. Jan 1 2021;20(1):531-537.
17. Liu NQ, Braakman RB, Stingl C, et al. Proteomics pipeline for biomarker discovery of laser capture microdissected breast cancer tissue. *J Mammary Gland Biol Neoplasia*. Jun 2012;17(2):155-64.
18. van der Ende EL, Meeter LH, Stingl C, et al. Novel CSF biomarkers in genetic frontotemporal dementia identified by proteomics. *Ann Clin Transl Neurol*. Apr 2019;6(4):698-707.
19. Vizcaíno JA, Côté RG, Csordas A, et al. The PRoteomics IDentifications (PRIDE) database and associated tools: status in 2013. *Nucleic Acids Res*. Jan 2013;41(Database issue):D1063-9.
20. Remmele W, Stegner HE. [Recommendation for uniform definition of an immunoreactive score (IRS) for immunohistochemical estrogen receptor detection (ER-ICA) in breast cancer tissue] Vorschlag zur einheitlichen Definition eines Immunreaktiven Score (IRS) für den immunhistochemischen Östrogenrezeptor-Nachweis (ER-ICA) im Mammakarzinomgewebe. *Pathologe*. May 1987;8(3):138-40.
21. Gu Z, Eils R, Schlesner M. Complex heatmaps reveal patterns and correlations in multidimensional genomic data. *Bioinformatics*. Sep 15 2016;32(18):2847-9.
22. Fu X, Gharib SA, Green PS, et al. Spectral index for assessment of differential protein expression in shotgun proteomics. *J Proteome Res*. Mar 2008;7(3):845-54.
23. Love MI, Huber W, Anders S. Moderated estimation of fold change and dispersion for RNA-seq data with DESeq2. *Genome Biology*. 2014/12/05 2014;15(12):550. doi:10.1186/s13059-014-0550-8

24. Krämer A, Green J, Pollard J, Jr., Tugendreich S. Causal analysis approaches in Ingenuity Pathway Analysis. *Bioinformatics*. Feb 15 2014;30(4):523-30.
25. Modlin IM, Shapiro MD, Kidd M. Carcinoid tumors and fibrosis: An association with no explanation. *Am J Gastroenterol*. 2004;99(12):2466-2478. doi:10.1111/j.1572-0241.2004.40507.x
26. Vazquez-Villa F, Garcia-Ocana M, Galvan JA, et al. COL11A1/(pro)collagen 11A1 expression is a remarkable biomarker of human invasive carcinoma-associated stromal cells and carcinoma progression. *Tumour Biol*. Apr 2015;36(4):2213-22.
27. Li T, Huang H, Shi G, et al. TGF-beta1-SOX9 axis-inducible COL10A1 promotes invasion and metastasis in gastric cancer via epithelial-to-mesenchymal transition. *Cell Death Dis*. Aug 28 2018;9(9):849.
28. Karagiannis GS, Petraki C, Prassas I, et al. Proteomic signatures of the desmoplastic invasion front reveal collagen type XII as a marker of myofibroblastic differentiation during colorectal cancer metastasis. *Oncotarget*. 2012;3(3):267-285. doi:10.18632/oncotarget.451
29. van Huizen NA, Coebergh van den Braak RRJ, Doukas M, Dekker LJM, JNM IJ, Luijder TM. Up-regulation of collagen proteins in colorectal liver metastasis compared with normal liver tissue. *J Biol Chem*. Jan 4 2019;294(1):281-289.
30. Lee KS, Park SJ, Kim SR, et al. Inhibition of VEGF blocks TGF-beta1 production through a PI3K/Akt signalling pathway. *Eur Respir J*. Mar 2008;31(3):523-31.
31. Wang J, Hu K, Cai X, et al. Targeting PI3K/AKT signaling for treatment of idiopathic pulmonary fibrosis. *Acta Pharm Sin B*. Jan 2022;12(1):18-32.
32. Shah T, Hochhauser D, Frow R, Quaglia A, Dhillon AP, Caplin ME. Epidermal growth factor receptor expression and activation in neuroendocrine tumours. *J Neuroendocrinol*. May 2006;18(5):355-60.
33. Cives M, Pelle E, Quaresmini D, Rizzo FM, Tucci M, Silvestris F. The Tumor Microenvironment in Neuroendocrine Tumors: Biology and Therapeutic Implications. *Neuroendocrinology*. 2019;109(2):83-99.
34. Sun Y, Zhang Y, Chi P. Pirfenidone suppresses TGF-β1-induced human intestinal fibroblasts activities by regulating proliferation and apoptosis via the inhibition of the Smad and PI3K/AKT signaling pathway. *Mol Med Rep*. Oct 2018;18(4):3907-3913.
35. Koundouros N, Pouligiannis G. Reprogramming of fatty acid metabolism in cancer. *British Journal of Cancer*. 2020/01/01 2020;122(1):4-22. doi:10.1038/s41416-019-0650-z

36. Li X, Zhang W, Cao Q, et al. Mitochondrial dysfunction in fibrotic diseases. *Cell Death Discovery*. 2020/09/05 2020;6(1):80. doi:10.1038/s41420-020-00316-9
37. Collard CD, Lekowski R, Jordan JE, Agah A, Stahl GL. Complement activation following oxidative stress. *Mol Immunol*. Sep-Oct 1999;36(13-14):941-8.
38. Freitas R, Fraga CAM. NF- κ B-IKK β Pathway as a Target for Drug Development: Realities, Challenges and Perspectives. *Curr Drug Targets*. 2018;19(16):1933-1942.
39. Crabtree JS, Singleton CS, Miele L. Notch Signaling in Neuroendocrine Tumors. *Front Oncol*. 2016;6:94.
40. Scott AT, Weitz M, Breheny PJ, et al. Gene Expression Signatures Identify Novel Therapeutics for Metastatic Pancreatic Neuroendocrine Tumors. *Clin Cancer Res*. Apr 15 2020;26(8):2011-2021.
41. Taniguchi K, Karin M. NF- κ B, inflammation, immunity and cancer: coming of age. *Nat Rev Immunol*. May 2018;18(5):309-324.
42. Kanaan R, Medlej-Hashim M, Jounblat R, Pilecki B, Sorensen GL. Microfibrillar-associated protein 4 in health and disease. *Matrix Biol*. May 26 2022;
43. Zhan S, Li J, Ge W. Multifaceted Roles of Asporin in Cancer: Current Understanding. Review. *Frontiers in Oncology*. 2019-September-24 2019;9doi:10.3389/fonc.2019.00948
44. Liu L, Yu H, Long Y, et al. Asporin inhibits collagen matrix-mediated intercellular mechanocommunications between fibroblasts during keloid progression. *The FASEB Journal*. 2021;35(7):e21705. doi:https://doi.org/10.1096/fj.202100111R
45. Tschumperlin DJ, Ligresti G, Hilscher MB, Shah VH. Mechanosensing and fibrosis. *The Journal of Clinical Investigation*. 2018;128(1):74-84. doi:10.1172/jci93561
46. Ear PH, Li G, Wu M, Abusada E, Bellizzi AM, Howe JR. Establishment and Characterization of Small Bowel Neuroendocrine Tumor Spheroids. *J Vis Exp*. Oct 14 2019;(152)
47. Kawasaki K, Toshimitsu K, Matano M, et al. An Organoid Biobank of Neuroendocrine Neoplasms Enables Genotype-Phenotype Mapping. *Cell*. 2020/11/25/ 2020;183(5):1420-1435.e21. doi:https://doi.org/10.1016/j.cell.2020.10.023
48. Laskaratos F-M, Mandair D, Hall A, et al. Clinicopathological correlations of mesenteric fibrosis and evaluation of a novel biomarker for fibrosis detection in small bowel neuroendocrine neoplasms. *Endocrine*. 2020;67(3):718-726. doi:10.1007/s12020-019-02107-4



Chapter 8

General discussion

General discussion

This thesis aimed at gaining better insight in the effect of current treatments for small intestinal neuroendocrine tumors (SI-NETs) on mesenteric metastases and fibrosis and also to further elucidate the processes involved in the development of SI-NET-associated mesenteric fibrosis. The implications of the main findings are discussed in this general discussion.

Palliative surgery for advanced SI-NETs with mesenteric disease

Mesenteric metastases are frequently present in SI-NETs and are known to induce fibrosis in the surrounding mesentery causing significant morbidity in SI-NET patients¹. Therefore, the current European Neuroendocrine Tumor Society (ENETS) guideline advises to consider palliative surgery in patients with advanced SI-NET and mesenteric metastases, even in asymptomatic patients². However, the studies on palliative surgery in advanced SI-NETs show conflicting results and there was a lack of studies analyzing asymptomatic SI-NET patients¹. As approximately 30-50% of SI-NET patients with mesenteric disease are asymptomatic, the benefits of prophylactic palliative surgery in these patients need to outweigh the risks^{3,4}. In **Chapter 3**, prophylactic palliative surgery was compared to symptomatic palliative surgery and there was no benefit on overall survival. A concurrent retrospective study confirmed our findings and found no difference in postoperative morbidity or mortality between prophylactic and symptomatic palliative surgery⁴. Moreover, this study found that prophylactic palliative surgery was associated with more reoperations due to bowel obstruction⁴. This suggests that next to having little benefit compared to surgery in a symptomatic stage, palliative prophylactic surgery may have additional risks. Since all studies until now were retrospective and had conflicting results, there is a clear need for a prospective study to assess the effect of prophylactic palliative surgery in advanced SI-NETs. Until that time, the decision needs to be made on an individual basis by a multidisciplinary team with careful weighing of the risks and benefits. In order to aid this assessment of risks and benefits, it is important to know the prognosis of mesenteric disease and the potential effects of non-surgical treatments on mesenteric metastases and fibrosis.

Progression of mesenteric disease

Unfortunately, the development of mesenteric disease over time was scarcely studied. There is only one study evaluating the progression of mesenteric metastases over time⁵. This study by Makridis and colleagues was performed before the widespread introduction of somatostatin analogues (SSAs), which are now the first line of treatment for low-grade advanced SI-NETs^{6,7}. Therefore, we evaluated the progression of mesenteric metastases over time in the era of targeted therapy. In **Chapter 2**, we described the very slow growth of mesenteric metastases. During follow-up, growth of the dominant mesenteric metastases was reported in only 13.5% of patients with a median time to growth of 40 months. Moreover, the development of mesenteric metastases, while not present at baseline, was very uncommon (2.6%). This suggests that different protumorigenic and prometastatic pathways might be dominant in mesenteric disease as compared to other metastatic locations. These findings are important to consider when assessing for disease progression and therapeutical response as there might be a discrepant behavior of mesenteric metastases as compared to other locations.

Effect of targeted therapy on mesenteric metastases and fibrosis

The effects of targeted treatment options for metastasized SI-NETs on mesenteric metastases and fibrosis have also been scarcely evaluated. Currently, SSAs are first line treatment options for low-grade metastasized SI-NETs with proven efficacy on tumor growth control and reduction of carcinoid syndrome symptoms⁷. However, it is unclear if the reduction on tumor growth also extends to mesenteric metastases. Moreover, SSAs are known to attenuate fibrosis in other diseases such as peritoneal sclerosis and pulmonary and liver fibrosis⁸⁻¹⁰. However, the effect of SSAs on the prevention or regression of mesenteric fibrosis has not been studied. In **Chapter 2**, we describe the development of mesenteric disease in a large cohort of patients. Unfortunately, as 91.2% of patients with mesenteric disease received SSAs treatment, it was not possible to evaluate the antitumor growth and antifibrotic effect of SSAs on SI-NET mesenteric metastases and fibrosis. As SSAs are now the first line treatment for low grade metastasized SI-NETs, the question of the effect of SSAs on mesenteric disease development and progression in SI-NETs will probably remain unanswered.

In **Chapter 2**, we also evaluated the effect of peptide receptor radionuclide therapy with ^{177}Lu -DOTATATE (PRRT) and found that this highly effective treatment option for SI-NETs resulted only in a size reduction of mesenteric metastases in 3.8% of patients as compared to an overall objective response rate of 12.9% when assessing all tumor lesions. Furthermore, next to having almost no effect on size reduction of mesenteric metastases, PRRT can cause bowel obstruction in SI-NET patients with mesenteric or peritoneal disease¹¹. These findings elucidate the importance of an individual management plan for patients with mesenteric metastases because a patient with an indication for undergoing PRRT might benefit from prophylactic surgery. Also, these findings stress the need to analyse other targeted treatments for their effects on mesenteric metastases and fibrosis in order to be able to correctly weigh the risks and benefits of treatment options and sequencing of treatments.

Predictors for symptomatic mesenteric disease

Next to evaluating the effect of different treatment options on mesenteric disease, it is important to be able to identify patients at risk for symptomatic mesenteric disease in order to optimize individual disease management. In this thesis, we tried to achieve this in two ways.

First, we analyzed our cohort of SI-NETs patients for the risks of developing mesenteric disease. Interestingly, we found sex to be associated with the risk of developing mesenteric fibrosis, next to the already known factors such as increased 5-hydroxyindoleacetic acid (5-HIAA) urinary excretion and a large size of the mesenteric metastasis (**Chapter 3**). Moreover, male sex was also associated with a higher risk of growth of a known mesenteric metastasis (**Chapter 2**). However, the odds ratio was not very high (OR 2.67) and it did not predict the development of symptomatic disease. Therefore, there is a need for a better prediction of symptomatic mesenteric disease.

Our second approach was to make prediction models based on systematic evaluation of CT imaging and CT-based radiomics as described in **Chapter 4**. The radiomics model had a similar performance as the multidisciplinary neuroendocrine tumor board. However, the individual clinicians had a poor interobserver agreement, making the prediction less reliable as the performance could vary depending on the presence of individual clinicians in a tumor board. As we believe the radiomics model for predicting

symptomatic mesenteric disease in SI-NET patients could have clinical value, we are now conducting a validation study. If the model retains a reliable performance, further prospective studies are needed to assess the clinical benefit to patients.

Next to demonstrating new avenues for developing tools to aid the prediction of the individual prognosis of SI-NETs and guide the selection of treatment options, the above-mentioned studies have also elucidated potential new pathways involved in the pathogenesis of mesenteric metastases and fibrosis.

New insights in the development of mesenteric metastases and fibrosis

As described in **Chapter 2** and **3**, we found a potential protective effect of female sex for the development of mesenteric disease. In **Chapter 5**, we have analyzed this in greater detail. Women younger than 50 years had less mesenteric metastases than older women or men. On the other hand, the rate of distant metastatic disease and hepatic metastases did not differ between the groups. Moreover, when young women had mesenteric metastases, the rate of mesenteric fibrosis was the same as in the other groups. This suggests a protective mechanism in young women which mainly affects the metastatic potential to the mesentery. However, the question remains how this effect is potentiated.

As the protective effect dissipates over time from the age of 50, it seems to be linked to the hormonal changes during the lifespan of women. In an attempt to elucidate the underlying potential pathophysiological mechanism, we analyzed the primary tumor and mesenteric metastases for the presence of sex steroid hormone receptors. Most importantly, using immunohistochemistry, the presence of the estrogen receptor alpha (ER α) was demonstrated in tumor cells and stroma, whereas androgen receptor (AR) staining was found in stromal cells only. Interestingly, there was no sex difference in the expression level ER α or AR, although patient numbers were low. However, as there are hormonal differences between premenopausal women compared to men and postmenopausal women, the effects potentiated by these sex steroid receptors probably differ between the groups. The exact effects and the interaction between other known protumorigenic and profibrotic pathways is worth further investigations.

Focusing back on our radiomics prediction models (**Chapter 4**), we can appreciate three findings that can aid our understanding of the development of symptomatic

mesenteric disease. First, the models including the dominant mesenteric metastasis did not result in any improved performance. So even though these mesenteric masses are the root from which the mesenteric fibrosis seems to develop, there were no radiological features that made a mass more or less likely to result in symptomatic disease. It is important to note that also features as volume and size were included.

Second, the radiomics model that only included the localization of the mesenteric metastatic mass in relation to the superior mesenteric artery (SMA) performed only slightly less than our optimal model based on the surrounding mesentery. This could be explained by the fact that more proximal lesions comprise a larger proportion of the intestinal blood flow, thereby increasing the risk for symptomatic disease. However, this finding could also point to other mechanistic factors involved in development of symptomatic mesenteric disease. As enterochromaffin cells and SI-NET cells are mechanosensitive, the localization of the mesenteric metastases within in the mesentery might result in different mechanic forces exerted on the tumor cells¹². This could affect the secretion of profibrotic factors resulting in desmoplasia. Therefore, it is an important avenue to investigate further in the validation study as it could result in identifying an easy predictor for symptomatic disease in the case of the former hypothesis or an interesting line of future research in case of the latter.

Finally, it is noteworthy that the best performing model was based solely on the mesentery surrounding the mesenteric mass. This highlights the importance of the interaction between SI-NET cells and the surrounding tissue in the development of symptomatic mesenteric disease. However, the analysis of the highly predictive variables in the radiomics models did not offer clear clues for identifying the underlying pathogenesis. Therefore, we conducted proteomics studies to investigate these local processes in greater details.

In **Chapter 6**, we have used proteomics to investigate proteins involved in the tryptophan metabolism. The analyzed proteins are, among others, involved in serotonin production and degradation¹³. Serotonin has been deemed one of the key factors contributing to SI-NET-associated fibrosis. We have shown that in patients with mesenteric fibrosis there were significantly less proteins present in the mesenteric stroma which are involved in serotonin degradation, such as monoamine oxidase A (MAO-A), compared to stroma of patients without mesenteric fibrosis. A lower rate of

serotonin degradation results in an increased bioactivity of serotonin and could increase the profibrotic potential of SI-NET cells in this environment^{14, 15}. This finding offers the first clue in understanding the difference in individual susceptibility for mesenteric fibrosis. Further research is necessary to determine if the lower abundance of serotonin degradation proteins is due to tumor-related processes or is a more inherent characteristic of the individual patient.

The next step was to analyze the proteomics data in a hypothesis-free method in order to potentially reveal new pathways involved in mesenteric fibrosis. As described in **Chapter 7**, we found only in the mesenteric stroma a clear proteome fingerprint associated with mesenteric fibrosis. The tumor cells showed no significant differences in protein abundance when comparing those from patients with and without mesenteric fibrosis. It is also important to note that the proteome of stroma from the primary tumor did not differ significantly between those from patients with and without mesenteric fibrosis. This again stresses the importance of the interaction between the tumor cells and the environment in the development of SI-NET-associated fibrosis. The mesenteric tumor cells were not significantly different from the primary tumor cells, but in some cases, they induced severe fibrotic reactions which were not seen in the stroma surrounding the primary tumor.

When we analyzed this mesenteric fibrotic proteome fingerprint, we could cluster the proteins in three Ingenuity Pathway analysis (IPA) networks. The first network included the multiple collagen subtypes that had a higher abundance in the fibrotic mesenteric stroma. These collagens are associated with extracellular matrix dysregulation towards increased invasion and desmoplasia. We demonstrated that the changes in collagen expression might be linked to vascular endothelial growth factor (VEGF) signaling and the phosphoinositide 3-kinase (PI3K)/Akt pathway. While overexpression of VEGF is well established in NETs and activation of Akt has been shown previously in SI-NETs, this was not previously linked to mesenteric fibrosis development.

The second IPA network included proteins involved in the fatty acid oxidation and inflammation. The lower abundance of proteins involved in mitochondrial fatty acid oxidation in the fibrotic mesenteric stroma is suggestive of mitochondrial dysfunction. Mitochondrial dysfunction can cause inflammation and fibrogenesis by higher level of reactive oxygen species (ROS) production. The link between the decreased fatty acid

oxidation and increased inflammation is further shown by the interaction in the network with increased abundance of complement C9 in patients with mesenteric fibrosis.

The third IPA network that we have identified consisted of various proteins present in the extracellular matrix. Many of these proteins are proteoglycans, such as asporin (ASPN) and microfibrillar-associated protein 4 (MFAP4) and are important constituents of the extracellular matrix. These proteins are essential for an appropriate balance between collagen synthesis and degradation. The increased abundance of these proteins in the mesenteric stroma of patients with mesenteric fibrosis is in line with a shift to more collagen synthesis. This results in changes of the mechanic properties of the extracellular matrix, disrupting the matrix-mediated intercellular mechanocommunications which results in increased secretion of profibrotic factors such as transforming growth factor beta (TGF β)¹⁶⁻¹⁸. A slight disruption in the balance of extracellular matrix remodeling can therefore create a profibrotic feedback loop as both fibroblasts and SI-NET cells are mechanosensing¹⁹. It is interestingly, therefore, to investigate the proteins in this network in greater detail as they could be the links between the extensive fibrogenesis seen in some patients and the known profibrotic factors secreted by SI-NETs. This, in turn, may result in identification of therapeutic targets,

Potential therapeutic options based on novel insights in mesenteric metastasis and fibrosis

These new insights in the development of mesenteric metastases and fibrosis might also have therapeutical implications that warrant further research. First, in **Chapter 5** we have described the potential protective effect of estrogen in the development of mesenteric metastases. Therefore, it would be interesting to explore if tamoxifen, a synthetic nonsteroidal selective estrogen receptor modulator, might have a beneficial role in SI-NET management. Tamoxifen is known for its antifibrotic effects and is used in the management of fibrotic disease such as retroperitoneal fibrosis^{20, 21}. Furthermore, a few cases in which tamoxifen was used in SI-NET patients and which resulted in tumor growth control and amelioration of carcinoid syndrome symptoms were already reported²²⁻²⁴. However, as noted earlier, it is important to understand that the processes involved in fibrogenesis are likely not to be the same as the processes involved in proliferation. Study

designs should take this into account and, therefore, separately assess a potential drug for each property.

Next, in **Chapter 6** we described aberrant tryptophan metabolism in patients with extensive mesenteric fibrosis with a lower level of serotonin degrading enzymes in the mesenteric stroma. Therefore, it would be of interest to investigate therapies that could increase the expression and activity of these enzymes. Valproic acid, an anticonvulsant, was found to be an inducer of MAO-A activity and may thus be a potential valuable therapeutic option in regulating serotonin-mediated fibrosis in SI-NETs²⁵. An additional benefit of valproic acid is its activity as a potent histone deacetylase inhibitor that has been demonstrated in NET cell lines to increase expression of somatostatin receptor 2 and thus potentially potentiates a cytotoxic effect of SSAs or PRRT^{26, 27}.

On the other hand, if there is decreased serotonin degradation, the balance could be restored by also decreasing serotonin production. Recently, telotristat ethyl, a tryptophan hydroxylase inhibitor, has shown to be effective for the treatment of carcinoid syndrome associated diarrhea²⁸. Moreover, treatment with telotristat ethyl lowered significantly the 5-HIAA urinary excretion, a marker of systemic serotonin production^{28, 29}. Lowering serotonin production could restore the balance between serotonin production and degradation and impair fibrogenesis. As telotristat ethyl is generally well tolerated, it could be suitable for the long-term use which is required to prevent a slow progressive process as mesenteric metastasis and fibrosis²⁸. Therefore, it would be worth exploring the effect of telotristat ethyl on SI-NET mesenteric disease within a clinical trial.

Lastly, we have described in **Chapter 7** multiple new proteins and pathways that are possibly involved in mesenteric fibrosis and which could be explored as therapeutic options. We describe a possible link between mesenteric fibrosis and VEGF signaling. Therefore, a tyrosine-kinase inhibitor (TKI) targeting VEGF signaling might have antifibrotic effects in SI-NETs³⁰. However, most TKIs have significant adverse events, precluding long-term prophylactic use against the development of mesenteric fibrosis. Moreover, since sunitinib, the only approved TKI for NET treatment, had only a limited effect on tumor growth in SI-NETs, it will have to be combined with other antitumor therapies which further precludes its clinical use³¹. Until the development of better tolerated TKIs, the use of TKIs to prevent fibrogenesis does not seem clinically viable.

To explore other treatment options such as targeting the proteoglycans and complement activation, first the role of these signalling pathways in SI-NET and mesenteric fibrosis development needs to be better understood.

References

1. Niederle B, Pape UF, Costa F, et al. ENETS Consensus Guidelines Update for Neuroendocrine Neoplasms of the Jejunum and Ileum. *Neuroendocrinology*. 2016;103(2):125-38.
2. Partelli S, Bartsch DK, Capdevila J, et al. ENETS Consensus Guidelines for the Standards of Care in Neuroendocrine Tumours: Surgery for Small Intestinal and Pancreatic Neuroendocrine Tumours. *Neuroendocrinology*. 2017;105(3):255-265. doi:10.1159/000464292
3. Laskaratos FM, Walker M, Wilkins D, et al. Evaluation of Clinical Prognostic Factors and Further Delineation of the Effect of Mesenteric Fibrosis on Survival in Advanced Midgut Neuroendocrine Tumours. *Neuroendocrinology*. 2018;107(3):292-304.
4. Daskalakis K, Karakatsanis A, Hessman O, et al. Association of a Prophylactic Surgical Approach to Stage IV Small Intestinal Neuroendocrine Tumors With Survival. *JAMA Oncol*. Feb 1 2018;4(2):183-189.
5. Makridis C, Rastad J, Oberg K, Akerström G. Progression of metastases and symptom improvement from laparotomy in midgut carcinoid tumors. *World J Surg*. Sep 1996;20(7):900-6; discussion 907.
6. Makridis C, Ekblom A, Bring J, et al. Survival and daily physical activity in patients treated for advanced midgut carcinoid tumors. *Surgery*. Dec 1997;122(6):1075-82.
7. Pavel M, O'Toole D, Costa F, et al. ENETS Consensus Guidelines Update for the Management of Distant Metastatic Disease of Intestinal, Pancreatic, Bronchial Neuroendocrine Neoplasms (NEN) and NEN of Unknown Primary Site. *Neuroendocrinology*. 2016;103(2):172-85.
8. Lang A, Sakhnini E, Fidder HH, Maor Y, Bar-Meir S, Chowers Y. Somatostatin inhibits pro-inflammatory cytokine secretion from rat hepatic stellate cells. *Liver International*. 2005;25:808-816. doi:10.1111/j.1478-3231.2005.01057.x
9. Ertilav M, Hur E, Bozkurt D, et al. Octreotide lessens peritoneal injury in experimental encapsulated peritoneal sclerosis model. *Nephrology*. 2011;16:552-557. doi:10.1111/j.1440-1797.2011.01460.x
10. Borie R, Fabre A, Prost F, et al. Activation of somatostatin receptors attenuates pulmonary fibrosis. *Thorax*. 2008;63:251-258. doi:10.1136/thx.2007.078006
11. Strosberg JR, Al-Toubah T, Pellè E, et al. Risk of Bowel Obstruction in Patients with Mesenteric or Peritoneal Disease Receiving Peptide Receptor Radionuclide Therapy. *J Nucl Med*. Jan 2021;62(1):69-72.

12. Byrnes KG, Walsh D, Walsh LG, et al. The development and structure of the mesentery. *Communications Biology*. 2021/08/18 2021;4(1):982. doi:10.1038/s42003-021-02496-1
13. Roth W, Zadeh K, Vekariya R, Ge Y, Mohamadzadeh M. Tryptophan Metabolism and Gut-Brain Homeostasis. *International Journal of Molecular Sciences*. 2021;22(6):2973.
14. Mohammad-Zadeh LF, Moses L, Gwaltney-Brant SM. Serotonin: a review. *J Vet Pharmacol Ther*. Jun 2008;31(3):187-99.
15. Mann DA, Oakley F. Serotonin paracrine signaling in tissue fibrosis. *Biochimica et Biophysica Acta (BBA) - Molecular Basis of Disease*. 2013/07/01/ 2013;1832(7):905-910. doi:https://doi.org/10.1016/j.bbadis.2012.09.009
16. Kanaan R, Medlej-Hashim M, Jounblat R, Pilecki B, Sorensen GL. Microfibrillar-associated protein 4 in health and disease. *Matrix Biol*. May 26 2022;
17. Zhan S, Li J, Ge W. Multifaceted Roles of Aspirin in Cancer: Current Understanding. Review. *Frontiers in Oncology*. 2019-September-24 2019;9doi:10.3389/fonc.2019.00948
18. Liu L, Yu H, Long Y, et al. Aspirin inhibits collagen matrix-mediated intercellular mechanocommunications between fibroblasts during keloid progression. *The FASEB Journal*. 2021;35(7):e21705. doi:https://doi.org/10.1096/fj.202100111R
19. Tschumperlin DJ, Ligresti G, Hilscher MB, Shah VH. Mechanosensing and fibrosis. *The Journal of Clinical Investigation*. 2018;128(1):74-84. doi:10.1172/jci93561
20. van Bommel EF, Hendriksz TR, Huiskes AW, Zeegers AG. Brief communication: tamoxifen therapy for nonmalignant retroperitoneal fibrosis. *Ann Intern Med*. Jan 17 2006;144(2):101-6.
21. Mikulec AA, Hanasono MM, Lum J, Kadleck JM, Kita M, Koch R. Effect of tamoxifen on transforming growth factor β 1 production by keloid and fetal fibroblasts. *Archives of Facial Plastic Surgery*. 2001;3:111-114. doi:10.1001/archfaci.3.2.111
22. Stathopoulos GP, Karvountzis GG, Yiotis J. Tamoxifen in carcinoid syndrome. *N Engl J Med*. Jul 2 1981;305(1):52.
23. Myers CF, Ershler WB, Tannenbaum MA, Barth R. Tamoxifen and Carcinoid Tumor. doi: 10.7326/0003-4819-96-3-383_1. *Annals of Internal Medicine*. 1982/03/01 1982;96(3):383-383. doi:10.7326/0003-4819-96-3-383_1
24. Moertel CG, Engstrom PF, Schutt AJ. Tamoxifen Therapy for Metastatic Carcinoid Tumor: A Negative Study. *Annals of Internal Medicine*. 1984/04/01 1984;100(4):531-532. doi:10.7326/0003-4819-100-4-531

25. Wu JB, Shih JC. Valproic acid induces monoamine oxidase A via Akt/forkhead box O1 activation. *Mol Pharmacol*. Oct 2011;80(4):714-23.
26. Veenstra MJ, van Koetsveld PM, Dogan F, et al. Epidrug-induced upregulation of functional somatostatin type 2 receptors in human pancreatic neuroendocrine tumor cells. *Oncotarget*. Mar 13 2018;9(19):14791-14802.
27. Arvidsson Y, Johanson V, Pfragner R, Wängberg B, Nilsson O. Cytotoxic Effects of Valproic Acid on Neuroendocrine Tumour Cells. *Neuroendocrinology*. 2016;103(5):578-591. doi:10.1159/000441849
28. Kulke MH, Horsch D, Caplin ME, et al. Telotristat ethyl, a tryptophan hydroxylase inhibitor for the treatment of carcinoid syndrome. *Journal of Clinical Oncology*. 2017;35:14-23. doi:10.1200/jco.2016.69.2780
29. Pavel M, Gross DJ, Benavent M, et al. Telotristat ethyl in carcinoid syndrome: safety and efficacy in the TELECAST phase 3 trial. *Endocr Relat Cancer*. Mar 2018;25(3):309-322.
30. Qu K, Huang Z, Lin T, et al. New Insight into the Anti-liver Fibrosis Effect of Multitargeted Tyrosine Kinase Inhibitors: From Molecular Target to Clinical Trials. Mini Review. *Frontiers in Pharmacology*. 2016-January-18 2016;6doi:10.3389/fphar.2015.00300
31. Kulke MH, Lenz HJ, Meropol NJ, et al. Activity of sunitinib in patients with advanced neuroendocrine tumors. *J Clin Oncol*. Jul 10 2008;26(20):3403-10.



Chapter 9

Summary

Samenvatting

Summary

Mesenteric fibrosis is a hallmark of small intestinal neuroendocrine tumors (SI-NETs) and can lead to severe complications such as intestinal obstruction, ischemia, and perforation. It is induced by various bioactive molecules secreted by SI-NETs, such as serotonin. In recent decades, the survival of SI-NETs patients has increased due to the development of targeted treatment options, such as somatostatin analogues (SSAs), everolimus, and peptide receptor radionuclide therapy with ^{177}Lu -DOTATATE (PRRT). As patients are living longer, the lack of treatment options for mesenteric fibrosis becomes more evident as they suffer more from its complications. Currently, the management of mesenteric fibrosis is limited to surgery. To improve SI-NET patient care, it is important to find better treatment options. Therefore, it is essential to gain a better understanding of the mechanisms involved in mesenteric fibrosis development and the effect of different medical therapies on it. **Chapter 1** of this thesis provides a broader introduction to SI-NETs, mesenteric fibrosis, and the aims of this thesis.

In **Chapter 2**, we assessed the development and progression of mesenteric metastases in the era of targeted therapy. We found that the mesenteric metastases had a very slow growth rate, with only 13.5% of patients showing objective growth during follow-up, with a median time to growth of 40 months. Moreover, the development of mesenteric metastases, if not present at baseline, was very rare. We assessed patients and disease characteristics as potential predictors for growth, and only male sex was found to be a significant predictor for growth of mesenteric metastases. Finally, we found that the effect of PRRT on mesenteric metastases size is very limited, as it resulted in an objective response in only 3.8% compared to an objective response rate of 12.8% when assessing all tumor target lesions.

In **Chapter 3**, we assessed different surgical strategies for mesenteric fibrosis. To date, surgery is the only effective treatment for symptoms caused by mesenteric metastases and fibrosis. Debate continues regarding the benefit of prophylactic surgery in asymptomatic

patients compared to symptomatic surgery or no surgery. We found no benefit of prophylactic surgery on overall survival. However, it is possible that some patients at high risk of developing symptoms may benefit from earlier surgery.

In **Chapter 4**, we analyzed CT scans of patients with asymptomatic and symptomatic mesenteric disease to identify those at high risk for symptomatic disease. We found that the radiomics model based solely on the mesentery surrounding the dominant mesenteric metastases had the best performance. The addition of data extracted from the mesenteric metastases or known clinical disease prediction factors did not improve this performance. The radiomics model showed comparable performance to systematic evaluation by clinicians and a multidisciplinary tumor board. However, the clinicians exhibited poor interobserver agreement, which could lead to less reproducible predictions compared to the radiomics model.

Next, we focus on elucidating the processes that cause fibrogenesis in SI-NET patients. In **Chapter 5**, we analyzed a cohort of SI-NET patients and found a clear sexual dimorphism regarding the rate of mesenteric disease. Younger women were less likely to develop mesenteric metastases and, consequently, less likely to develop mesenteric fibrosis. When analyzing the potential underlying mechanism of this sexual dimorphism, we found expression of estrogen receptor alpha (ER α) in tumor cells and the surrounding stroma, as well as androgen receptor (AR) expression in the stromal compartment. We noted a strong correlation of ER α expression in tumor cells of primary tumors and mesenteric metastases, but no correlation of the stroma expression of ER α or AR between primary tumor and mesenteric metastases. Interestingly, there was also no sex difference in the rate of positive staining for ER α or AR.

Serotonin has been identified as a primary driver of SI-NET-associated fibrogenesis. However, individual differences in susceptibility to its profibrotic effects have been observed. To gain insight into the underlying mechanisms of these differences, we utilized a proteomics-based approach to analyze tryptophan and serotonin metabolism pathways

in SI-NET patients with and without mesenteric fibrosis in **Chapter 6**. Our findings suggest that serotonin is less efficiently metabolized in patients with mesenteric fibrosis compared to those without, leading to prolonged bioactivity of serotonin.

In **Chapter 7**, we conducted a detailed analysis of the proteome of primary SI-NETs and paired mesenteric metastases from patients with and without mesenteric fibrosis. Using liquid chromatography-mass spectrometry-based proteomics, we identified a total of 2988 proteins. Unsupervised hierarchical clustering revealed a clear dichotomy between tumor samples and stroma samples, and further showed a close clustering of fibrotic mesenteric metastasis stroma samples, which separated them from stroma samples of primary tumors and non-fibrotic mesenteric metastases. Comparing samples of patients with mesenteric fibrosis to those without, we found 36 proteins with a significantly different abundance. Even though these proteins were also found in different tissue groups; the differential abundance was only present in the mesenteric metastasis stroma samples. Analysis of these proteins showed higher abundance in patients with mesenteric fibrosis of complement C9, various collagens, and proteoglycans associated with extracellular matrix dysregulation, and an association with platelet-derived growth factor (PDGF), transforming growth factor beta (TGF β), and vascular endothelial growth factor (VEGF) signaling. Proteins involved in fatty acid oxidation were found to have a lower abundance in patients with mesenteric fibrosis.

In **Chapter 8**, a general discussion reviews the findings from the preceding chapters in a broader context and proposes future research directions.

Samenvatting

Mesenteriale fibrose is een van de kenmerken van neuro-endocriene tumoren welke ontstaan in de dunne darm (SI-NET) en dit kan ernstige complicaties veroorzaken, zoals darmobstructie, ischemie en perforatie. Mesenteriale fibrose vindt plaats rond een mesenteriale uitzaaiing van de SI-NET. De SI-NET scheidt verschillende bioactieve moleculen af, zoals serotonine, welke onder andere fibrosevorming kunnen veroorzaken. De afgelopen decennia is de overleving van patiënten met een SI-NET toegenomen dankzij de ontwikkeling van gerichte behandelingsopties zoals somatostatine-analogen (SSAs), everolimus en peptide receptor radionuclide therapie met ^{177}Lu -DOTATATE (PRRT). Hierdoor is het ontbreken van goede behandelingsopties voor mesenteriale fibrose belangrijker geworden omdat patiënten langer overleven en daarom meer de problemen veroorzaakt door mesenteriale fibrose gaan ervaren. Momenteel is chirurgisch ingrijpen de enige behandelingsoptie voor mesenteriale fibrose. Echter dit betreft een ingrijpende operatie met belangrijke risico's op complicaties. Om de zorg voor SI-NET patiënten te verbeteren, is het belangrijk om betere behandelopties te ontwikkelen. Hiervoor is het essentieel om meer inzicht te krijgen in de mechanismen die betrokken zijn bij de ontwikkeling van mesenteriale fibrose. In **Hoofdstuk 1** wordt een uitgebreide introductie gegeven over SI-NETs en mesenteriale fibrose en wordt het doel van dit proefschrift toegelicht.

In **Hoofdstuk 2** werd het ontstaan en de progressie van mesenteriale uitzaaiingen in het tijdperk van verbeterde en gerichte therapie van SI-NETs onderzocht. We vonden dat de mesenteriale uitzaaiingen een zeer trage groeisnelheid hebben, waarbij slechts bij 13,5% van de patiënten objectieve groei werd aangetoond tijdens de follow-up met een mediane tijd tot groei van 40 maanden. Bovendien was het ontstaan van mesenteriale uitzaaiingen, als deze niet aanwezig waren bij eerste diagnose van de SI-NET, zeer zeldzaam. Patiënt- en tumorkenmerken werden beoordeeld als potentiële voorspellers voor groei en alleen mannelijk geslacht bleek een significante voorspeller te zijn voor de groei van mesenteriale uitzaaiingen. Tenslotte bleek PRRT een beperkt effect op de grootte van mesenteriale uitzaaiingen te hebben. PRRT resulteerde in een objectieve respons bij slechts 3,8%

van de mesenteriale uitzaaiingen in vergelijking met een objectieve respons van 12,8% wanneer alle tumordoellaesies werden beoordeeld.

Vervolgens hebben we verschillende chirurgische strategieën voor mesenteriale fibrose beoordeeld. Chirurgie is tot op heden de enige effectieve behandeling voor symptomen veroorzaakt door mesenteriale metastasen en fibrose. Er is echter discussie of profylactische chirurgie in een asymptomatisch stadium beter is dan chirurgie in een symptomatisch stadium. In **Hoofdstuk 3** vergeleken we profylactische palliatieve chirurgie met symptomatische palliatieve chirurgie of geen chirurgie en vonden geen voordeel van profylactische chirurgie op de overleving van patiënten. Dit sluit echter niet uit dat sommige patiënten met een hoog risico op het ontwikkelen van symptomatische ziekte baat kunnen hebben bij chirurgie in een eerder stadium.

Om patiënten met een hoog risico op symptomatische mesenteriale ziekte te identificeren, analyseerden we in **Hoofdstuk 4** de CT-scans van patiënten met asymptomatische en symptomatische mesenteriale ziekte met behulp van systematische evaluatie door klinici en met radiomics. Hierbij had het radiomics-model, dat uitsluitend is gebaseerd op het mesenterium rond de dominante mesenteriale uitzaaiing, de beste prestaties. Het radiomics-model werd niet verbeterd door gegevens toe te voegen die waren geëxtraheerd uit de mesenteriale uitzaaiingen of bekende klinische ziektevoorspellers. Het radiomics-model toonde een vergelijkbare prestatie als systematische evaluatie door klinici en een multidisciplinaire tumorraad. De klinici hadden echter een slechte score-overeenkomst tussen de waarnemers, wat kan resulteren in minder replicerbare voorspellingen in vergelijking met het radiomics-model.

Vervolgens richt het proefschrift zich op het ophelderen van de processen die fibrogenese veroorzaken bij SI-NET patiënten. In **Hoofdstuk 5** analyseerden we een cohort van SI-NET patiënten en vonden we een duidelijk seksueel dimorfisme met betrekking tot de frequentie van mesenteriale ziekte. Jongere vrouwen hadden minder kans op het ontwikkelen van mesenteriale uitzaaiingen en vervolgens minder kans op het ontwikkelen van mesenteriale fibrose. Bij het analyseren van het mogelijke onderliggende mechanisme van dit seksuele dimorfisme, vonden we expressie van oestrogenreceptor-alfa (ER α) in

tumorcellen en het omringende stroma. Androgeenreceptor (AR) expressie was alleen aanwezig in het stromale compartiment. Hoewel er een sterke correlatie was van ER α -expressie in tumorcellen van primaire tumoren en die in mesenteriale uitzaaiingen, was er geen correlatie van de stromale expressie van ER of AR tussen de primaire tumor en mesenteriale uitzaaiing. Interessant genoeg was er ook geen sekseverschil in de mate van positiviteit van de kleuring voor ER α of AR.

Zoals eerder genoemd, wordt serotonine beschouwd als de belangrijkste aanjager van SI-NET-geassocieerde fibrogenese. Er zijn echter individuele verschillen in de gevoeligheid voor de profibrotische effecten van serotonine. Om inzicht te krijgen in de onderliggende mechanismen van deze individuele verschillen, analyseerden we in **Hoofdstuk 6** de tryptofaan en serotonine metaboliseroute in SI-NET-patiënten met en zonder mesenteriale fibrose. Gebruikmakend van proteomics, vonden we een lagere expressie van serotonine-metaboliserende enzymen in het mesenteriale stroma van patiënten met mesenteriale fibrose in vergelijking met patiënten zonder mesenteriale fibrose. Deze bevinding suggereert dat serotonine minder efficiënt wordt gemetaboliseerd bij patiënten met mesenteriale fibrose en derhalve langer bioactief kan blijven.

In **Hoofdstuk 7** hebben we het proteoom van primaire SI-NETs en gepaarde mesenteriale uitzaaiingen van patiënten met en zonder mesenteriale fibrose uitgebreider geanalyseerd. Met behulp van vloeistofchromatografie-massaspectrometrie-gebaseerde proteomics werden in totaal 2988 proteïnes geïdentificeerd. Ongesuperviseerde hiërarchische clustering toonde een duidelijke dichotomie tussen tumorweefsel en stromaweefsel. Bovendien toonde het een nauwe clustering van stroma van fibrotische mesenteriale uitzaaiingen waarbij er een heldere scheiding was met componenten van stroma van primaire tumoren en niet-fibrotische mesenteriale uitzaaiingen. Verder vonden we 36 proteïnes met een significant verschillend abundantie tussen patiënten met mesenteriale fibrose en zonder mesenteriale fibrose. Hoewel deze proteïnes in verschillende weefselgroepen werden gevonden, was de differentiële abundantie alleen aanwezig in het stroma van mesenteriale uitzaaiingen. Analyse van deze proteïnes toonde een hogere abundantie bij patiënten met mesenteriale fibrose van complement C9, verschillende collagenen en proteoglycanen geassocieerd met ontregeling van de

extracellulaire matrix en een associatie met PDGF-, TGF β - en VEGF-signaal transductie. Proteïnes die betrokken zijn bij vetzuuroxidatie vertoonden een lagere abundantie bij patiënten met mesenteriale fibrose.

Ten slotte bevat **Hoofdstuk 8** een algemene discussie waarin de bevindingen beschreven in de vorige hoofdstukken in een breder perspectief worden geplaatst en voorstellen worden gedaan voor toekomstig onderzoek.



Appendix

Erasmus MC PhD Portfolio

List of publications

Dankwoord

Curriculum Vitae



Erasmus MC PhD Portfolio

Name PhD student:	Anela Blažević
Erasmus MC department:	Internal Medicine, Section of Endocrinology
Research School:	Molecular Medicine
PhD period:	2017 - 2023
Promotors	prof.dr. Wouter W. de Herder prof.dr. Leo J. Hofland
Co-promotor	dr. Richard A. Feelders

Training	Year	Workload (ECTS)
General Academic Courses		
Survival Analysis	2017	0.6
Systematic literature retrieval in Pubmed and Embase	2017	0.6
Endnote	2017	0.2
Basic Introduction Course on SPSS	2017	1
Biomedical English Writing	2017	2
Biostatistical Methods I: Basis Principles	2017	5.7
Biostatistical Methods II: Classical Regression Models	2017	4.3
Scientific Integrity	2018	0.3
Python programming	2022	2.5
Clinical Courses		
Postgraduate Course 14 th Annual ENETS Conference for the Diagnosis and Treatment of Neuroendocrine Tumor Disease	2017	0.6
Postgraduate Course 15 th Annual ENETS Conference for the Diagnosis and Treatment of Neuroendocrine Tumor Disease	2018	0.5
prIME Masterclass Neuroendocrine Tumors	2018	1
Postgraduate Course 16 th Annual ENETS Conference for the Diagnosis and Treatment of Neuroendocrine Tumor Disease	2019	0.3

Training	Year	Workload (ECTS)
Conferences – oral presentations		
ESE Young Endocrinologist and Scientists (EYES) Meeting, Porto	2017	1
Young Dutch Society for Endocrinology (JNVE) Conference, Leiden	2017	1
Dutch Endocrine Meeting, Noordwijkerhout	2018	1
Annual European Neuroendocrine Tumor Society (ENETS) Conference, Barcelona	2018	1
Science Days Internal Medicine, Antwerp	2018	1
Annual European Neuroendocrine Tumor Society (ENETS) Conference, Barcelona	2019	1
Annual European Neuroendocrine Tumor Society (ENETS) Conference, online	2020	1
Conferences – poster presentations		
Science Days Internal Medicine, Antwerp	2017	0.7
European Congress of Endocrinology (ECE)	2018	0.7
Teaching		
Invited lectures		
Erasmus Endocrinology Course, Noordwijkerhout	2018	1
Annual North American Neuroendocrine Tumor Society (NANETS), Seattle	2018	1
Dutch ENETS Congress Update, Rotterdam	2019	1
ESE Young Endocrinologist and Scientists (EYES) Meeting, Athens	2019	1
Dutch Academic Research Update, Rotterdam	2021	1
Annual Dutch Society for Surgery (NVvH) Spring meeting, online	2021	1
Dutch Endocrine Meeting, Noordwijkerhout	2022	1
Medical curriculum		
First year medical students, clinical courses on thyroid and adrenal disease	2017-2018	2
Clinical technology students, clinical courses on thyroid and adrenal disease	2017-2018	2
Grants and prizes		
Best poster prize (basic science), ENETS	2018	
Meeting Grant, European Society of Endocrinology	2019	
Best oral abstract (clinical science), ENETS	2019	
ESE Basic Science Meeting Grant, European Society of Endocrinology	2019	
Travel Grant, ENETS	2020	

List of publications

Blazevic A, Iyer AM, van Velthuysen MF et al. Aberrant tryptophan metabolism in stromal cells is associated with mesenteric fibrosis in small intestinal neuroendocrine tumors. *Endocr Connect*. 2022 Mar 1;EC-22-0020

Blazevic A, Iyer AM, van Velthuysen MF, et al Sexual Dimorphism in Small-intestinal Neuroendocrine Tumors: Lower Prevalence of Mesenteric Disease in Premenopausal Women. *J Clin Endocrinol Metab*. 2022 Apr 19;107(5):e1969-e1975

Blazevic A, Starmans MPA, Brabander T et al. Predicting symptomatic mesenteric mass in small intestinal neuroendocrine tumors using radiomics. *Endocr Relat Cancer*. 2021 Jun 21;28(8):529-539

Blazevic A, Brabander T, Zandee WT et al. Evolution of the Mesenteric Mass in Small Intestinal Neuroendocrine Tumours. *Cancers* 2021 Jan 25;13(3):443

Hoorn EJ, **Blazevic A**, Versmissen J and Rabelink NM. A 59-year-old woman with pressing thirst. *Kidney Int*. 2019 Nov;96(5):1245-1246

Blazevic A, Hofland J, Hofland LJ et al. Small intestinal neuroendocrine tumours and fibrosis: an entangled conundrum. *Endocr Relat Cancer* 2018; 25: R115-R130

Blazevic A, Zandee WT, Franssen GJH et al. Mesenteric fibrosis and palliative surgery in small intestinal neuroendocrine tumours. *Endocr Relat Cancer* 2018; 25: 245-254

Blazevic A, Hunze J, Boots JM. Severe hypophosphataemia after intravenous iron administration. *Netherlands Journal of Medicine* Jan 2014; 72(1): 49-53.

Dankwoord

Promoveren is een weg die je niet alleen af kunt leggen. Dit proefschrift zou dan ook onvolledig zijn zonder een dankwoord gericht aan degene die hebben bijgedragen aan de manuscripten die dit proefschrift vormgeven en die mij hebben gesteund en geholpen.

Als eerste gaat veel dank uit naar mijn promotoren. Geachte **prof.dr. de Herder**, beste Wouter, ik wil je bedanken voor het vertrouwen wat je altijd in mij had. Je liet me vrij om mijn eigen weg in het onderzoek te vinden en daarmee het pad te volgen waar ik in geloofde. Dat heeft ervoor gezorgd dat ik mijn hele promotietraject met veel passie en overtuiging heb kunnen uitvoeren. Maar naast de vrijheid was je er ook altijd om me te steunen en van advies te voorzien als het nodig was. Deze mentor rol heb je later ook vervuld toen ik fellow endocrinologie werd. Naast de enorme ervaring die je altijd wilde delen in combinatie met een goede (soms wat lange) anecdote, zorgde je er ook voor dat je je als fellow gezien en gehoord voelde.

Geachte **prof.dr. Hofland**, beste Leo, dankzij jou heb ik naast klinisch onderzoek ook prachtig basaal wetenschappelijk werk kunnen doen. Bedankt voor alle waardevolle discussies, die we onder andere tijdens onze wekelijkse besprekingen hebben gevoerd. Je oog voor details en zorgvuldigheid is bewonderingswaardig en heeft mij helpen groeien als onderzoeker.

Geachte **dr. Feelders**, beste Richard, in 2015 kwam ik naar het Erasmus MC voor mijn polistage en had ik het geluk dat jij mijn supervisor werd. Je zag mijn enthousiasme voor wetenschap en zorgde er onder andere voor dat ik op dit promotietraject kon starten waarin mijn liefde voor basaal onderzoek gecombineerd kon worden met klinisch werk. Je uitgebreide expertise op zowel neuroendocriene tumoren als bijnier pathologie zorgde altijd voor een verfrissende invalshoek tijdens besprekingen, en resulteerde meermaals in nieuwe projecten. Daarvoor wil ik je bedanken en ik hoop dat we nog lang kunnen blijven samenwerken.

Geachte leden van de leescommissie, **prof.dr. Nieveen Van Diekum**, **prof.dr. Spaander** en **prof.dr. Verburg**, hartelijk dank voor het plaatsnemen in de leescommissie en voor het beoordelen van het manuscript. Daarnaast wil ik ook de overige leden hartelijk danken voor het plaatsnemen in de promotiecommissie. Ik verheug me erop met u van gedachten te kunnen wisselen over de studies en hypothesen beschreven in dit proefschrift.

Dan natuurlijk alle dank voor de collega's uit het lab. **Peter**, **Fadime** en **Rosanna**, ik was jullie gezamenlijk project en dat zorgde ervoor dat ik altijd op jullie expertise kon bouwen tijdens mijn experimenten. Dank jullie wel voor jullie begeleiding. **Dr. Iyer**, beste Anand, halverwege mijn promotietraject kwam jij ons team ondersteunen en wat een geluk was dat voor mij. Met name je hulp bij de analyse van de proteomics data was van onschatbare waarde. Vele uren hebben gependend te bedenken wat de beste wijze van analyse was en welk verhaal we op de voorgrond moesten zetten. En dan natuurlijk de verbindende factor op het lab, **Annelies**. Dank je wel voor al je hulp gedurende de jaren. Ik kon altijd bouwen op je strategisch inzicht en advies voor alle promotie-gerelateerde zaken maar heb ook ontzettend van je warmte en gezelligheid genoten.

Daarnaast was ik ook vaak op het *Metabolism and Reproduction* lab te vinden. Geachte **dr. Visser**, beste Jenny, dank je wel voor je gastvrijheid op het lab. Beste **Gido**, nu alweer dr. Snaterse, ik was overtuigd dat steroïdhormonen ook een rol speelden bij pathogenese van neuroendocriene tumoren en wil je bedanken voor jouw expertise die me heeft geholpen deze hypothese verder te kunnen onderzoeken. **Martin**, dank je wel voor je hulp bij experimenten, je luisterend oor en je ijskoude culinaire traktaties. Verder wil ik ook alle andere collega's, **Patric**, **Cobie**, **Anke**, **Selvetta**, **Keng**, **Karina** en **Loes** bedanken voor de samenwerking. En tot slot, **Bas**, helaas moeten we je gezelligheid nu missen. Je was er altijd, vooral in die zomers met een verlate verdieping en wanneer ik als een hulpeloze klinische promovendus naar lab apparatuur aan het kijken was.

Geachte **dr. Hofland**, beste Hans, ik wil je ontzettend bedanken voor alle ondersteuning en adviezen die je me over de jaren hebt gegeven. Je kritische blik zorgde ervoor dat iedere paper beter werd maar heeft ook geholpen mijn doelen scherper te krijgen. Ik

heb bewondering voor je tomeloze inzet en liefde voor de wetenschap en geneeskunde. Je begeleiding, waarbij ik altijd probeerde aan je verwachtingen te voldoen, heeft me ontzettend doen groeien als wetenschapper en arts, dank je wel daarvoor.

Geachte **dr. van Velthuisen**, beste Loes, ik heb genoten van onze besprekingen. Na een tocht naar het Josephine Nefkens instituut kwam ik altijd terug met frisse enthousiasme. Jouw blik op mesenteriale fibrose en neuroendocriene tumoren is verfrissend en je vragen altijd scherp. Je ondersteuning heeft de stukken in dit proefschrift duidelijker en samenhangender gemaakt en je hebt me ontzettend geholpen om overkoepelend beeld van de pathogenese van mesenteriale fibrose te vormen.

Geachte **drs. Franssen** en **dr. van Ginhoven**, beste Gaston en Tessa, zonder de samenwerking met jullie als endocriene chirurgen was dit proefschrift er niet geweest. Ook ben ik dankbaar voor de kansen die jullie mij hebben gegeven om als beschouwend arts onze bevindingen over de chirurgische aspecten rondom mesenteriale fibrose op congressen te delen. Tot slot wil ik jullie ook bedanken voor de gezelligheid en begeleiding als fellow endocrinologie.

Geachte **dr. Brabander**, beste Tessa, je was daar aan het begin van mijn promotietraject om mij de principes en valkuilen van het beoordelen van mesenteriale fibrose te leren. Verder wil ik je bedanken voor je waardevolle inbreng bij het opzetten van de studies beschreven in dit proefschrift waarvoor je ook een enorme hoeveelheid CT-scans voor hebt herbeoordeelt.

Geachte **dr. Zandee**, beste Wouter, dank je wel voor het wegwijs maken in het wereld van het NET-onderzoek. Ook is de database die jij zorgvuldig hebt bijgehouden en verbeterd de basis geweest van veel manuscripten en daarmee essentieel voor dit proefschrift.

Geachte **dr. Starmans**, beste Martijn, dank je wel voor hele fijne samenwerking. Je bent een echte bruggenbouwer en maakt de ingewikkelde techniek van radiomics en machine learning toegankelijk voor ons klinici. Onze samenwerking heeft er ook voor gezorgd dat

ik weer de liefde voor programmeren hervond. Ik hoop dan ook in toekomst met je te kunnen blijven samenwerken.

Geachte **dr. Zajec** en **dr. van Huizen**, beste Marina en Nick, jullie hulp bij het proteomics project was onmisbaar. Daarnaast zijn jullie goede vrienden geworden. Nick, ik waardeer jou nuchterheid. Marina, obožavam tvoju vatru.

Alle overige co-auteurs, **Lindsey Oudijk**, **Roy Dwarkasing**, **Renza van Gils**, **Stefan Klein**, **Wiro Niessen** en **Theo Luider**, dank jullie wel voor jullie bijdrage aan dit proefschrift. Ook wil de **afdeling pathologie** en in het bijzonder **Thierry van den Bosch** bedanken voor hun samenwerking.

Geachte **dr. Coopmans** en **drs. Van der Valk**, beste Eva en Eline, wij zijn ongeveer samen gestart met ons promotietraject en wat een geluk was dat. In de afgelopen jaren heb ik jullie leren kennen ambitieuze en talentvolle vrouwen en zijn jullie waardevolle vriendinnen geworden. Ons verschil in karakter zorgde ervoor dat bij obstakels jullie nieuwe paden vooruit konden tonen en problemen goed in perspectief kwamen. Ook zijn we samen door verschillende levensfasen gegaan, van trouwen tot een gezin starten en dit zorgt voor een bijzondere band. Ik ben dan ook ontzettend blij dat jullie mijn paranimfen zijn

Beste **Amber**, **Sara**, **Noémie**, **Ilva**, **Merijn**, **Leonora**, **Claudia**, **Julie**, **Ticiania** en **Charlotte**, dank jullie wel voor de gezelligheid op de “5de” en daarbuiten. Ook bedankt voor alle steun en begrip bij de obstakels die ik tegenkwam. Het is altijd ontzettend fijn om te weten dat je niet alleen in een bootje zit en na even gelucht te hebben kon ik er altijd weer met frisse moed en ideeën tegenaan.

Naast de mede-promovendi, zijn er ook klinische collega's die in het bijzonder wil bedanken voor hun steun tijdens promotietraject. Beste **Maud**, je grote hart en toewijding is er niet alleen voor je patiënten, maar ook voor je vrienden ben je er altijd. Ik verheug me dat we nu weer collega's worden en hoop nog vaak om op jouw (of binnenkort op mijn) dakterras te kunnen genieten van een wijntje en goed gesprek. Beste **Rosa**, tijdens

de vele koffiemomentjes gedurende onze polistage hebben wij elkaar leren kennen en ik ben jouw ongezouten mening ontzettend gaan waarderen. Ook hoop ik dat nu je een nieuw avontuur tegemoet gaat, we elkaar niet uit het oog verliezen en samen met **Carmen** en **Marieke** het Tribunaal sterk voortgezet gaat worden. Beste **Zana**, jij begrijpt mijn Slavische ziel en jouw empathie zorgt ervoor dat je er precies bent op de momenten dat het nodig is.

Beste **Karin**, **Loyal** en **Evert**, dankzij jullie werd het begin van de differentiatie een duik in het diepe met zwembandjes aan. Beste **Kim**, **Sanne**, **Tim**, **Mark** en **Caroline**, jullie waren de beste collega's die je je kon wensen. Jullie stonden altijd klaar als de druk te hoog opliep en er was veel gezelligheid van Indische rijsttafels tot feestvieren met A.C. Milan hooligans.

Dan mijn liefste vriendinnen, ik voel mij zo gezegend met jullie in mijn leven. Lieve **Elan**, je kent me als geen ander en in jouw blik zie ik mijn echte zelf terug. Ook al zijn onze levens vaak een andere kant op gegaan, het heeft ons nooit gescheiden. Je bent er altijd voor mij en daar ben ik je ontzettend dankbaar voor. Beste **Jennifer**, samen hebben we een grote stap gezet en gezorgd dat er een begin is van een commune met vrienden. Ik bewonder jouw loyaliteit en zorgzaamheid en prijs me ontzettend gelukkig dat ik in de ontvangende cirkel zit. Lieve **Siobhan**, jouw warmte straalt naar iedereen door. Ik waardeer je empathie en vind het zo bijzonder hoe geliefd jij iedereen om je heen laat voelen, dank je wel daarvoor. Beste **Kristi**, je bent een heerlijke chaotische powervrouw. Ik bewonder je energie en veerkracht en ook al zijn onze afspraakjes nu we mamma's zijn minder wild, maakt dat het niet minder leuk. Lieve **Vandhana**, in veel opzichten zijn we elkaars tegenpolen en heb ik dan ook veel van je geleerd. Beste **Lisa**, de afgelopen jaren heb je hoge bergen beklommen en ik ben blij dat je nu weer in Nederland bent. Lieve **Merel**, de tofste meid van het Honours programme. Van feestjes en weekendjes weg tot kopjes thee op de bank, je bent de afgelopen jaren een luisterend oor, steunende schouder en waardevolle vriendin geweest, dank je wel daarvoor. Beste **Maaike**, jouw energie kent geen grenzen en volgens mij heeft jouw week veel meer dan 168 uur. Ondanks alle avonturen, ambities en afstand, blijf je tijd maken voor onze vriendschap en dat waardeer ik heel erg.

Draga **Mimi** i dragi **Tata**, hvala Vam za sve. Jullie hebben me geleerd kritisch te zijn, te durven denken en te staan voor mijn mening. Jullie vertrouwen in mij heeft ervoor gezorgd dat ik altijd mijn hart durfde te volgen. Ik ben jullie daar ontzettend dankbaar voor want dat pad heeft me nu hier gebracht.

Je leerde me lichter te zijn tot ik durfde te vliegen. Je was het anker die mij de diepte van liefde toonde. Lieve **Ivan**, *it had to be you.*

Curriculum Vitae

Anela Blažević was born on January 21st, 1988 in Zenica, Former Yugoslavia. She graduated from the Erasmiaans Gymnasium cum laude in 2006 and started her study of Medicine at the Erasmus University in Rotterdam, the Netherlands. During the first years of Medical School, she took part in the Erasmus MC Honours Class, an extra program to get acquainted with the cutting edges between Medicine, Science and Society. Inspired by this program, she started concurrently with Medical School training for a Bachelor of Arts degree in the Philosophy of Science. She graduated in 2012 with her bachelor thesis entitled '*Pragmatic Confusion: a Critical Appraisal of Bennett & Hackers' Philisophical Foundations of Neuroscience*'. She continued to obtain Master of Science degree in Neuroscience. Her Master thesis was entitled '*Exploring the Role of α CAMKII on the Retention of Fear Memories*' and was awarded with a Assistantship Award from the Royal Dutch Academy of Science and Arts (KNAW). In 2013, she graduate from Medical School cum laude and she started her residency in Internal Medicine at the Ikazia Hospital in Rotterdam. Subsequently, she continued her clinical training at the Erasmus Medical Center. In 2017, she started her PhD training at the Laboratory of Neuro-Endocrinology of the Department of Internal Medicine of the Erasmus Medical Center, under the supervision of prof.dr. W.W. de Herder, prof.dr. L.J Hofland and dr. R.A. Felders. She presented her research at several national and international meetings, and was the winner of best oral presentation at the European Neuroendocrine Tumor Society Conference in 2019. In 2020, she started her Fellowship Endocrinology which she finished in 2022. Currently, she works as an Endocrinologist.



